EVALUATION OF FIBER REINFORCED POLYMER (FRP) STRENGTHENING FOR DETERIORATED BRIDGE BENT CAPS

by

YAZAN ALMOMANI

Presented to the Faculty of the Graduate School of

The University of Texas at Arlington in Partial Fulfillment

of the Requirements

for the Degree of

DOCTOR OF PHILOSOPHY

THE UNIVERSITY OF TEXAS AT ARLINGTON

August 2018

Acknowledgments

First and foremost, I acknowledge my gratitude to my God for giving me the strength to complete this research. My deepest appreciation goes to my advisor Dr. Nur Yazdani for his generous guidance, consistent support and advice through all stages of this research work. I am thankful to Dr. Shih-Ho Chao, Dr. Raad Azzawi and Dr. Bill Carroll for readily accepting to serve on my dissertation committee. I want to thank them for their support during my study. I will always be thankful to the Civil Engineering Department at UT Arlington for supporting me throughout my research work.

I am thankful to my friends Dr. Eyosias Beneberu, Santosh Timilsnia, Tariq Al Jaafreh, Natawut Chaiwino, Towfiqul Quadir, Dr. Mina Riad, Ankita Lad, and Zaid Momani for all the help during the research work.

I am deeply grateful to my family who stood by my side through the entirety of this research.

July 12, 2018

Abstract

EVALUATION OF FIBER REINFORCED POLYMER (FRP) STRENGTHENING FOR DETERIORATED BRIDGE BENT CAPS

Yazan Almomani, PhD

The University of Texas at Arlington, 2018

Supervising Professor: Nur Yazdani

Deterioration of aging highway bridges has been a serious concern in the U. S. A. Almost 39% percent of all bridges in the country have passed their 50-year design life, and approximately 9% of these bridges are structurally deficient due to concrete deterioration and truck weight increases on highways. Compared to superstructures, the deterioration of bridge substructures and associated repair/strengthening/evaluation has received much less attention in previous studies. A reinforced concrete bridge built in 1940 and located in Dallas, Texas, exhibited moderate to severe corrosion related concrete deterioration in the bent caps. Eight such bent caps were selected herein for repair, carbon FRP (CFRP) strengthening for strength gain and confinement, long-term durability, and evaluation. The in-situ performance of the carbon FRP (CFRP) system of bent cap strengthening was evaluated through full-scale load testing. The

investigation consisted of three phases: static load testing of deteriorated bent caps before repair and CFRP strengthening, repair/strengthening of the bent caps using an epoxy mortar and longitudinal/transverse CFRP laminates, and follow-up load testing after CFRP repair/strengthening. Test data comparison showed a reduction in the live load strains ranged from 20 to 28% due to a contribution of the CFRP and concrete repair on the strength and stiffness of the bent caps. Numerical models were performed to investigate the flexural behavior of the bridge in the undamaged, damaged, and repaired states. The bent caps after being repaired show that the flexural capacity of the damaged bent caps has been improved.

Table of Contents

Acknowledgments iii

Abstract iv

Table of Contents vi

List of Figures x

List of Tables xv

Chapter 1 INTRODUCTION 1

1.1 Background 1

1.2 Problem Statement 5

1.3 Objectives 7

1.4 Organization of the Dissertation 8

Chapter 2 LITERATURE REVIEW 10

2.1 Introduction 10

2.2 Concrete Deterioration 11

2.2.1 Carbonation-Induced Corrosion 14

2.2.2 Chloride-Induced Corrosion 15

2.3 Concrete Inspection 16

2.4 Concrete Repair 19

2.4.1 Concrete Repair Materials 21

2.4.2 Concrete Repair Methods 22

2.5 CFRP Strengthening 28
2.6 Numerical Modeling 31
2.7 Non-destructive Load Test 32
Chapter 3 CONCRETE REPAIR AND CFRP STRENGTHENING 40
3.1 Bridge Description 40
3.2 Visual Inspection 43
3.3 Concrete Surface Preparation 45
3.4 Formwork Installation and Pouring 49
3.5 Patching 52
3.6 CFRP Preparation and Application 53
3.6.1 CFRP Preparation 53
3.6.2 CFRP Application 54
3.6.3 CFRP Protection 56
3.6.4 Pull off test 56
Chapter 4 NON-DESTRUCTIVE LOAD TESTING 58
4.1 Load Testing Instrumentation before Repair 58
4.2 Load Testing Procedures 64
4.2.1 Marking on the Roadway 65
4.2.2 Truck Live Load 66
4.2.3 Diagnostic Load Tests 67
4.2.3.1 Static Load Test 67

4.2.3.1 Crawl Speed Test 70
4.3 Load Testing after Repair 74
Chapter 5 FINITE ELEMENT MODELING 77
5.1 Introduction 77
5.2 Material Properties 78
5.2.1 Concrete 78
5.2.2 Steel Reinforcement 81
5.2.3 FRP 81
5.2.4 Bond between FRP and Concrete 84
5.3 Element Types 85
5.4 Model Geometry 85
5.4.1 Model Geometry of before Repair Bent Cap 87
5.4.2 Model Geometry of after Repair Bent Cap 89
5.5 Meshing and Boundary Conditions 91
5.6 Loads 94
Chapter 6 LOAD TESTS AND FINITE ELEMENT MODELING RESULTS 96
6.1 Load Tests Results 96
6.1.1 Comparison between before and after Repair Load Tests 97
6.1.2 Load Cases 102

6.2 Model Calibration 103
6.3 Model Results 108
6.3.1 Strain Results 108
6.3.2 Neutral Axis Location 110
6.3.3 Deterioration Effect 111
6.4 Bent Cap Capacity before and after Repair 115
Chapter 7 CONCLUSIONS AND RECOMMENDATION 119
7.1 Summary 119
7.2 Summary of Findings and Conclusions 119
7.3 Future Research 121
Appendix A SUMMARY OF BRIDGE REPAIR MANUALS FOR ALL STATES HIGHWAY 122
References 136
Biographical Information cxlii

List of Figures

Figure 1-1 Overheight vehicle crash causes significant bridge damage in Indianapolis, Indiana. (FOX59, 2017) 2

Figure 1-2 Performance history of a bridge (Carolin, 2003)..... 3

Figure 2-1 Age of America's bridges (ASCE 2017) 10

Figure 2-2 Initiation and propagation periods for steel corrosion in concrete (Zhoa and Jin 2016)..... 13

Figure 2-3 Concrete deficiencies: (a) Crack in concrete bent cap, (b) Concrete spalling due to contaminated drainage, (c) Concrete spalling on bent cap (d) Collision damage to concrete pier column (FHWA 2012) 18

Figure 2-4 Concrete removal (Nemtai 2006) 23

Figure 2-5 Saw cutting the perimeter (Rec 24

Figure 2-6 Concrete removal around the rebar: (a) before removal, (b) after removal (Nemati 2006) 24

Figure 2-7 Repair methods: (a) Form and Cast-in-Place (b) Form and pump (c) Trowel applied (d) Dry-mix Shotcrete 27

Figure 2-8 Figure 2 8 First impact damaged beam repair with CFRP: (a) The impact damaged beam (b) CFRP u-wrap was applied (c) The repaired beam after five years (Bradberry and Wallace 2003) 30

Figure 2-9 Finite element mesh of middle span (Chajes et al. 1996)..... 32

Figure 2-10 Instrumentation of the bridge (Hag-Elsafi et al. 2000) 35
Figure 2-11 Locations of GFRP and CFRP plates (Stallings 2000) 36
Figure 2-12 Load positions (Stallings 2000) 37
Figure 3-1 Top view of US 80 Bridge-Dallas, Texas (Google Maps) 40
Figure 3-2 Two traffic lanes of the WB bridge (Google Maps) 41
3-3 Cross-section view of the WB bridge 42
Figure 3-4 Deterioration of the bridge bent caps: (a) Bent Cap 35, (b) Bent Cap 37, (c) Bent Cap 40, (d) Bent Cap 41 44
Figure 3-5 Plan view of the eight selected bent caps 45
Figure 3-6 Concrete Surface Preparation: (a) Chipping out loose concrete and saw cut the edges, (b) Removing concrete around the rebars, (c) Cleaning the repair area using high-pressure water pump 47
Figure 3-7 Concrete Surface Preparation: (a) Chipping out loose concrete and saw cut the edges, (b) Removing concrete around the rebars, (c) Cleaning the repair area using high-pressure water pump 48
Figure 3-8 Formwork installation and pouring: (a) Steel cleaning and water spraying, (b) Bonding agent application, (c) Formwork installation and poring, (d) Formwork removal, (e) Curing compound spraying 51
Figure 3-9 Patching mortar application 52
Figure 3-10 Sandblasting the repaired area 53

Figure 3-11 CFRP application: (a) Cutting CFRP sheets, (b) Applying CFRP sheets, (c) CFRP sheets after curing 55
Figure 3-12 Protection top coat application 56
Figure 3-13 Pull off test (a) Preparing the CFRP surface (b) Dolly placing (c) Pulling out the sample (d) Concrete failure sample 57
Figure 4-1 3-D model of the selected bridge 59
Figure 4-2 Instrumentation plan for bent caps 37 and 36 60
Figure 4-3 Instrumentation plan for bent cap 35 61
Figure 4-4 Data acquisition system location 61
Figure 4-5 Strain gages installation: (a) Marking, (b) Grinding, (c) Appling acetone, (d) Applying water, (e) Applying epoxy, (f) Installing strain gage, (g) Bent cap 37, (h) Bent cap 36 63
Figure 4-6 Marking the roadway 65
4-7 Dimensions of the dump trucks 66
Figure 4-8 Stop location at bent cap 37 68
Figure 4-9 Stop location at bent cap 36 68
Figure 4-10 Stop location at bent cap 35 69
Figure 4-11 Trucks stopped at Bent cap 37 69
Figure 4-12 Loading Path One 71
Figure 4-13 Loading Path Two 72
Figure 4-14 Loading Path One & Two 73

Figure 4-15 Instrumentation plan for bent cap 37 75
Figure 4-16 Instrumentation plan for bent cap 36 75
Figure 4-17 Instrumentation plan for bent cap 35 76
Figure 5-1 Uni-axial stress-strain curves of concrete (Saenz 1964) 79
Figure 5-2 Stress-strain curve for typical reinforcing steel bar (Obaidat 2011) 81
Figure 5-3 Stress-strain curves for typical fiber, resin and FRP composite (Piggot, 2002) 83
Figure 5-4 Abaqus element families 85
Figure 5-5 Abaqus model geometry 86
Figure 5-6 Reinforcement cage model 87
Figure 5-7 Deteriorated bent cap model 88
Figure 5-8 Repair mortar model 90
Figure 5-9 FRP sheets model 91
Figure 5-10 Mesh used in the model 93
Figure 5-11 Model Boundary condition in Abaqus 93
Figure 5-12 bridge model using CSIBridge 94
Figure 5-13 Surface loads model 95
Figure 6-1 Strain comparison of span two of bent cap 37 98
Figure 6-2 Strain comparison of span three of bent cap 37 99
Figure 6-3 Strain comparison of span three of bent cap 35 99

Figure 6-4 Strain comparison of span one of bent cap 37 100
Figure 6-5 Strain comparison of span one of bent cap 35 100
Figure 6-6 strain measurement for the load cases (a) before repair, (b) after repair 103
Figure 6-7 Concrete coring procedures: (a) Taking the cores, (b) GPR scanning, (c) Setting up the compression machine, (d) Tested sample 105
Figure 6-8 FEM results vs. experimental results..... 108
Figure 6-9 Measured vs. FEM (a) before repair, (b) after repair 109
Figure 6-10 FEM results for the bent cap before and after repair 110
Figure 6-11Neutral Axis Location 111
Figure 6-12 Tensile strain for all models..... 113
Figure 6-13 HL-93 truck vs. TxDOT truck (a) bent cap before repair, (b) bent cap after repair 114
Figure 6-14 Cracked section of the bent cap before repair..... 116
Figure 6-15 Cracked section of the repaired bent cap..... 116
Figure 6-16 Crack pattern for the bent cap before repair..... 117
Figure 6-17 Cracks pattern for the bent cap after repair..... 118
Figure 6-18 bent cap capacity 118

List of Tables

Table 2-1 Sample of a summary for concrete repair manuals for all states highway 21

Table 3-1 Estimation of the concrete spalling quantities of the eight selected bent caps..... 46

Table 4-1 Axle weights for the dump trucks..... 66

Table 4-2 Axle weights for the dump trucks..... 74

Table 5-1 material properties of FRP laminates 83

Table 5-2 Depth of concrete spalling 88

Table 6-1 Compressive strength of the bent caps 106

Table 6-2 Section loss variation..... 112

Chapter 1
INTRODUCTION

1.1 Background

The United States has a growing number of bridges which are considered structurally or functionally obsolete. If a bridge is both structurally and functionally obsolete, it is only considered as a structurally deficient bridge. According to the ASCE 2017 report card America's infrastructure, functionally obsolete bridges are approximately 13.6% of U.S. bridges in 2016. Functionally obsolete bridges can be defined as bridges that are not able to meet the current standards or serve current traffic demand due to insufficient lanes or narrow lanes or shoulders (ASCE Report Card 2017).

One in 10 (10.1%) of the U.S. bridges are considered structurally obsolete. Typically, these bridges have been limited to light vehicles, closed to traffic or required rehabilitation. Structurally deficient means there are members of the bridge that need to be monitored and/or repaired. These bridges require load restrictions, which can significantly increase the driving time for large vehicles such as delivery trucks (ASCE Report Card 2017). However, a significant number of bridges are damaged each year due to

structural deterioration or extreme events such as fire, earthquakes, and accidents as shown in Figure 1-1.

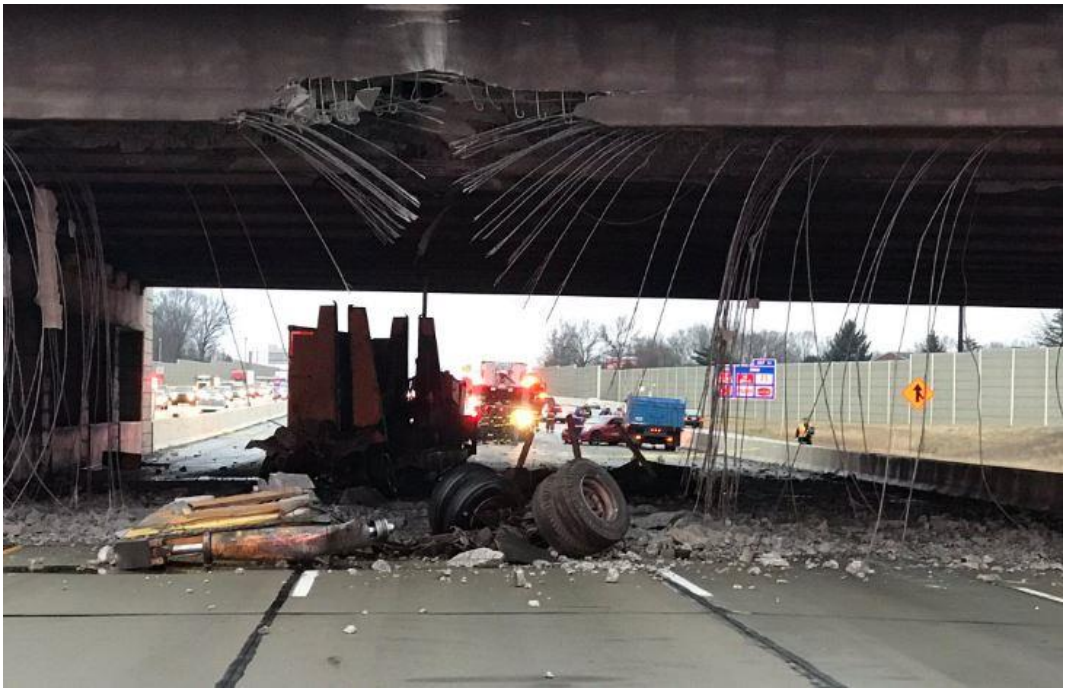

Figure 1-1 Overheight vehicle crash causes significant bridge damage in Indianapolis, Indiana. (FOX59, 2017)

Texas Department of Transportation (TxDOT) maintains over 33,000 on-system bridges, approximately 85% of these bridges have concrete spans and/or have concrete members in all types of bridges (Yang et al. 2011). Concrete bridge members are in need to be repaired and rehabilitated as their service lives are exceeding. Deterioration is one of the main issues that affect the bridge service life due to steel corrosion, freeze-

thaw, sulfate attack, degradation induced by deicing salts, and alkali-silica reaction (Kim et al. 2008). Retrofitting or replacement is required when a structural member is subjected to extensive damage which could result in a loss of the ultimate strength. The prioritization for rehabilitation or replacement is based on the bridge deficient degree in meeting the public demands (Branco and de Brito 2004). An alternative solution of replacement is to improve the capacity of these bridges by retrofitting the deficient members as shown in Figure 1-2. Concrete rehabilitation could result in a significant cost savings and capacity improvement throughout the service life of the bridge.

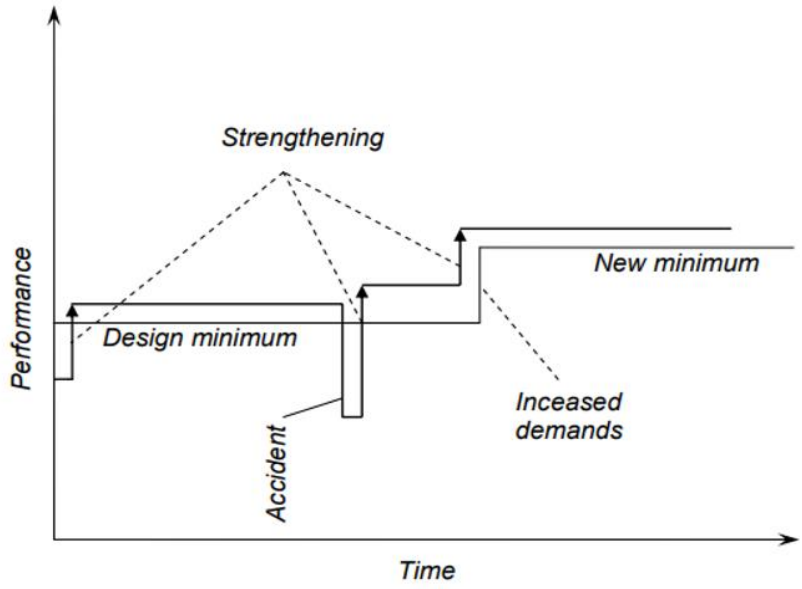

Figure 1-2 Performance history of a bridge (Carolin, 2003).

Rehabilitation can be performed using several methods such as steel or concrete jacketing, external post-tensioning, externally bonded steel plates, and externally bonded Fiber Reinforced Polymer (FRP). The development of external FRP composite laminate material has recently become a common method of rehabilitation. The great success of using FRP in rehabilitation of concrete members was due to their ease in handling, light weight, high strength-to-weight ratio, resistance to corrosion, and high tensile strength (Stallings et al. 2000). There are several forms of FRP materials which are ranging from factory-made laminates to dry fiber sheets which used as wrapping material (ACI 440.2R 2017).

FRP is comprised of fibers embedded in a polymeric resin matrix that serves as a protective binder to the reinforcing fibers and bonding agent to the substrate (Pino et al. 2017). The advantages of using FRP include an active load-carrying mechanism, effective stress redistribution of existing reinforcement, enhanced durability and serviceability, and improved shear and flexural capacities (Kim 2008). FRP composites exhibit excellent tensile strength in the fiber direction and relatively low strength in the fiber transverse direction, which demonstrates an orthotropic behavior of the system (Pino et al. 2017).

1.2 Problem Statement

Over 50% of all bridges in the United States were built before 1940, and approximately 42% of these bridges are structurally deficient (Klaiber 1987). This alarming statistic highlights the importance of developing reliable and cost-effective repair, strengthening, and evaluation techniques for existing bridge structures. This research aims to develop a FRP strengthening scheme for such deteriorated bridge bent caps. The effectiveness of the procedure is being tested on the 87 years old US-80 bridge over East Fork Trinity, Forney, Texas.

Texas has many old concrete bridges that have deteriorated substantially with age due to concrete spalling and steel corrosion. Bridges need repair if deterioration has resulted in a loss of load capacity. While some bridges only exhibit minor deterioration but were designed for live loads less than the modern traffic loads. There is currently a lack of understanding throughout the bridge repair industry regarding when certain repair procedures are applicable. Applying an inadequate or incorrect repair procedure has no guarantee of providing any benefit over taking no action (Ainge 2009).

Developing repair and strengthening techniques of bridge substructures is the focus of this study. Research focused on bridge substructure repair and strengthening is much less common than research

focusing on superstructure members. Since bridge bent caps considered as bridge substructure, there currently exists no document which effectively evaluates the possible repair methods for bridge substructure (Tilly 2011). This study attempts to maximize the reliability and the efficiency of repairs that are conducted on concrete substructures which could result in significant cost savings throughout the service life of the bridge.

Each bridge should be inspected every two years according to (FHWA, 2012). Most bridges are evaluated using basic models that depend on the bridge properties and dimensions determined from original design plans and/or notes made from visual inspections. Generally, the individual who inspects a bridge is not directly involved in either the rating or the analysis of the bridge. Consequently, ratings determined in that way may not always perfectly reflect a bridge's actual safe load-carrying capacity (Micheal 1997). There is no such recommendation when it comes to the evaluation of FRP repaired and bridge substructures. This study will focus on how experimental load testing can be used to evaluate the bridge bent caps and to develop relatively simple, yet accurate, numerical bridge models, and how these models can, in turn, be used to rate the bridge substructures.

1.3 Objectives

This study investigates the performance of bridge bent cap structure that experienced significant deterioration. This study aims to improve the public safety by ensuring the bridge bent cap structures are strong and safe in carrying the anticipated traffic loading by improving efficient bent cap repair and guidelines for CFRP application. Due to lack of research regarding bridge substructures repairing and strengthening, the performance of the bent caps strengthened with CFRP composite is evaluated by analytical models and experimental tests. A significant improvement in bridge structures is expected through the developed knowledge, guidelines, analytical and test methods for the bridge substructures. The proposed research involves repair, instrumentation, CFRP application, load testing before and after repair, modeling and model calibration of the bridge bent caps located on US 80 highway over East Fork Trinity River. The research was conducted with the following main objectives:

- Developing a strategy for efficient bent cap repair and strengthening.
- Investigating and comparing the performance of deteriorated bent caps with an undamaged bent cap to study the effect of deterioration on the bent caps.

- Comparing the performance of selected bent caps before and after CFRP rehabilitation to evaluate the effectiveness of the CFRP strengthening technique.
- Performing a static and crawl speed load tests to investigate the overall performance of bridge bent caps.
- Performing a theoretical modeling of the bridge structure using structural analysis programs (CSIBridge) to investigate the critical load testing paths.
- Performing a realistic 3D finite element model of FRP strengthened concrete bridge bent caps.
- Calibrating the 3D finite element model based on the experimental load testing results, and hence, capture the behavior of the in-service bridge bent caps.
- Developing load testing guidelines and recommendations for FRP-strengthened bridge bent caps using the results of the experiment and the numerical model.

1.4 Organization of the Dissertation

This dissertation is organized into seven chapters. The content of each chapter is described as follows.

- *Chapter 2- Literature Review*

This chapter presents a review of the concrete repair, FRP strengthening, the conducted research on the bridge load tests and the numerical models.

- *Chapter 3- Concrete Repair and CFRP Strengthening*

  This chapter represents the bridge bent caps visual inspection, repair procedures, and CFRP application.

- *Chapter 4*- Non-Destructive load testing:

  This chapter represents the instrumentation plan and the procedures of before and after repair non-destructive load tests.

- Chapter 5- *Numerical Modelling*

This chapter discusses the material and geometry of the numerical modeling of the bridge bent cap and the calibration of the non-destructive load test data.

- *Chapter 6- Results and Discussion*

This chapter represents the results of the nondestructive load testing and the numerical model.

- *Chapter 7- Conclusions and Recommendations*

Finally, a summary of findings, conclusions, and future recommendations are presented in Chapter 7.

Chapter 2
LITERATURE REVIEW

2.1 Introduction

The U.S. has 614,387 bridges, almost 39% are 50 years or older as shown in Figure 2-1 (ASCE 2017). There is an average of 188 million trips daily across structurally deficient bridges. The average age of bridges in the U.S. is 43 years old and will continue increasing as many of the US bridges are close to the end of their design life. The most recent estimate of U.S. bridge rehabilitation is $123 billion. Most of the bridges were designed for an average lifespan of 50 years, so that growing number of bridges will need replacement or rehabilitation (ASCE 2017).

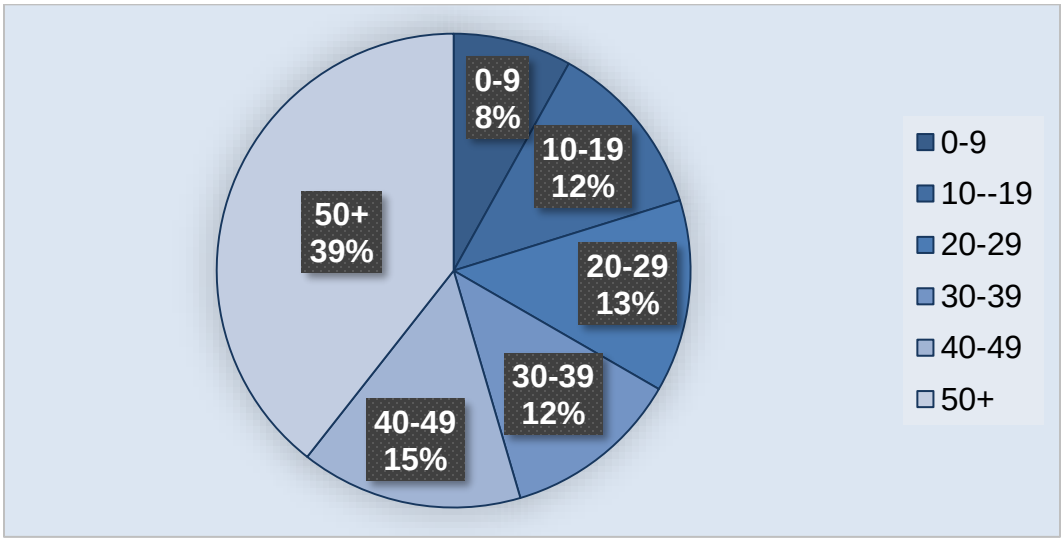

Figure 2-1 Age of America's bridges (ASCE 2017)

2.2 Concrete Deterioration

Corrosion of reinforcing steel is the leading cause of concrete deterioration. Corrosion occurs when steel exposes to either chlorides or carbon. Chlorides are often existent in seawater and deicing agents, while carbonation is caused by atmospheric CO2 penetrating the concrete. Corrosion produces materials that can increase the volume of the reinforcement by three to six times (Smith and Virmani 1996). When the corroding steel expands, it creates tensile stresses which damage the surrounding concrete since the concrete has a low tensile strength. The damage may be excessive cracking, spalling and separation of concrete cover, loss of bond between concrete and reinforcements, and eventually decreasing in the member bearing capacity (Lu et al. 2017).

Concrete provides a protective coating that prevents the water and oxygen from accessing the steel surface. Additionally, the concrete has a very high alkalinity solutions, which produces a very thin protective coating on the steel (a passive film) which limits the metal loss from the steel surface due to corrosion to about 0.1 - 1.0 μm/year (Hansson et al. 2007). Therefore, within a 75-year lifetime, the reinforcing steel would not be corroded, also the corrosion volume would not be sufficient to create any damaging stresses within the concrete.

Reinforced concrete service life can be divided into two separate phases, as shown in Figure 2.2. The first one is the initiation of corrosion, which is the amount of time needed for chloride ions to reach the steel interface in sufficient amounts to initiate active corrosion (Zhoa and Jin, 2016). The duration of the first (initiation) phase depends on the penetration rate of the aggressive agents through the concrete cover and the corrosion resistance properties of the reinforcement steel in the cementitious environment (Trejo et al. 2009). Design codes normally define minimum cover depths to control the corrosion rate (Zhoa and Jin 2016). The second phase is the propagation of corrosion, which initiates when the steel is depassivated and eventually results in a limit state being reached. This phase is usually identified by the serviceability failure associated with cracking or separation of the concrete cover (Zhoa and Jin 2016). The propagation phase mainly depends on the rate of corrosion of the reinforcement (Trejo et al. 2009).

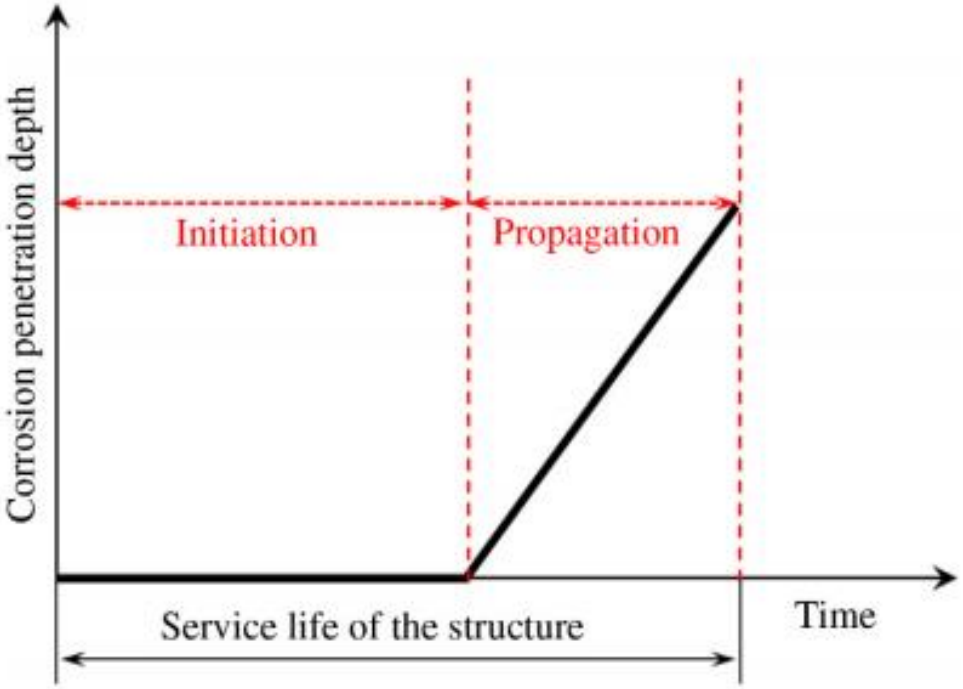

Figure 2-2 Initiation and propagation periods for steel corrosion in concrete (Zhoa and Jin 2016).

Concrete corrosion causes significant and costly maintenance problems for concrete bridge members. However, there are some methods attempting to prevent chloride penetration by using of admixtures and changing the concrete mixture design, improving the concrete cover over reinforcement, cathodic protection, and using of epoxy-coated reinforcement (Smith and Virmani 1996).

2.2.1 Carbonation-Induced Corrosion

Carbonation is a neutralizing process, which consists of carbon dioxide gas dissolution in the atmosphere with the alkaline hydroxides in the concrete. This process induces acid, which neutralizes the pore water alkalies. These carbonic acids penetrate the concrete without damaging, but just attack the steel and neutralize the alkalies in the pore water, mainly forming calcium carbonate that lines the pores: as described by equation (2-1) and (2-2) (Zhoa and Jin 2016).

$$CO_2 + H_2O \text{ ---> } H_2CO_3 \qquad 2\text{-}1$$

$$Ca(OH)_2 + H_2CO_3 \text{ ---> } CaCO_3 + 2H_2O \qquad 2\text{-}2$$

In this circumstance, the carbonation process reduces the value of pH at the surface layer of concrete to less than 8.3. Therefore, the passive film made of pH is no longer stable and causes initiation of the active corrosion. The corrosion process is relatively homogeneous, unlike chloride-induced corrosion. Moreover, the products of corrosion tend to be more soluble in the neutral carbonated concrete. Also may spread out to the surface as rust stains on the concrete rather than condensing in the concrete cover and causing damage stresses and cracking. Corrosion rates due to carbonation are lower than those due to chlorides, but over a long period, the cross-section of the reinforcing steel can be reduced significantly even in presence of little visible damage to the concrete (Poursaee 2016).

2.2.2 Chloride-Induced Corrosion

Chloride can be existed in concrete due to deicing salts or the use of contaminated chloride admixtures (Poursaee 2016). The mechanism of breaking down the passive film by the chloride ions is not fully understood since the passive film is too thin to be examined which the process occurs inside the concrete (Hansson et al. 2007). Chloride ions compete with OH ions for the Fe^{2+} ions producing a soluble complex of iron chloride forms that can diffuse away from the anode, destroying the protective layer of $Fe(OH)_2$ and permit corrosion to continue: as described by equations (2-3) and (2-4) (Zhoa and Jin 2016).

$$Fe^{2+} + 2Cl^- + 4H_2O \text{ ---> } FeCl_2.4H_2O \qquad 2\text{-}3$$

$$FeCl_2.4H_2O \text{ ---> } Fe(OH)_2 + 2Cl^- + 2H^+ + 2H_2O \qquad 2\text{-}4$$

A breaking down of the passive film needs sufficient concentration of chloride in the pore solution; then the chloride ions can depassivate steel and cause pitting corrosion to occur. The chloride concentration threshold or critical value needs to be reached so the corrosion will occur. The determination of threshold value under various circumstances is a very complicated problem (Zhoa and Jin 2016). The complexity and variety of the chloride threshold are due to several factors that can affect the corrosion: w/c ratio, type and specific surface area of the cement, mixture proportions of the concrete, using of supplementary cementing materials

(SCM), sulfate content, curing conditions, age and environmental history of the concrete, temperature and relative humidity of the environment, degree of carbonation of the concrete, and roughness and cleanliness of the reinforcement (Hansson et al., 2007). Therefore, many studies suggested that at a threshold level of 0.2% chloride by weight of cement the corrosion can be observed when the water and oxygen are available or up to 1.0% or more if water and oxygen are excluded (Zhoa and Jin 2016).

2.3 Concrete Inspection

Good bridge inspection and assessment is essential to document the bridge situation and to protect the public's safety and investment in bridge structures. Most highway agencies follow Federal Highway Administration (FHWA) inspection procedures including Texas Department of Transportation (TxDOT). FHWA Inspection Manual provides three different methods to inspect a concrete structure; visual, physical, and advanced inspection. Visual inspection involves reviewing the previous inspection report, visually examining the members of the bridge, a visual assessment to identify obvious deficiencies. Visual inspection can be performed for the following concrete deficiencies (FHWA 2012):

- Cracking (see Figure 2-3 (a))
- Spalling (see Figure 2-3 (b) and (c))

- Collision damage (see Figure 2-3 (d))
- Other causes (temperature changes, fire damage, moisture absorption, chemical attack, design and construction faults, differential movement of foundation, and unintended objects in concrete).

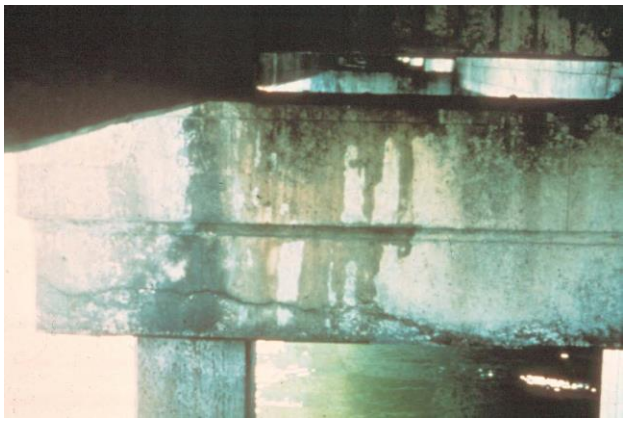

(a)

(b)

(c)

(d)

Figure 2-3 Concrete deficiencies: (a) Crack in concrete bent cap, (b) Concrete spalling due to contaminated drainage, (c) Concrete spalling on bent cap (d) Collision damage to concrete pier column (FHWA 2012)

An in-depth inspection is another type of visual inspection. It is an inspection at a distance no more than an arm's length of one or more members below or above the water level to estimate all deficient surfaces visually. Physical inspection uses inspection hammer to identify any delaminated area which has a distinctive hollow "clacking" sound when tapped with a hammer. The properties of found cracks during the visual inspection like location, length, and width of cracks need to be measured and recorded. An advanced inspection methods must be used if the extent of the deficiency is hard to be determined by the visual and physical inspection methods described above.

Advanced inspection methods can be carried out using non-destructive methods such as; Acoustic wave sonic/ultrasonic velocity measurements, Electrical methods, Delamination detection machinery, Ground-penetrating radar and Impact-echo testing (FHWA 2012).

2.4 Concrete Repair

Reinforced concrete has proved to having high structural performance and durability as structural material (Nemati 2006). Nonetheless, one should note that considering the reinforced or prestressed concrete as a maintenance-free structure is a faulty assumption (Smoak 2002). The durability and maintenance requirements

of concrete structures should be to an anticipated design life incorporates a planned maintenance program (Mays 2002). Concrete structures show the degree of deterioration in the form of cracking, spalling and disintegration (Sudhakumar, 2001).

Concrete repair is a method that restores a deteriorated concrete member to a service level equal to or almost equal to the as-built condition (Weyers 1993). The selection of proper repair methods and materials is important for bridge engineering. The repair materials depend on the available repair construction timeframe and the volume and area of concrete to be repaired (Smoak 2002). In addition to describing the most appropriate repair methods, expected service life and average cost are included in each repair method. In general, the repair method decision is open to interpretation. However, some highway agencies provide recommendations for selecting the repair method for concrete deterioration. In this study, a summary of repair manuals for all states highway was carried out to compare the different repair methods for concrete bridge superstructures and concrete substructure such as bent caps. A sample of the summary is as shown in Table 2-1, while a complete table is attached to Appendix A.

Table 2-1 Sample of a summary for concrete repair manuals for all states highway

#	State	Bent Cap Repair	FRP	Concrete Repair
1	Louisiana	✘	✘	Evaluation procedure is only provided.
2	Colorado	• Limit of removal of concrete (0.5-1)'' beyond the face of the reinforcing steel. • Apply patching material.	• FRP for Substructure: Columns repair: 1) Place concrete sealer on top of concrete columns. 2) Provide 4" gaps between FRP placement areas. No concrete sealer shall be placed in the area.	1) Patching
3	Nevada	• External Pier Cap Post-Tensioning: Tensioning strand or rods can be placed externally on the cap to add compression to the cap. Brackets, distribution plates and other components are needed to transfer the post-tensioning forces to the cap. If aesthetics is a concern, the cap can be widened with ducts placed internally for the post-tensioning. Post-tensioning is usually symmetrical to the cap so that an eccentric force is not introduced. The designer must look at the stressing sequence to ensure that the	• FRP for Superstructures: Inadequate internal shear reinforcement or damaged reinforcement can be strengthened with externally applied, fiber-reinforced polymer (FRP) laminate reinforcement bonded to the surfaces of the webs. Bending capacity can also be increased with the application of FRP reinforcement.	1) Patching. 2) Polymer Concrete Overlay 3) Resin Overlay 4) Waterproof Membrane/Asphalt Overlay 5) Epoxy-Resin Injection 6) Crack Sealant 7) Silane Seal 8) Joint Rehabilitation and Replacement 9) Upgrade/Retrofit Bridge Rails 10) Scour Mitigation 11) External Pier Cap Post-tensioning 12) Micropile Underpinning

2.4.1 Concrete Repair Materials

In the first half of the century, concrete repair materials were relatively simple. It mainly involved using a Portland cement mortar to replace the damaged or deteriorated concrete. Since the 1960's, new improved concrete repair materials have been introduced. These materials have ranged from polymer modifiers for Portland cement-based products (primarily styrene butadiene, acrylic and some vinyl copolymers) to pure polymers such as epoxy resins (Morgan, 1996).

Morgan (1996) has attempted to categorize different types of repair materials based on the deterioration condition and location in the concrete member. He proposed that if the deterioration of original concrete was as a result of aggressive exposure conditions, such as chemical attack or high wear/abrasion, the most appropriate repairing material is using a higher strength and more chemically resistant resin mortar (Polymer concrete). For vertical or overhead surfaces, If thin hand-applied repairs are proposed, the most suitable repair material choice is using a polymer modified cementitious mortar, with superior adhesion, cohesion, and thickness of build-up characteristics. If the repairing is required to be applied at below-freezing temperatures, or rapid setting and hardening and early strength gain properties are wanted then the most appropriate repairing materials that with high early heat of reaction, such as certain resin mortars (e.g., vinyl ester resins), magnesium phosphate cement or accelerated high alumina cement (Morgan, 1996).

2.4.2 Concrete Repair Methods

Many concrete repair failures have accrued since the first concrete was placed (Smoak 2002). Before any repair is carried out the causes of the damage must be identified (Allen et al. 1992). The next step must be to consider the objective of the repair, which will generally be to regain or improve one or more requirements such as; structural strength, durability,

function, and appearance. The most common requirement in repair work is the restoration of durability (Allen et al. 1992). The first stage of repair work is to remove unsound concrete as shown in Figure 2-4. Shoring of the deteriorated members must be provided before starting removals if structural integrity affected by the removals (Nemati 2006). The repair area needs to be saw cut to a depth of about one inch to provide a neat edge as shown in Figure 2-5.

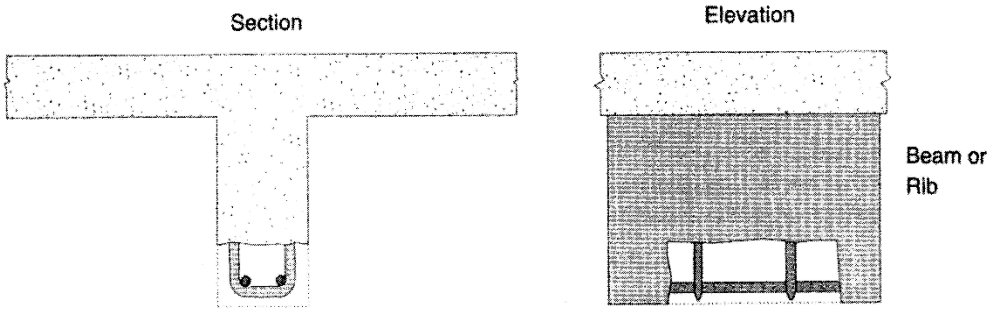

Figure 2-4 Concrete removal (Nemtai 2006)

Figure 2-5 Saw cutting the perimeter (Rec

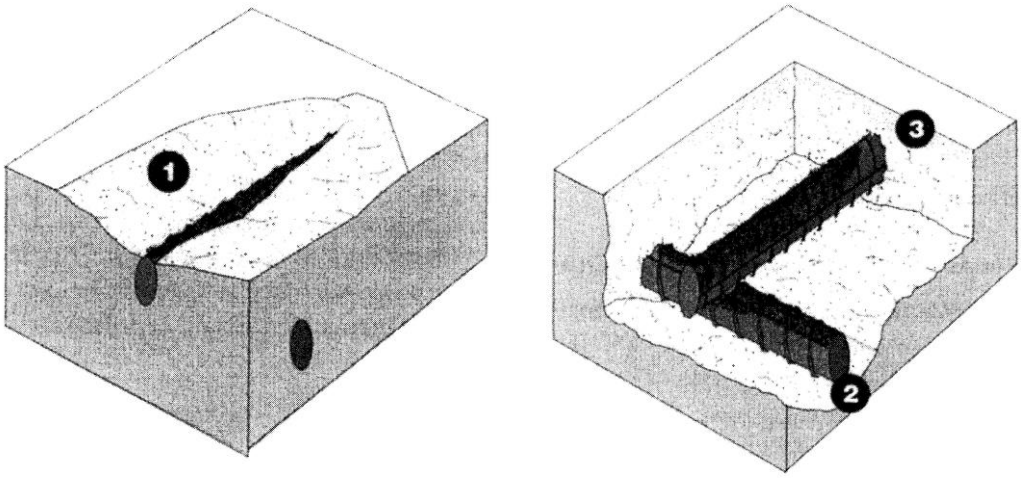

(a) (b)

Figure 2-6 Concrete removal around the rebar: (a) before removal, (b) after removal (Nemati 2006)

The next stage is to remove the concrete around any exposed corroded rebars. This stage will provide clearance under the corroded bars for cleaning and full and perfect circumference bonding to surrounding concrete and will secure the repair structurally as shown in Figure 2-6 (Nemati 2006). After concrete removal and preparation of the reinforcing steel are completed, primary cleaning must be performed using shot blasting, sandblasting, or water blasting removes any weakened surfaces resulting from the initial concrete removal. Bonding between the new repair material and the parent concrete depends upon the repairing material interlocking and reacting with the surface of the prepared concrete. The bonding agent is significant to ensure intimate contact with prepared surfaces; however, if a self-bonding repairing material is used, it should have sufficient binder (e.g., epoxy resin, cement paste) for substrate wetting (Nemati 2006).

Nemati (2006) compared the repair methods such as shotcrete, form and pour, and trowel applied material based on the depth and location of the repair area. The first method is Form and Cast-in-Place by placing the repairing materials into a formwork surrounded all exposed sides as shown in Figure 2-7 (a). Rodding or conventional vibration is used to consolidate the repairing material which is poured into the formwork. This method works for columns, walls, and exterior slab edges. The second method is Form

and pump where the repairing material is mixed then pumped to the formwork by concrete lines until the outlet point is filled and pressurized. This method is perfect for Overhead and vertical applications where there is a congestion in reinforcement, ribs, beam bottoms, slab soffits. The third method is Trowel applied which repair material is transported to the prepared substrate using a trowel or any other suitable tool. This method works for thin repairs. The fourth method is the Dry-mix Shotcrete where the dry or slightly damp repairing material is put in the shotcrete machine and mixed with compressed air. Then using a hose, the mixture is transported to the exit nozzle where water and admixtures, if any, are introduced. At the end, the materials are propelled onto the prepared surface with a force of the compressed air. This method is appropriate for large vertical and overhead repairing.

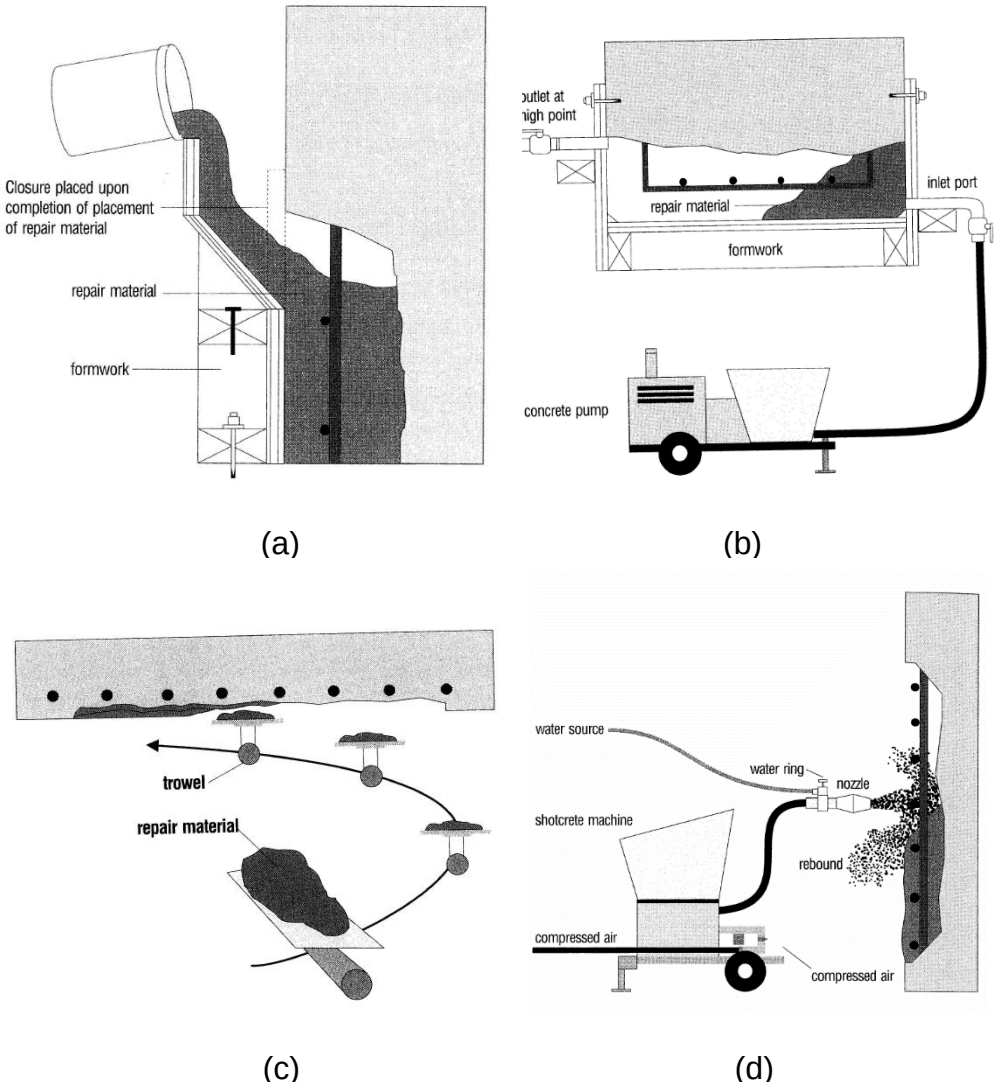

Figure 2-7 Repair methods: (a) Form and Cast-in-Place (b) Form and pump (c) Trowel applied (d) Dry-mix Shotcrete

2.5 CFRP Strengthening

The development of external FRP composite laminate material has recently become a conventional method of rehabilitation. The great success of using FRP in the rehabilitation of concrete members was due to their properties such as resistance to corrosion, lightweight, ease in dealings with, high strength-to-weight ratio, and high tensile strength (Stallings et al. 2000). These materials are generally available in more than one forms such as factory-made laminates, strips, rods and dry fiber sheets that can be wrapped to conform with the shape of a structural element before adding the polymer resin (ACI 440.2R, 2017). FRP is comprised of fibers embedded in a polymeric resin matrix that serves as a protective binder to the reinforcing fibers and bonding agent to the substrate (Pino et al. 2017). The advantages of the FRP application include increasing shear and flexural capacities, enhanced durability and serviceability, enhanced the overall structural performance, and effective stress redistribution of existing reinforcement (Kim 2008). FRP composites have high tensile strength in the fiber direction and relatively low strength in the fiber transverse direction, which demonstrates an orthotropic behavior of the system (Pino et al. 2017).

TxDOT started using FRP in 1999 and has rehabilitated many concrete bridges, resulting in considerable time and money savings (Yang et al.

2011). TxDOT used FRP materials to solve many issues such as; damage of the reinforced concrete structures due to the corrosion of reinforcement steel, girders damaged due to vehicle impacts on the bridges, concrete bridges with no visual signs of distress but are load-posted or otherwise deficient in load rating, and inadequate shear reinforcements in girders and bent caps by current standards or that show service cracking (Bradberry and Wallace 2003).

The first impact damaged beam in Texas repaired using CFRP is shown in Figure 2-8(a) (Bradberry and Wallace 2003). An exterior prestressed beam was hit by an overheight truck, damaging the bottom flange and severely cracking the entire web. TxDOT engineers decided to wrap the repair area with CFRP, which could add tensile strength, shear strength, and robustness to the repair. The repair option was selected after a comparison between replacement and repair. One ply of a continuous CFRP “U” wrap, covering the entire bottom flange and the web between the two diaphragms, was then installed using wet lay-up techniques as shown in Figure 2-8(b). The bridge was repaired in 5 days with a total direct cost of $47,000. The installed CFRP was inspected five years later with no sign of delamination

or other deterioration of the CFRP composite (Figure 2c) (Bradberry and Wallace 2003).

(a) (b)

(c)

Figure 2-8 Figure 2 8 First impact damaged beam repair with CFRP: (a) The impact damaged beam (b) CFRP u-wrap was applied (c) The repaired beam after five years (Bradberry and Wallace 2003)

2.6 Numerical Modeling

Finite Element Models (FEM) can be verified and adjusted by diagnostic tests (Beal 1998). Under the diagnostic type test, the selected load is placed at designated locations on the bridge, and the effects of this load on individual members of the bridge are measured by the instrumentation attached to these members (Lichtenstein 1995). Strain sensors locations should be selected so that the analytical model can be validated (AASHTO 2011). The theoretical model of the bridge capacity requires information about the effect of deterioration, load distribution, support behavior, and material properties (Nowak and Saraf 1996).

FEM used in conjunction with load testing has been proven to be efficient in load rating and structural evaluation of bridge structure. As a result of a successful bridge load test, the engineer achieves greater confidence in the analytical model used to predict the live load effects on the bridge. Chajes et al. (1997) created a FEM of the structure's main span with thin plate elements superimposed on a two-dimensional grid made up of line elements as shown in Figure 2-9. The FEM was found to be in good agreement with field tests.

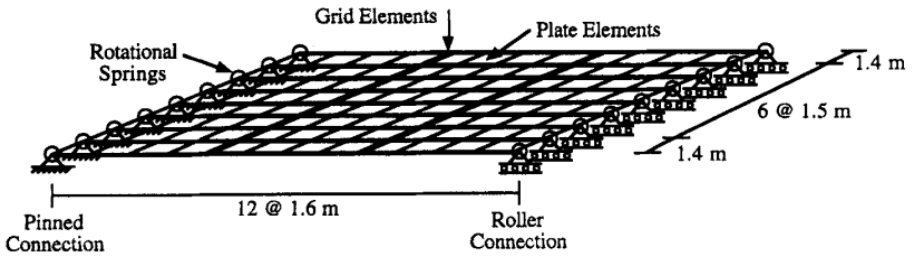

Figure 2-9 Finite element mesh of middle span (Chajes et al. 1996)

A calibrated FEM can be a powerful tool to understand and analyze the overall bridge behavior. Typically, based on analytical calculations and experimental responses, FE model is adjusted by providing an objective way of quantifying the differences in the experimental and analytical responses. The calibration process can be well suited for computerized automation by reduced it to a general optimization problem (Wang et al. 2007).

2.7 Non-destructive Load Test

Experimental load testing of bridges has been a reliable method used for load rating and evaluation of bridges. The manual of the American Association of State Highway and Transportation Officials (AASHTO) for Bridge Evaluation (2011) defines the load testing as the measurement and observation of the bridge response subjected to predetermined loadings

without causing changes in the elastic response of the structure. Two types of load tests are presented for bridge evaluation; diagnostic tests and proof tests. Chajes et al. (1997) define the diagnostic load test as the measurement of a bridge response by placing a predetermined load at different locations along the tested bridge. The loading is typically near the bridge's rated capacity. A numerical model of the bridge is developed based on the measured response, which can estimate the maximum allowable load. Diagnostic load testing improves the understanding of the behavior of bridges to reduce uncertainties related to boundary conditions, material properties, cross-section contributions, the effectiveness of repair, and the influence of damage and deterioration (AASHTO 2011). In a proof test, the loads are applied incrementally to the bridge until either a wanted load is reached, or a predetermined limited state is exceeded. The flexural capacity of the bridge can be determined based on the maximum load reached. However, diagnostic tests are usefull for estimating the bridge's capacity with such a short testing time, a lower cost, and less disruption to traffic (Chajes et al. 1997).

In general, the load carrying capacity predicted from analytical methods is often lesser than the actual capacity of a bridge conducted through field testing due to conservative assumptions have been in the design phase (Ren et al. 2007). Therefore, bridge load carrying capacity

conducted through live load testing provides a more accurate than the analytical one. Instruments such as strain gages and displacement transducers and had been used successfully to measure the absolute movement and strain of structural members (Collins 2010).

Hag-Elsafi et al. (2000) performed load tests to evaluate FRP composite laminates that used in strengthening an old age reinforced concrete T-beam bridge in Rensselaer County, New York. The bridge is supported by 26 beams spaced at 1.37 m center to center. The bridge experienced a leakage at the end joints led to concrete delamination and freeze-thaw cracking and at different locations. Bridge load testing before and after FRP rehabilitation was performed to evaluate the effectiveness of the strengthening system and explore its effect of structural behavior. Nine beams of the bridge were instrumented.

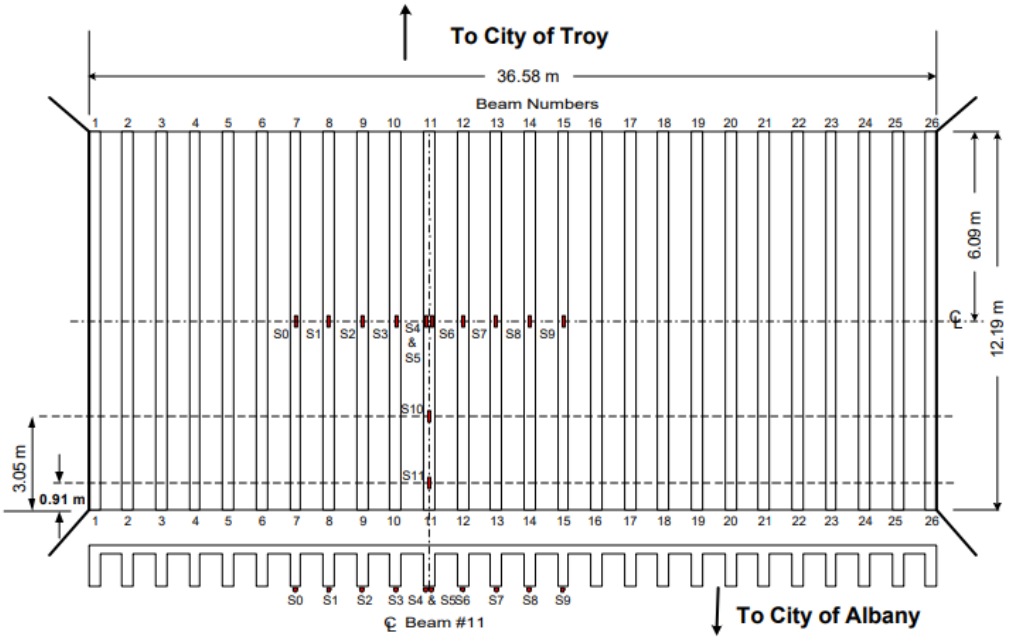

Figure 2-10 Instrumentation of the bridge (Hag-Elsafi et al. 2000)

The design of the FRP for flexural and shear was based on the assumption that the loss in reinforcing steel rebar area due to corrosion is 15%. Using strain data, the researchers were able to compare “before” and “after” live load distribution factors. They concluded that the system of laminate slightly reduced the stresses in main steel rebar and reasonably improved the distribution of transverse live load to the bridge beams, under service loads. Also concluded that the total cost of repairing was around $300,000 whereas the replacement of the structure required $1.2 million.

Stallings et al. (2000) performed load testing of bridge girders before and after strengthening with FRP plates. The bridge was built in 1952, located on Alabama Highway 110, and consists of seven simple spans. The bridge was originally designed for H15-44 design loading, which corresponds to an applied live load bending moment for the girders equal to 63% of the *HS20-44* and the results were a reduction in the reinforcing bar stresses and vertical mid-span deflections of the girders. The girders exhibited flexural cracks and minor spalling. FRP plates repair are applied on one span of the bridge. A CFRP plate was applied to each girder at their bottom surfaces, and a GFRP plate was applied to each side of the four girders, as shown in Figure 2-11.

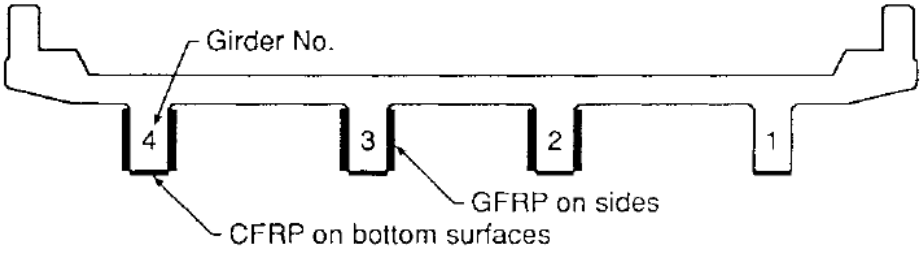

Figure 2-11 Locations of GFRP and CFRP plates (Stallings 2000)

Two trucks used in the load test which had a three-axle configuration with a gross vehicle weight of 346 kN distributed. Static and dynamic tests

were performed on the bridge with different load positions as shown in Figure 2-12. Spacings between the trucks were chosen to produce the most extreme load conditions possible.

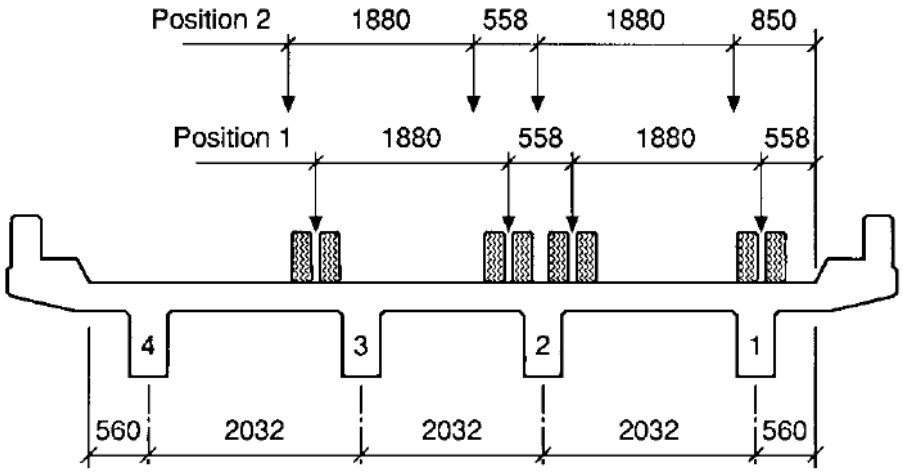

Figure 2-12 Load positions (Stallings 2000)

A decrease in steel reinforcing bar stresses and vertical mid-span deflections was observed in the repaired bridge. The Reductions of reinforcing bar stresses ranged from 4% to 9% for the dynamic tests and from 4% to 12% for the static tests. The reductions in the Girder deflection ranged from 7% to 12% for the dynamic tests and from 2% to 12% for the static tests. These reductions prove that the FRP plates were behaving as an effective component of the girder cross sections.

Pantelides et al. (1999) performed load tests on a bridge cap beam column-joint before and after CFRP strengthening to verify the

effectiveness of the rehabilitation. The bridge was built in 1962, and exhibited severe corrosion of the shear reinforcement and bottom flexural reinforcement in the cap beam. The bridge cap beam column-joint was strengthened using CFRP to restore structural integrity and improve resistance to seismic loading. The load tests results showed that using CFRP composite was effective in strengthening the cap beam-column joints with increasing in shear stresses of 35%, while the maximum lateral load capacity was increased by 16%. The displacement ductility was improved from 2.8 for the as-built bent to 6.3 for the retrofitted bent.

Hag-Elsafe et al. (2002) conducted a diagonstic load testing to evaluate FRP plates strengthened bridge bent cap located in Chemung County, New York. The bridge was built in 1954 and carries around 2000 vehicles a day. The superstructure dead load increased because of adding a concrete wearing surface and a median barrier. Therefore, the bridge bent cap experienced flexural and shear cracking. Bonded FRP composite plates were considered for strengthening the bridge bent cap. Diagnostic load tests were performed before and after rehabilitation, to study effectiveness of the FRP system. Based on the test results, the system moderately reduced live load stresses in the steel reinforcement bars in the negative and positive moment regions by about 10 and 6 percent, respectively. However, this is a very small difference which is also

supported by the fact that the bent cap stiffness did not exhibit a significant change after installation of the plates. This study investigates the performance of bridge bent cap structure that experienced significant deterioration. This study aims to improve the public safety by ensuring the bridge bent cap structures are strong and safe in carrying the anticipated traffic loading by improving efficient bent cap repair and guidelines for CFRP application. Due to lack of research regarding bridge substructures repairing and strengthening, the performance of the bent caps strengthened with CFRP composite is evaluated by analytical models and experimental tests. A significant improvement in bridge structures is expected through the developed knowledge, guidelines, analytical and test methods for the bridge substructures.

Chapter 3
CONCRETE REPAIR AND CFRP STRENGTHENING

3.1 Bridge Description

The west bound of US 80 over East Fork Trinity River Bridge located in Dallas, Texas was selected for this study as shown in Figure 3-1. The average daily traffic on this bridge is around 29,000 vehicles (NBI 2016). The WB bridge is part of a four-lane highway system providing two lanes of vehicles in the east and west direction as shown in Figure 3-2. The WB bridge is simple girder spans, cast in place reinforced concrete with 52 spans spaced at 25 ft. The bridge has an eight-inch composite deck. The bridge is not skewed and has a 41.75 ft. clear roadway width with two 12 ft. traffic lanes. It has 6.5 ft. and 11 ft. Shoulders on the south and north side, respectively.

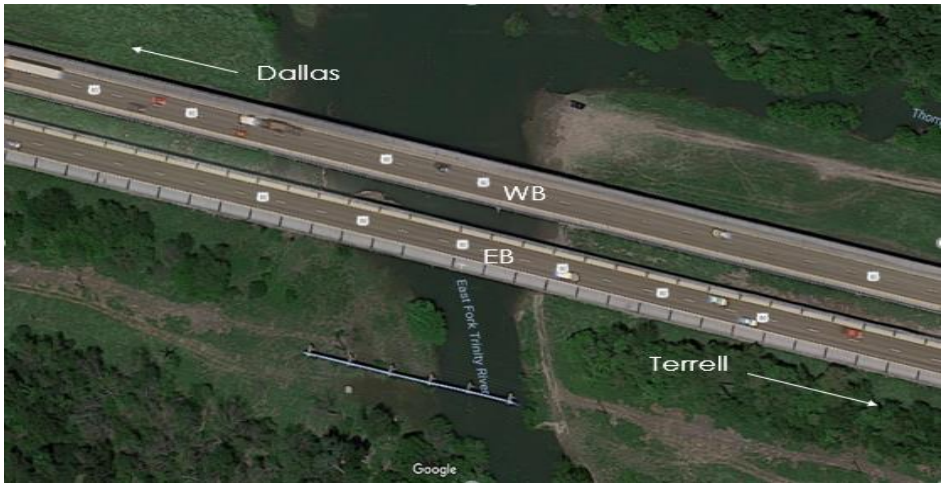

Figure 3-1 Top view of US 80 Bridge-Dallas, Texas (Google Maps)

Figure 3-2 Two traffic lanes of the WB bridge (Google Maps)

The bridge was constructed in 1940 and widened in 1970. The bridge cross section originally consisted of six concrete T-beams, while three I-beams were added later for the widened part as shown in Figure 3-3. Concrete compressive strength of 2000 psi and reinforcing steel yield strength of 33000 psi were specified for the bridge at the time of construction. The bridge was originally designed for an AASHTO H-15 design loading, which corresponds to an applied live load truck of 30 kips.

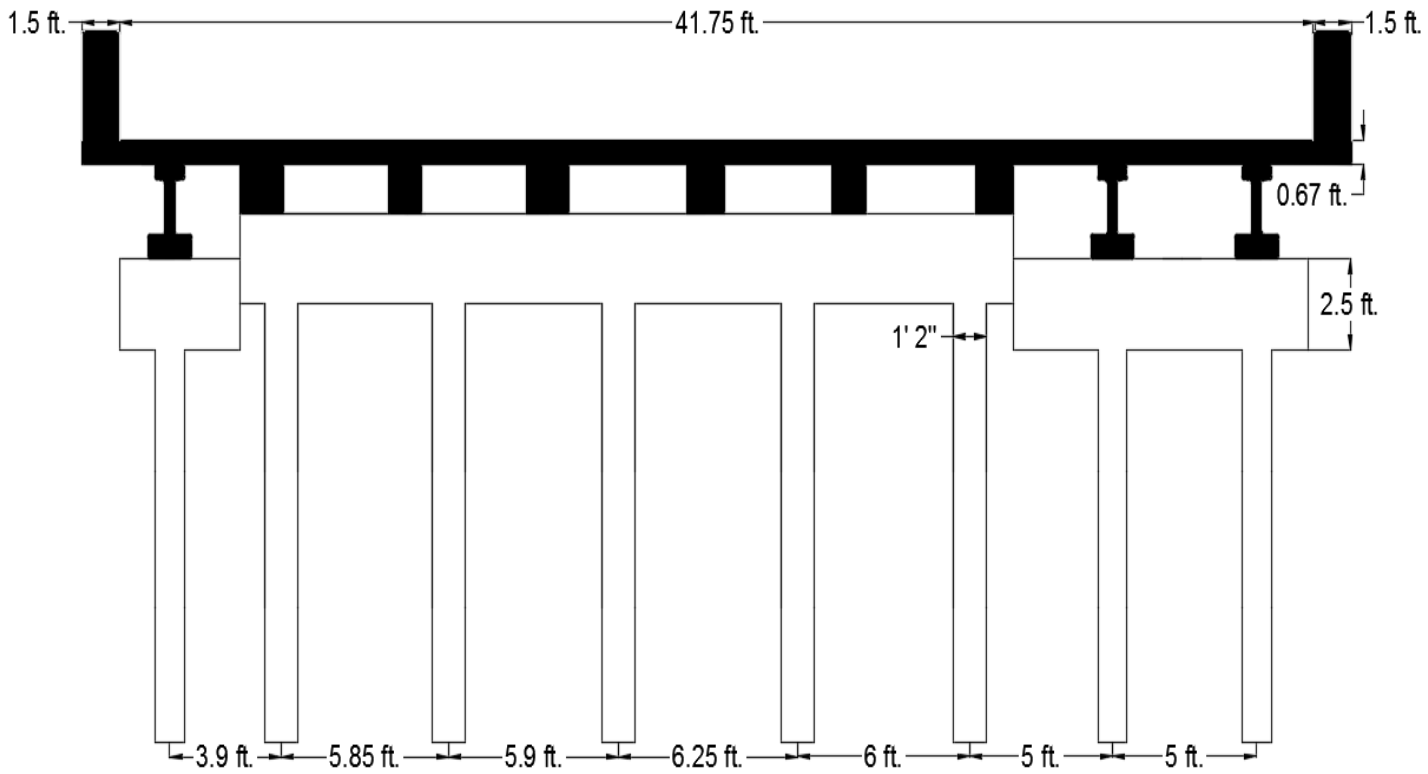

3-3 Cross-section view of the WB bridge

3.2 Visual Inspection

Bridge inspection is usually performed every two years to determine the physical and functional condition for most normal bridges (TxDOT 2018). The most recent official inspection report of the WB bridge was performed in March 2016. The deck and superstructure conditions were classified as fair condition, while the substructure as poor condition. A visual inspection of the bridge bent caps was carried out as part of this study in October 2016. The bridge bent caps exhibited a significant amount of concrete spalling as shown in Figure 3-4. Flexural and shear reinforcements exposed in some spalled areas and experienced excessive corrosion. A green residue resulted from water drainage was seen on the concrete spalling areas which caused some steel corrosion. The concrete spalling extended from the bottom up to the side of the bent caps. Eight bent caps were selected for repair and rehabilitation, three of them were selected for load testing.

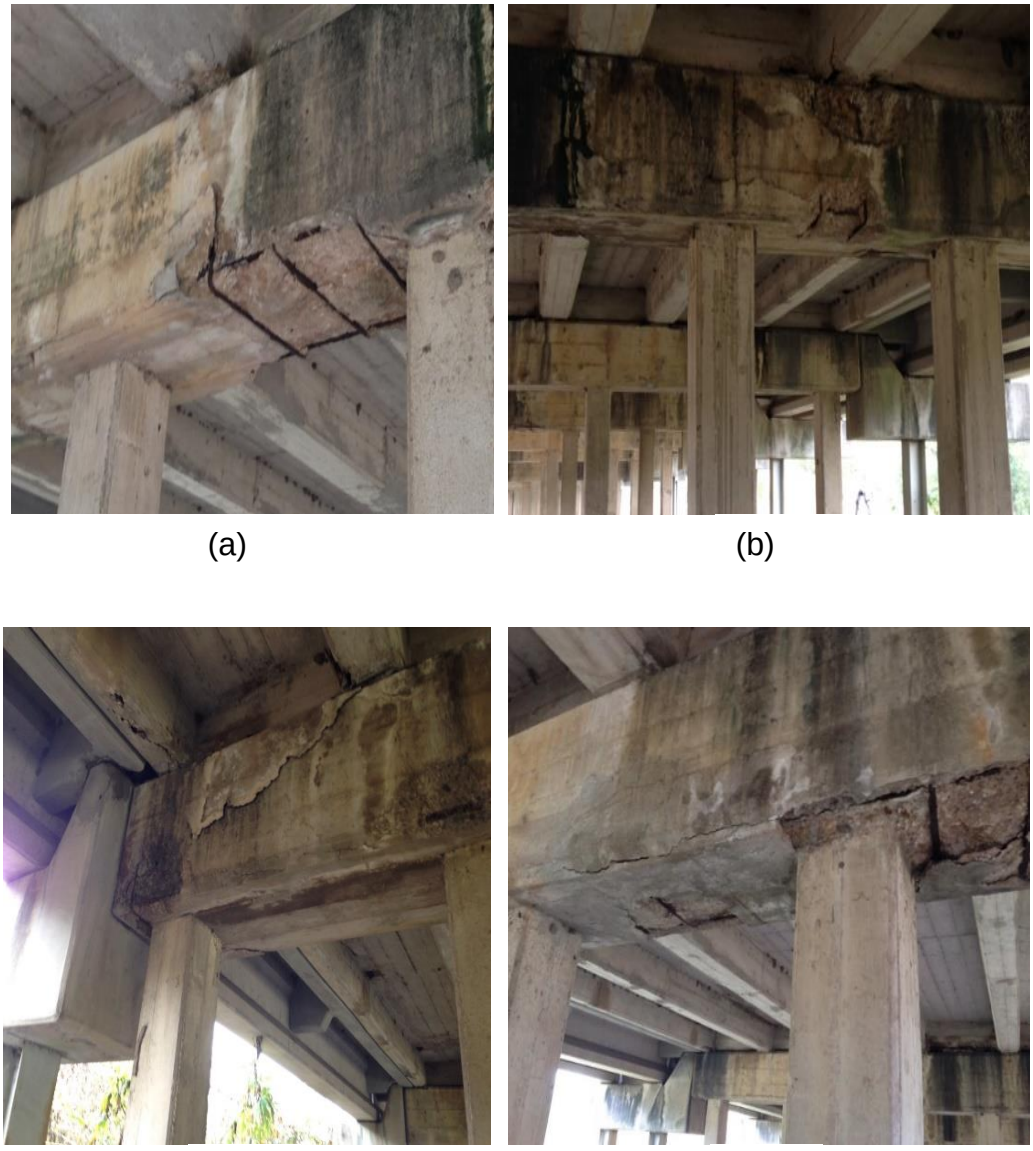

(a) (b)

(c) (d)

Figure 3-4 Deterioration of the bridge bent caps: (a) Bent Cap 35, (b) Bent Cap 37, (c) Bent Cap 40, (d) Bent Cap 41

3.3 Concrete Surface Preparation

The first step in the CFRP repair procedures is to prepare the concrete surface. Eight bent caps 42 through 35 were selected for repair as shown in Figure 3-5. According to TxDOT repair manual, spalls can be categorized as minor, intermediate, or major based on severity (TxDOT 2017). The bridge bent caps spalls were specified as Intermediate spalls due to spalls depth was more than 1 in. in some areas and extensive steel exposure and corrosion. An estimation of the amount of the concrete spalling for the eight selected bent caps was provided by TxDOT based on visual inspection, as shown in Table 3-1.

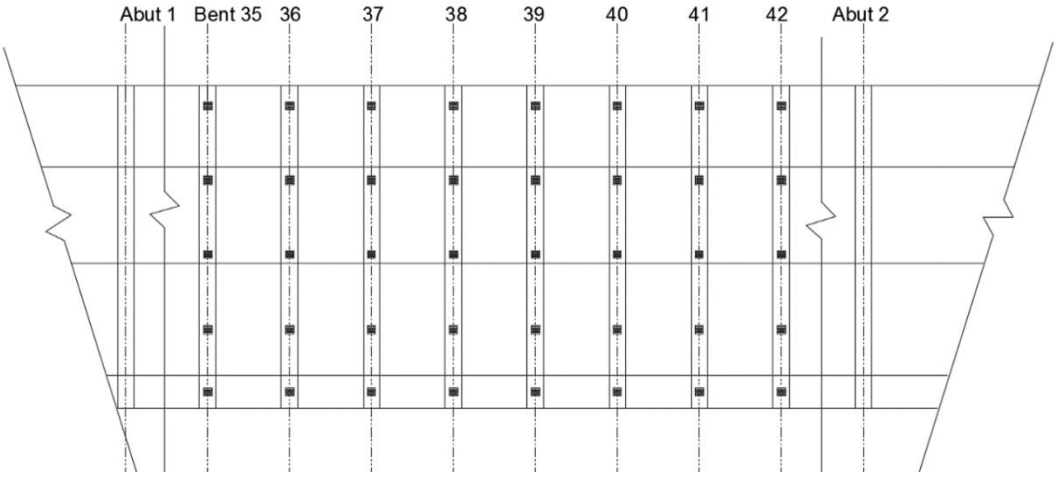

Figure 3-5 Plan view of the eight selected bent caps

Table 3-1 Estimation of the concrete spalling quantities of the eight selected bent caps

Bent Cap	West face (ft^2)	East face (ft^2)	Down face (ft^2)	Top face (ft^2)	Total (ft^2)
35	10	16	20	4	50
36	8	8	8	0	24
37	18	8	8	0	34
38	12	10	8	0	30
39	6	8	4	0	18
40	8	12	6	0	26
41	16	4	8	0	28
42	4	12	0	0	16
					226

TxDOT “Concrete Repair Manual” was followed for the repair procedures as shown in Figure 3-6. Damaged or loose concrete was removed using eight-pound power-driven chipping hammers. The concrete around the bars was removed for any mild reinforcement exposed more than half the reinforcement perimeter or exhibited significant corrosion by providing ¾-inch clearance or 1.5 times the largest sized aggregate in the repair material, whichever is greater, between the steel and surrounding concrete to permit adequate flow of the repair material. The patch

perimeters were saw-cut to eliminate feathered edges and to ensure that the repair material will be applied in depths no less than half an inch. A handheld grinder was used to square the patch perimeters. The substrate was roughened to ensure that there would be a mechanical bond between the patch material and the parent concrete. The repair area was cleaned using a towable washer equipped with 3500 psi pressure pump to remove all dust and dirt.

(a)

(b)

(c)

Figure 3-7 Concrete Surface Preparation: (a) Chipping out loose concrete and saw cut the edges, (b) Removing concrete around the rebars, (c) Cleaning the repair area using high-pressure water pump

3.4 Formwork Installation and Pouring

Appropriate repair materials and methods differ significantly depending on the spall depth, size, and configuration (horizontal, vertical, or overhead) (TxDOT 2017). Formwork method must deliver the selected repair material to the prepared substrate with accurate results. The properties of repair materials generally specified are the compressive strength, bond strength, shear strength, and those properties that influence volume changes, such as drying shrinkage, modulus of elasticity, and coefficient of thermal expansion.

The materials used in bent caps repair were approved by TxDOT "Material Producer List" (MPL) (TxDOT 2016). Formwork was used for overhead spalls at the bottom face with depth larger or equal to one inch. Form and pour pre-extended SikaCrete 211 SCC Plus mortar with a compressive strength of 6500 psi was used. The mortar specifications recommended using a bonding agent before placing the mortar to achieve a good bond between the new mortar and the repair area. Sika® Armatec® 110 EpoCem was used as a bonding agent and steel corrosion protection. A concrete screw gun was used to place the two sides studs to the columns. The repair procedures were as follows:

1. The steel reinforcement was cleaned using a wire brush to remove all the corrosion rust. (Figure 3-7(a)).

2. The repair area was sprayed with water to achieve the Saturated Surface Dry (SSD) condition. (Figure 3-7 (a)).
3. Two studs were placed on the columns face to hold the bottom formwork. (Figure 3-7 (a)).
4. The bonding agent was applied to the steel and concrete. (Figure 3-7 (b)).
5. The bottom formwork was placed, and then the side plywood was attached. (Figure 3-7 (c)).
6. The mortar was mixed and poured inside the formwork. (Figure 3-7 (c)).
7. The formwork was removed after 36 hr. (Figure 3-7 (d)).
8. The mortar was sprayed by a curing compound. (Figure 3-6 (e)).

(a)

(b)

(c)

(d)

(e)

Figure 3-8 Formwork installation and pouring: (a) Steel cleaning and water spraying, (b) Bonding agent application, (c) Formwork installation and poring, (d) Formwork removal, (e) Curing compound spraying

3.5 Patching

Patching mortar was placed after formwork installation and pouring was performed. Patching mortar was only applied to vertical repair areas. The specified mortar is SikaQuick VOH with a compressive strength of 5500 psi. The repair area was sprayed with water to achieve the SSD condition, then trowel or other suitable placing tools were used to transport the mortar to the prepared substrate as shown in Figure 3-8. The repair material is pressed into the substrate to develop intimate contact without voids.

Figure 3-9 Patching mortar application

3.6 CFRP Preparation and Application

3.6.1 CFRP Preparation

Surface preparation for CFRP application was achieved by sandblasting the repaired areas after 28 days of formwork pouring and patching to ensure that the mortar achieved the desired compressive strength as shown in Figure 3-9. The surface profile of the repaired area was prepared to a minimum Concrete Surface Profile (CSP) 3 as defined by the International Concrete Repair Institute (ICRI 2007). The surface profile is critical in providing a good bond between the CFRP and the concrete surface.

Figure 3-10 Sandblasting the repaired area

3.6.2 CFRP Application

CFRP was applied to the repaired area for the eight selected bent caps. Standard Specifications for Construction and Maintenance of Highways, Streets, and Bridges (TxDOT 2014), was followed for the CFRP application. It requires CFRP should be applied at a temperature between 50°F and 95 °F. Therefore the CFRP was applied at an average ambient temperature of 83°F and in the absence of direct light to prevent any undesirable problems with the epoxy. The CFRP application was started when the temperature was cooling down to prevent the phenomena of outgassing of the concrete which might increase the voids under the CFRP. The CFRP was applied at the bottom face parallel to the bent cap span for strengthening in flexural, while perpendicular to the bent cap span for strengthening in shear. Two types of epoxy were used to attach the CFRP to the bent caps; type I Sikadur 300 and type II Sikadur 330 with tensile strength 55 MPa and 24.8 MPa, respectively. The CFRP was Sika Wrap Hex 117C with 24 in. Width for flexure and 12 in. for shear. Figure 3-8 shows the CFRP application.

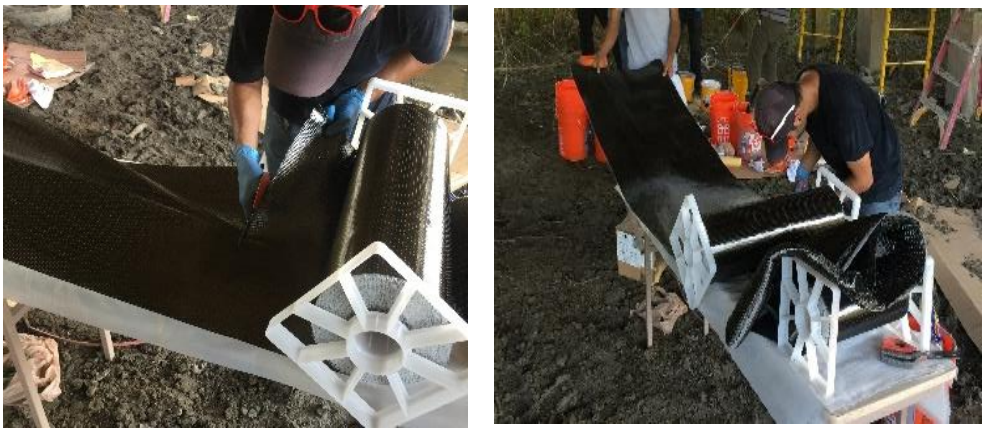

(a)

(b)

(c)

Figure 3-11 CFRP application: (a) Cutting CFRP sheets, (b) Applying CFRP sheets, (c) CFRP sheets after curing

3.6.3 CFRP Protection

A protection top coat was applied on the CFRP for weathering resistance. The white colored Sikagard 670w was used as shown in Figure 3-11.

Figure 3-12 Protection top coat application

3.6.4 Pull off test

The ASTM pull off test was performed on the CFRP as an indication of the strength of the bond in tension. Three direct pull-off tests to verify the bond strength were performed after the FRP had cured and before applying topcoats on the bent caps. The average tensile strength was 400 psi. The failure for one sample was fully in the concrete while the other two were in the bond-line between the CFRP and concrete. (Figure 3-12)

(a)

(b)

(c)

(d)

Figure 3-13 Pull off test (a) Preparing the CFRP surface (b) Dolly placing (c) Pulling out the sample (d) Concrete failure sample

Chapter 4
NON-DESTRUCTIVE LOAD TESTING

4.1 Load Testing Instrumentation before Repair

Instrumentation of the west bound of US 80 over East Fork Trinity River Bridge in Dallas, Texas was carried out in February 2017. A detailed plan was prepared for instrumentation, static and moving load testing. Girders, deck, and foundations were not within the scope of this study, only the substructure behavior was considered. A good instrumentation plan is a key to understanding the overall behavior of the bridge bent caps. A three-dimensional model of the selected bridge was carried out using CSIBridge software as shown in Figure 4-1. The bridge dimensions were found from the original plans while girders locations and dimensions were determined from the bridge site due to lack of some information given in the original hand-written plan. The CSIBridge model was performed to conduct the strain gages location, and critical positions of the trucks live load.

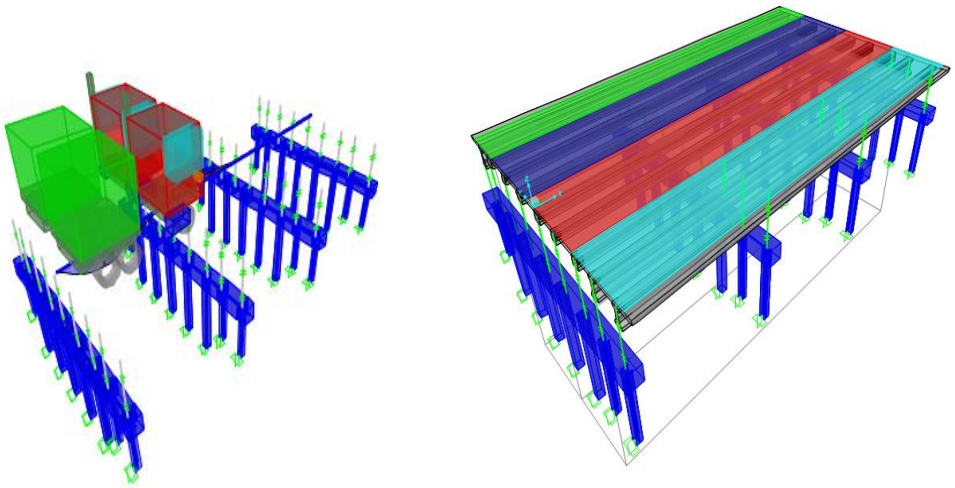

Figure 4-1 3-D model of the selected bridge

A total of 48 strain gages were installed on three different bent caps. Bent caps 37, 36, and 35 were selected for the load testing. Bent caps 37 and 35 represented a severe deterioration while bent cap 36 had a minor deterioration to study the effect of the deterioration on the bent caps. The selected bent caps were instrumented with concrete and shear strain gages. Bent caps 37 and 36 were fully instrumented, while bent cap 35 was partially instrumented due to limited channels in the data acquisition systems.

Strain gages were placed on the top and bottom of the same section of the bent cap to find the location of the neutral axis. Strain gages were attached along the column centerline to detect the negative moment in the represented bent caps. Strain gages were attached to the bent caps bottom face along the girder centerline to determine the applied positive moment. For shear investigation, strain gages were attached along the columns face

in two different locations for two bent caps. The layout of strain gages locations of different sections of the bent caps can be seen in Figure 4-2 and 4-3. The data acquisition systems were placed between bent cap 37 and 36 as shown in Figure 4-4. All strain gauge wires were extended to reach the data acquisition boxes. A Tokyo Sokki DS750 with capacity of 40 channels and a Micro measurement 8000 model DAQs with a capacity of 32 channels were used to collect the data at 100 Hz.

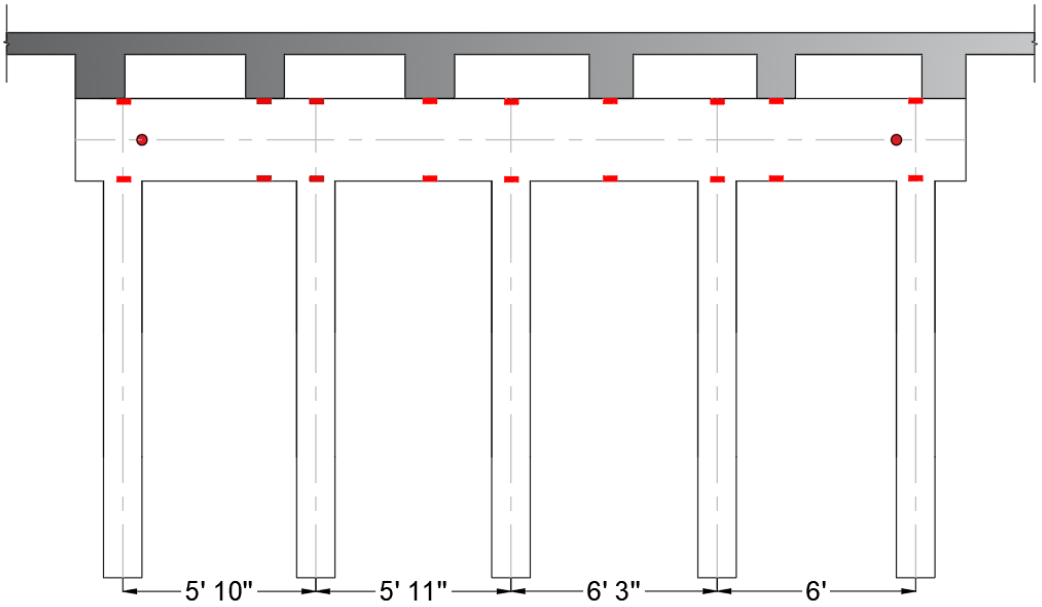

Figure 4-2 Instrumentation plan for bent caps 37 and 36

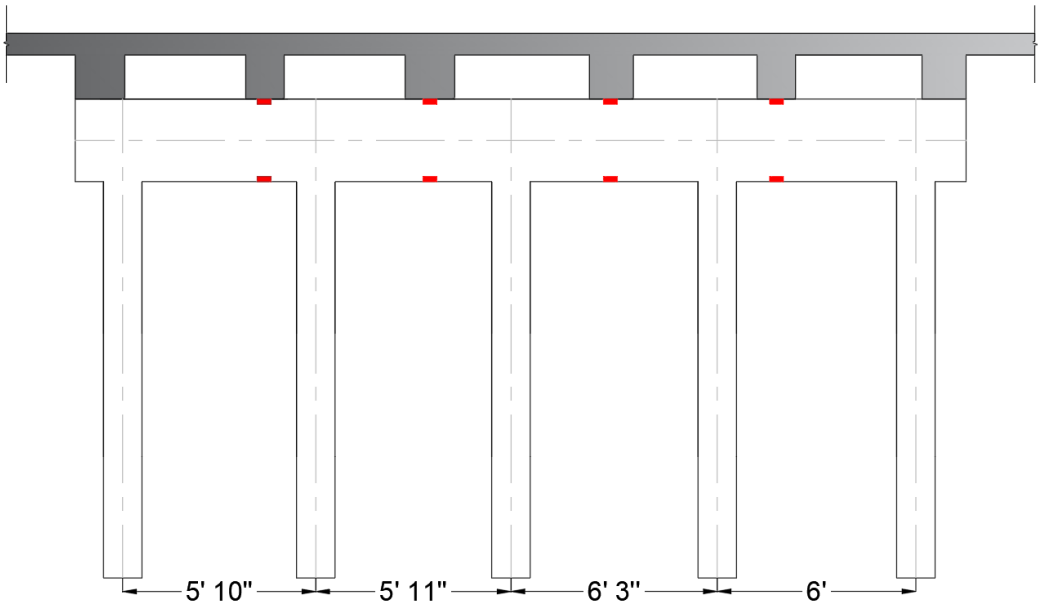

Figure 4-3 Instrumentation plan for bent cap 35

Figure 4-4 Data acquisition system location

The concrete and shear strain gages attached on the concrete surface require a detailed process which had to be followed to assure all the gages were properly working. The installation of strain gages in the concrete surface involved the following steps:

- Strain gages locations were marked on the concrete surface. (Figure 4-5(a))
- Concrete surface was smoothened and grinded by sander or grinder to achieve a uniform and even surface. (Figure 4-5(b))
- Concrete surface was cleaned with acetone to remove dirt, dust, and other particles. (Figure 4-5(c))
- Cleaning the area with water to remove the acetone from the surface. (Figure 4-5(d))
- A fast setting epoxy was applied on the area to fill the voids in the concrete and provide a smooth and even surface. (Figure 4-5(e))
- Strain gage was applied after the epoxy dried using special adhesive designed for bonding strain gages to concrete (Figure 4-5(f))
- Weather proof chemical called ‘Epoweld’ was applied as a coating on top of the strain gages to protect them from rain, dust, moisture, and other weather effects.

Bent caps 37 and 36 after strain gages installation are shown in Figures 4-5(g) and 4-5(h).

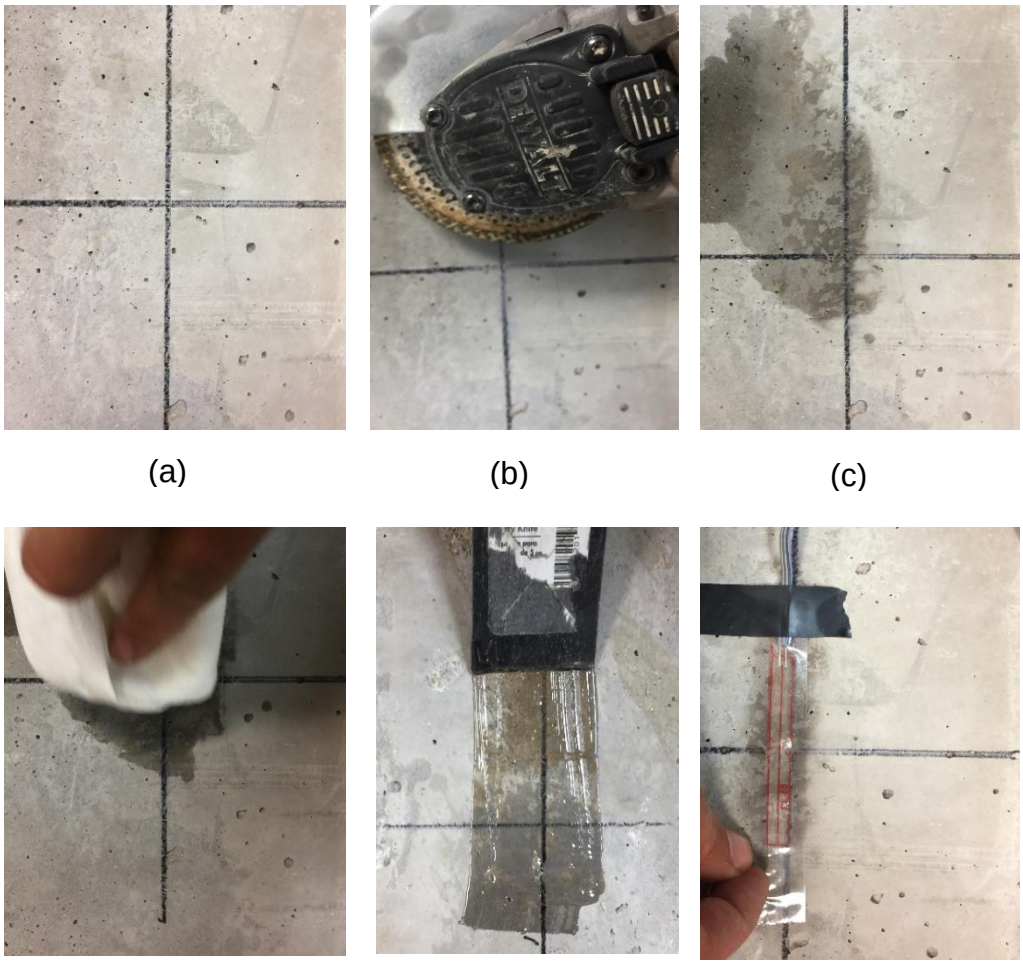

Figure 4-5 Strain gages installation: (a) Marking, (b) Grinding, (c) Appling acetone, (d) Applying water, (e) Applying epoxy, (f) Installing strain gage, (g) Bent cap 37, (h) Bent cap 36

4.2 Load Testing Procedures

Load testing before repair of the west bound US 80 Bridge was carried out in March 2017. The load testing required a complete closure of traffic to avoid any participation of other vehicles in the data collection. The bridge load testing was carried out during the night time due to high traffic volume during normal business hours. The testing procedures were explained to TxDOT personnel in advance to achieve safe traffic control. The load testing was carried out in four intervals to avoid traffic closure for more than 15 minutes. Vehicles could pass on the bridge between the different tests.

Various configurations of a single lane or multiple lanes were considered to perform an analysis for the bent caps. An important consideration in the design of bent caps is to determine the maximum or critical force effects by positioning live load lanes. Whether the truck is at the mid-span of a bridge or at the support, it influences the values of the moment and shear on the bent cap (Caltrans 2015). One truck should be placed in each lane. Transversely, if the bridge can fit four lanes, then up to four trucks can be placed on the bridge, one in each lane within a distance of 12 ft. (AASHTO LRFD 2014).

4.2.1 Marking on the Roadway

Marking on top of the bridge was performed one hour before the load testing started. The marking was made perpendicular to the traffic direction along the centerline of bent caps 38, 37, 36, 35, and 34. Bent cap 38 centerline was the starting point of the dump trucks paths while bent cap 34 was the end. Another marking was made parallel to traffic direction, two feet from the lane line to keep the position of the trucks fixed for all the loads configuration. The marking was made using duct tape and chalk as shown in Figure 4-6.

Figure 4-6 Marking the roadway

4.2.2 Truck Live Load

Two pre-weighed dump trucks were selected for the load testing. Weights of the dump trucks are shown in Table 4-1. The dimensions of the trucks are as shown in Figure 4-7.

Table 4-1 Axle weights for the dump trucks

	Axle 1 weight (lb.)	Axle 2 weight (lb.)	Axle 3 weight (lb.)	Total weight (lb.)
First Truck	11,100	20,000	19,600	50,700
Second Truck	11,300	19,400	19,000	49,700

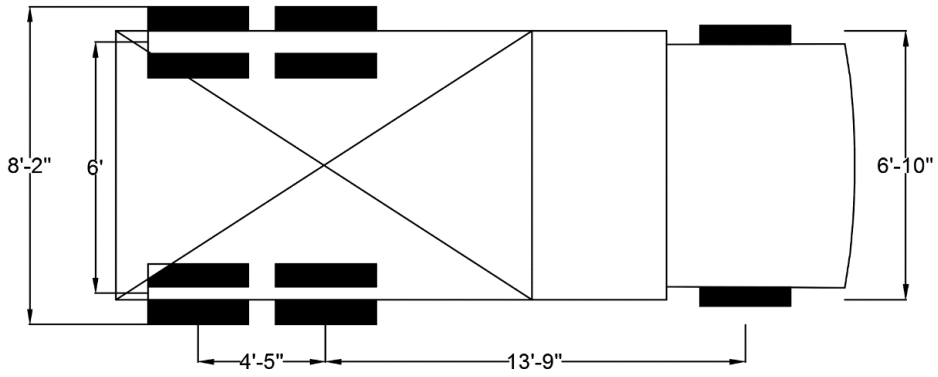

4-7 Dimensions of the dump trucks

4.2.3 Diagnostic Load Tests

Two types of diagnostic load tests were performed in this study. The first test called “crawl speed test” where trucks were moved at a speed of around five mph on the two marked paths. The speed of the truck was kept low so that no vibrations were produced. This helped to avoid any dynamic effects on the bridge. The second test is the “static test” where the trucks were stopped at critical locations on the bridge. Maximum positive moment can be reached when the middle axle of the truck is placed over the bent cap. Maximum negative moment can be reached when the trucks is placed in the middle of the bridge span between the bent caps.

4.2.3.1 Static Load Test

This method includes critical stop locations for the trucks to produce the maximum influence on the bridge. Placing the middle axle over the support would produce maximum reaction at interior bents when the long span is less than twice as long as short span (TxDOT 2015). The two dump trucks were placed over the support for the three selected bent caps as shown in Figures 4-8 through 4-11. Maximum positive moment can be reached at this critical location.

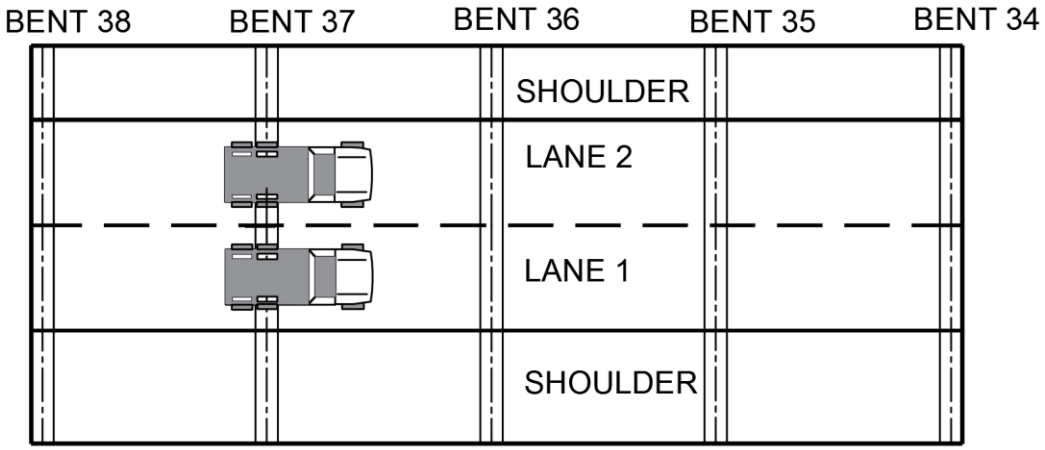

Figure 4-8 Stop location at bent cap 37

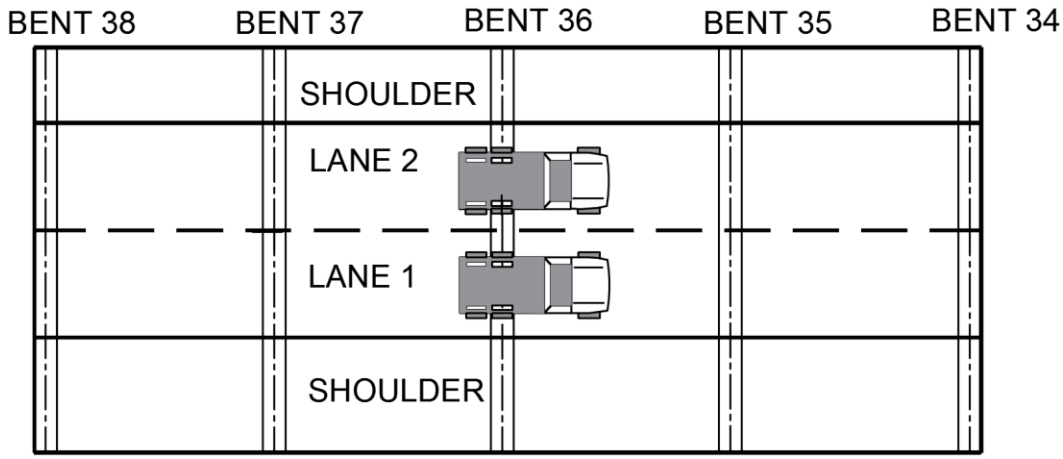

Figure 4-9 Stop location at bent cap 36

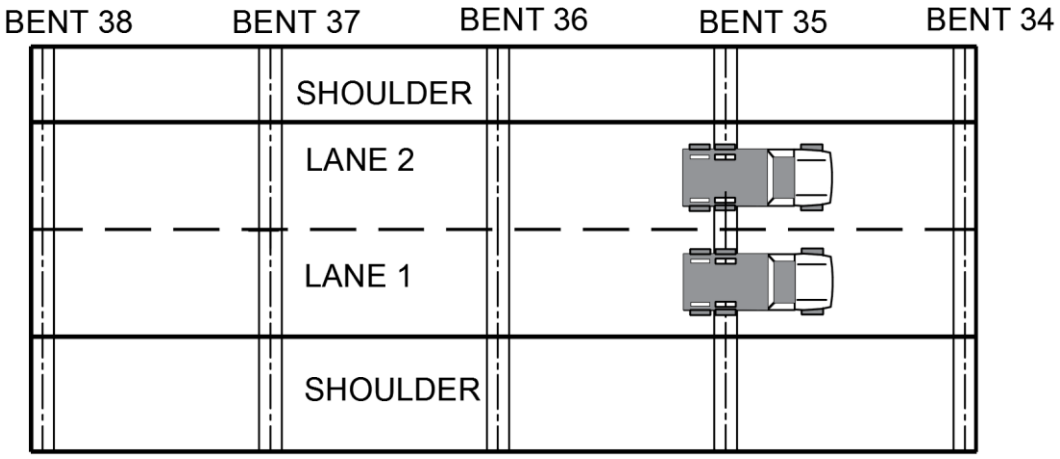

Figure 4-10 Stop location at bent cap 35

Figure 4-11 Trucks stopped at Bent cap 37

4.2.3.1 Crawl Speed Test

This method is used to consider the effect of moving loads on the overall response of the bridge bent caps. The dump trucks started moving from bent cap 38 at an approximate speed of 5 mph. The strain readings for the crawl speed runs were collected through the data acquisition system. Both lanes of the bridge were loaded separately and simultaneously as shown in Figures 4-12 through 4-14.

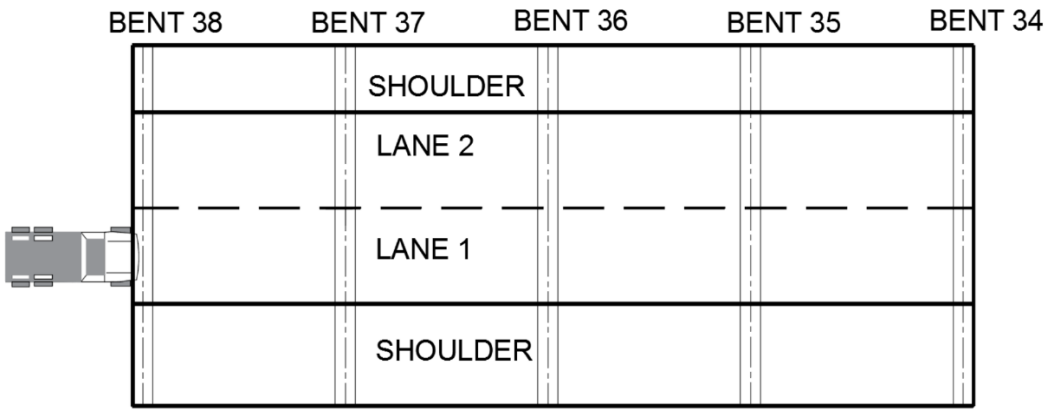

Figure 4-12 Loading Path One

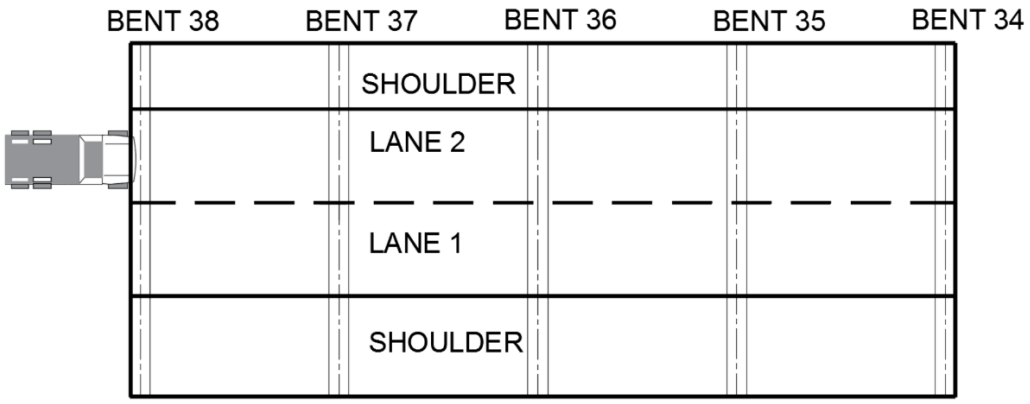

Figure 4-13 Loading Path Two

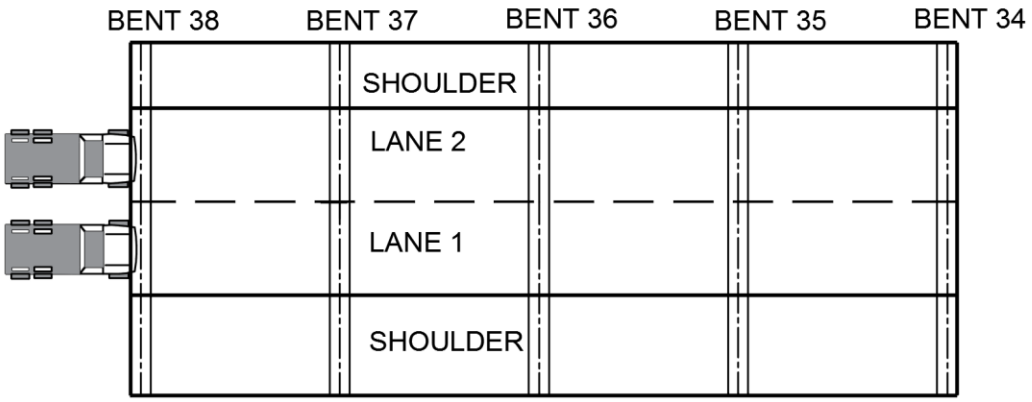

Figure 4-14 Loading Path One & Two

4.3 Load Testing after Repair

Instrumentation for load testing after repair and strengthening with CFRP was carried out in August 2017. The detailed plan discussed earlier was repeated for the after repair testing. However, some concrete strain gages were replaced by CFRP strain gages in the areas strengthened with CFRP. A total of 38 concrete and CFRP strain gages were installed in the three selected bent caps. The layout of strain gage locations in different sections in the bent caps can be seen in Figures 4-15 through 4-17. Concrete strain gages are marked by letter ‘’C’’, CFRP strain gages by letter “F” while shear strain gages by letter ‘’R’’. The load testing was performed same as before repair load testing as shown in Figure 30. The same dump trucks used for the before repair load test was used for the after repair test with a small difference in weight as shown in Table 4-2.

Table 4-2 Axle weights for the dump trucks

	Axle 1 weight (lb.)	Axle 2 weight (lb.)	Axle 3 weight (lb.)	Total weight (lb.)
First Truck	12,700	20,300	19,500	52,500
Second Truck	12,900	21,000	19,700	53,600

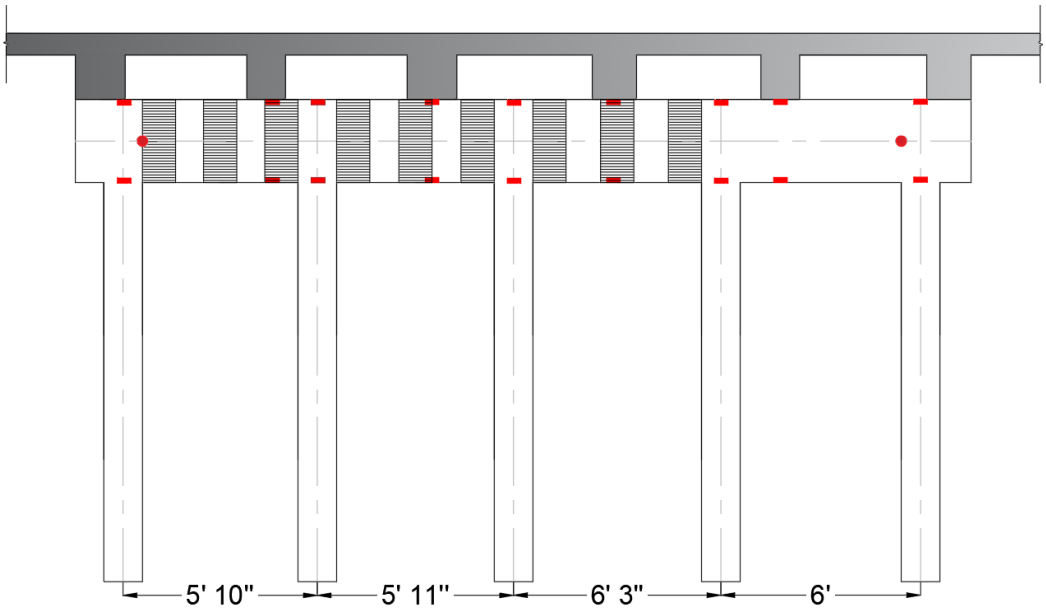

Figure 4-15 Instrumentation plan for bent cap 37

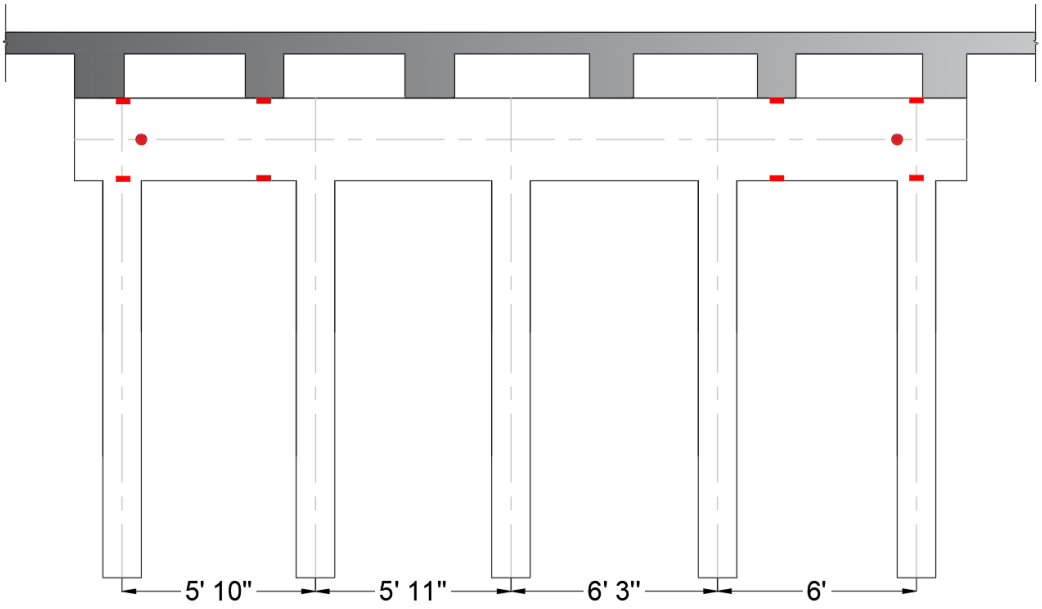

Figure 4-16 Instrumentation plan for bent cap 36

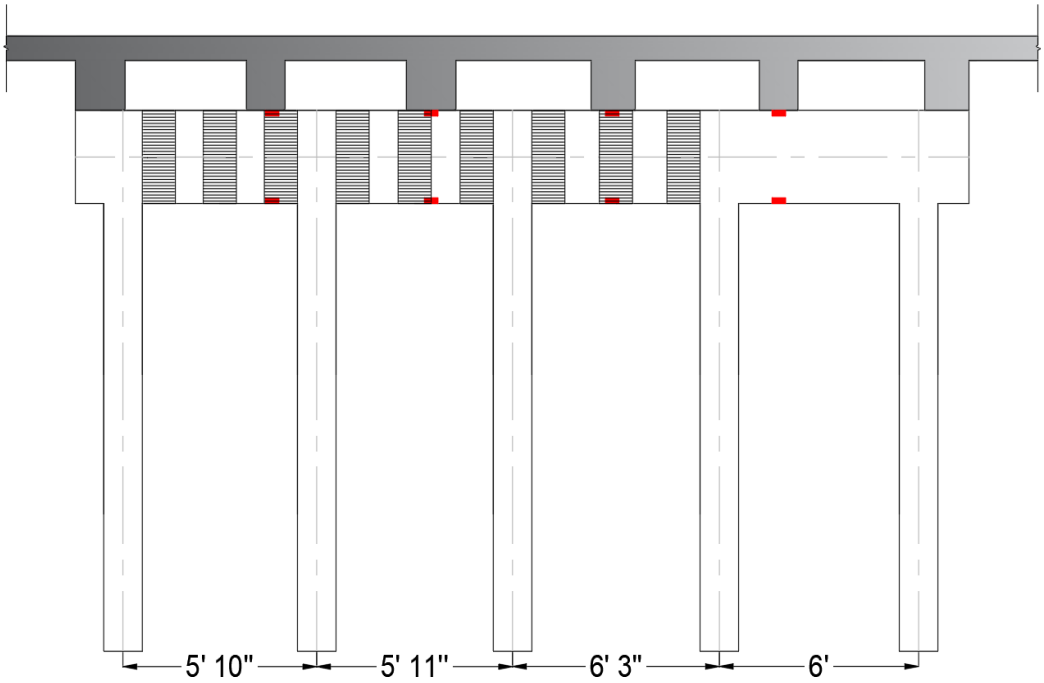

Figure 4-17 Instrumentation plan for bent cap 35

Chapter 5
FINITE ELEMENT MODELING

5.1 Introduction

The Finite Element Model (FEM) for the west bound of US 80 over East Fork Trinity River Bridge was created using a non-linear finite element software ABAQUS. It is provided with a wide selection of modeling capabilities which allow modeling different types of structural members, including FRP (Riad 2017). This study aims to develop a modeling framework to simulate the bridge bent cap retrofitted with FRP. This involves several aspects of theoretical and practical interest. Important issues including material models, element types, mesh, convergence and boundary conditions, are discussed in this chapter.

The FE model aims to calibrate the results obtained from the experimental load testing to investigate the performance of the bridge bent caps. The bent cap was modeled in 3D so that the overall structural response can be evaluated. Two FE models were developed to evaluate the FRP strengthened bridge bent caps. The first model was performed to capture the behavior of the deteriorated bent cap before repair which included concrete and steel sections loss due to spalling and corrosion, respectively. The second model was developed to evaluate the performance of the repair mortar and FRP composites.

5.2 Material Properties

5.2.1 Concrete

Concrete is the most important material available for construction. Concrete consists of aggregate, cement, water, and admixture. Generally, concrete is weak in tension and strong in compression. This is due to the presence of fine cracks in concrete, which have a little effect when concrete is subjected to compression loads since the loads cause the cracks to close and permit compression transfer. However, this is not the case for tensile loads (Mccormac and Brown 2015).

The stress-strain relationship of concrete is linear elastic under compression. However, the behavior becomes nonlinear after the initiation of micro-crack. When the ultimate compressive strength is reached, the stress decreases with increasing strain as shown in Figure 5-10(a) (Saenz 1964). The stress-strain response follows a linear elastic relationship under tension until the value of the failure stress is reached. The failure stress corresponds to the onset of microcracking in the concrete material. The formation of micro-cracks is represented by a softening stress-strain response, Figure 5-10(b). The tensile strength of concrete varies from about 8% to 15% of its compressive strength. Although tensile strength is normally neglected in design calculations, it is nevertheless an important property

that affects the sizes and extent of the cracks that occur (Mccormac and Brown 2015).

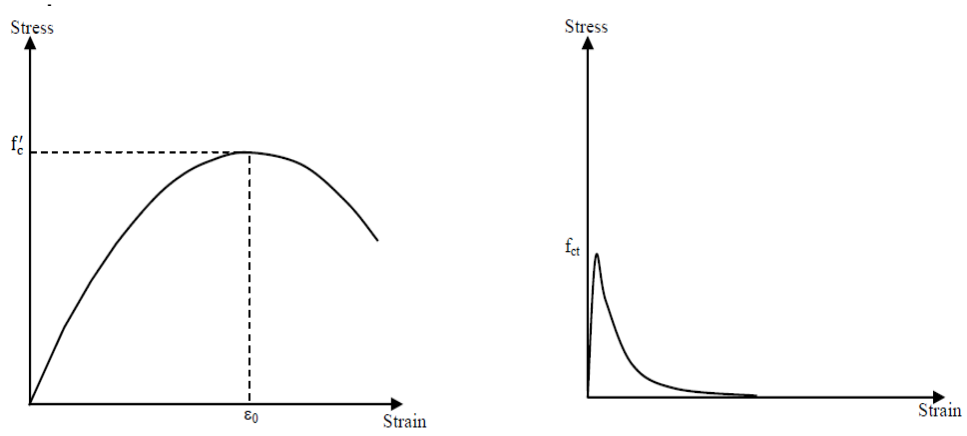

(a) (b)

Figure 5-1 Uni-axial stress-strain curves of concrete (Saenz 1964)

Concrete behavior can be predicted through several constitutive models. One of the models is the discrete crack model in which the cracks are defined along the element boundaries (Wu and Hemdan 2005). Another model is the smeared crack model which the cracks initiate when the principal tensile stress exceeds the tensile strength. The elastic modulus of the material is then assumed to be zero in the direction parallel to the

principal tensile stress direction (Pham et al. 2006). Another model is the plastic damage model which has been used successfully for predicting the response of standard concrete tests in both tension and compression. The concrete plastic-damage model assumes that the two main concrete failure mechanisms are cracking and crushing. Crack propagation is modeled using continuum damage mechanics, stiffness degradation (Obaidat 2011).

In this study, concrete compressive and tensile properties were modeled as concrete damaged plasticity. This model requires the values of elastic modulus, Poisson's ratio, the five plastic damage parameters and description of compressive and tensile behavior. The five plastic damage parameters are the dilation angle, the flow potential eccentricity, the ratio of initial equibiaxial compressive yield stress to initial uniaxial compressive yield stress, the ratio of the second stress invariant on the tensile meridian to that on the compressive meridian and the viscosity parameter that defines viscoplastic regularization. The values of the last four parameters were recommended by the Abaqus documentation for defining concrete material and were set to 0.1, 1.16, 0.66, and 0.0, respectively. The dilation angle and Poisson's ratio were chosen to be 37° and 0.2, respectively (Obaidat 2011).

5.2.2 Steel Reinforcement

Steel is initially linear-elastic for stress less than the initial yield stress. At ultimate tensile strain, tensile strength is reduced as shown in Figure 5-2. The constitutive model used to simulate the steel reinforcement was the classical metal elastic-perfectly plastic model (Obaidat 2011). The input for the steel model includes elastic modulus Poisson's ratio and yield stress. In this study, Poisson's ratio was assumed to be 0.3 while the yield strength was assumed to be 33 ksi.

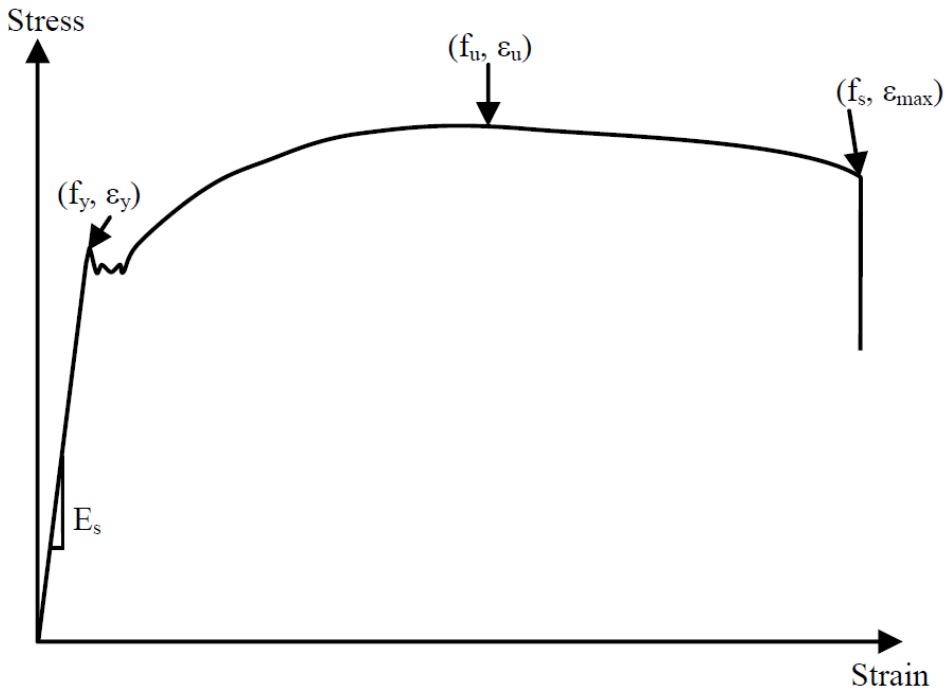

Figure 5-2 Stress-strain curve for typical reinforcing steel bar (Obaidat 2011)

5.2.3 FRP

The fiber behavior is linear elastic up to failure. Figure 5-3 shows the stress-strain relationship for fiber, matrix and the FRP composite (Piggot, 2002). The strain in fiber and matrix is the same before the yielding of the matrix. A knee will appear in the stress-strain curve after the yielding of the matrix since the matrix no longer contributes to the stiffness. The mechanical properties of composites are dependent on the fiber properties, matrix properties, fiber-matrix bond properties, fiber amount and fiber orientation distribution. An isotropic linear elastic model is usually used to model FRP plate behavior if the direction of fibers is parallel to that of the principal stresses (Obaidat 2011). In this study, the material properties of FRP laminates as provided from the manufacture are as shown in Table 5-1.

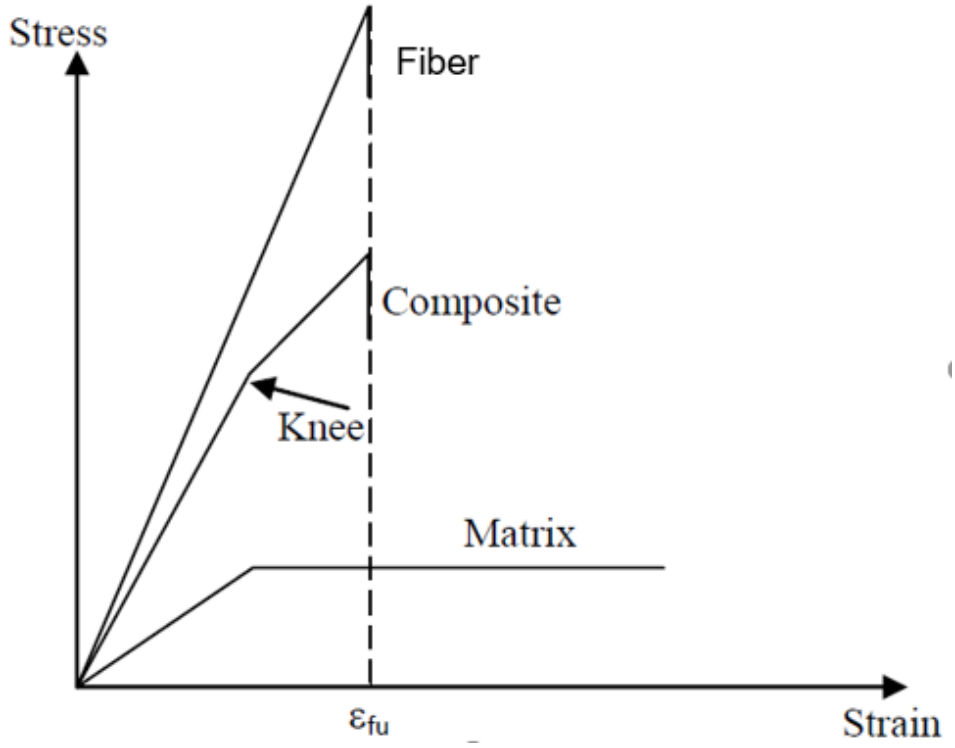

Figure 5-3 Stress-strain curves for typical fiber, resin and FRP composite (Piggot, 2002)

Table 5-1 material properties of FRP laminates

Cured Laminate properties	
Tensile Strength (psi)	105000
Tensile Modulus (psi)	8200000
Thickness (in.)	0.02
Elongation (εu)	0.01

5.2.4 Bond between FRP and Concrete

The modeling of the bond between FRP and concrete is very important since a perfect bond can overestimate the ultimate load and stiffness, compared to experimental results. Therefore, the cohesive model available in Abaqus is a better choice for representing the interface behavior. The cohesive model defines surfaces of separation and describes their interaction by defining a relative displacement at each contact point. The definition of the model is characterized by the parameters, initial stiffness, shear strength, fracture energy and curve shape of the bond slip model. However, Obaidat performed several simulations to find the values of initial stiffness, shear strength and fracture energy that gave the best fit, and the results were compared with experimental results from the literature. The following relations for initial stiffness $K_{0,}$ and shear strength τ_{max}, as a function of the adhesive and concrete properties, were proposed in Equation 5-1 and 5-2 (Obaidat 2011):

$$K_0 = 0.16 \frac{Ga}{ta} + 0.47 \qquad 5\text{-}1$$

$$\tau_{max} = 1.46\ Ga^{0.165}\ f_{ct}^{1.033} \qquad 5\text{-}2$$

where ta is the adhesive thickness in mm, Ga is the adhesive modulus in GPa and fct is the tensile strength of concrete in MPa. In this study, initial stiffness $K_{0,}$ and shear strength $\tau_{max,}$ of 576 Mpa and 1.93 Mpa were determined, respectively.

5.3 Element Types

Three-dimensional models were performed to get an accurate behaviour bridge bent cap. The modeling involved defining the geometry, boundary condition, material properties, loads, analysis methods and contact. The concrete was modeled using C3D8R (solid, eight-node) element. The FRP sheets were modeled using S4R (shell, 4-node) element. The reinforcing rebars were modeled using T2D2 (truss, 2-node) element. Figure 5-4 shows the element families that are used most commonly in Abaqus.

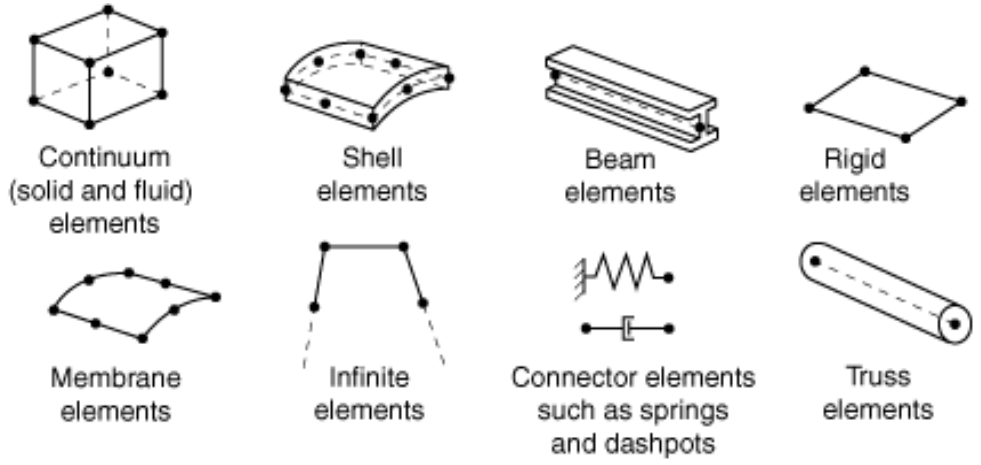

Figure 5-4 Abaqus element families

5.4 Model Geometry

The numerical modeling is developed with the goal of estimating the bridge bent caps behavior. The represented bridge was widened in 1970 by

adding two bent caps to the north and south side. The new bent cap has steel columns while the old one has concrete columns. Both bent caps were connected through two no. 3 dowels which allow the forces to be transferred. The dowels were modeled as a 3D solid element. Figure 5-5 and 5-6 show the model geometry and reinforcement, respectively.

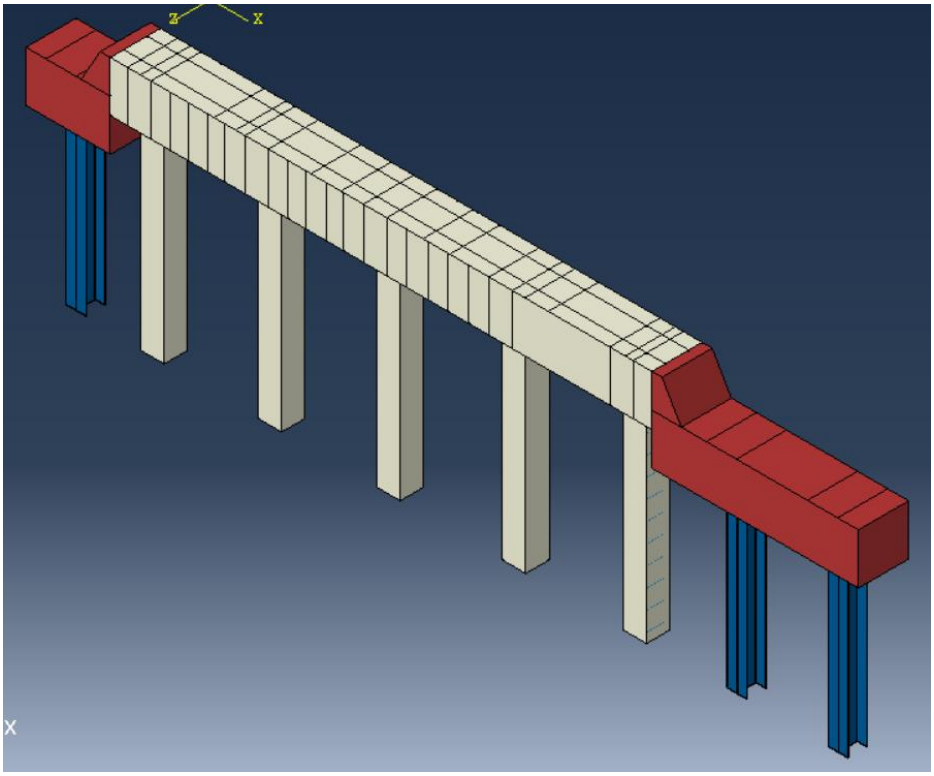

Figure 5-5 Abaqus model geometry

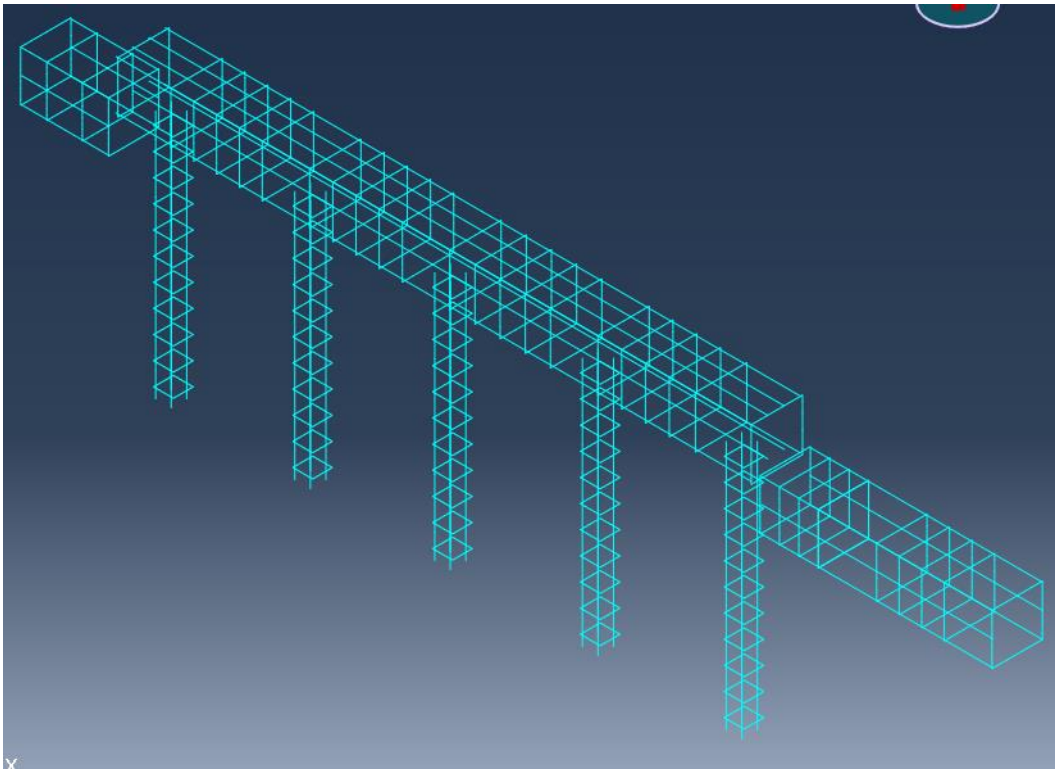

Figure 5-6 Reinforcement cage model

5.4.1 Model Geometry of before Repair Bent Cap

The model was performed to capture the behavior of the deteriorated bridge bent cap before repair which included concrete and steel sections loss due to spalling and corrosion, respectively. The concrete spalling locations and depths are as shown in Table 5-2. A section cut was created in Abaqus with different depths to represent the deterioration in the bent caps as shown in Figure 5-7. The model was used for calibration purposes for the before repair load test results.

Table 5-2 Depth of concrete spalling

Spalling Location	Depth (in.)
Span 1	1
Span 2	3
Span 3	2.5

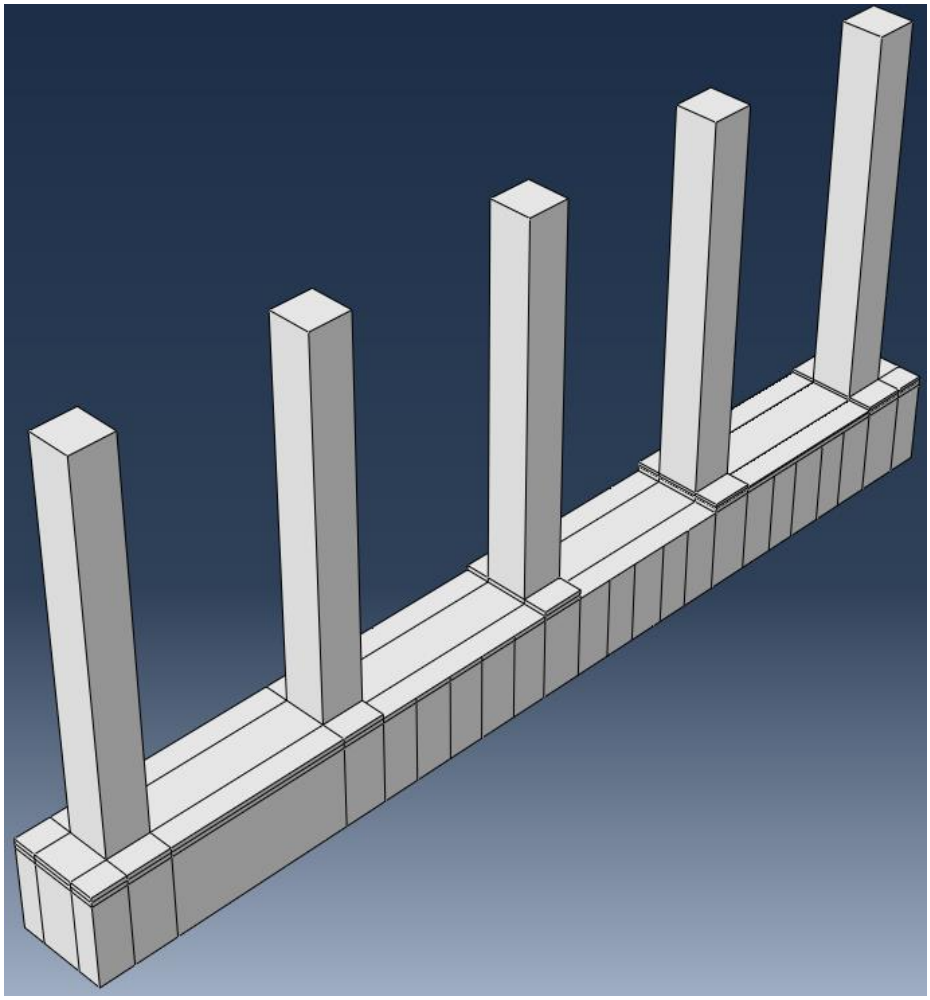

Figure 5-7 Deteriorated bent cap model

5.4.2 Model Geometry of after Repair Bent Cap

Repair mortar and FRP sheets were added to the model to evaluate their performance and calibrate the load test results. The first component added to the model is the repair mortar. It was modeled for the three deteriorated spans of the bent cap. The repair mortar compressive strength is 6500 psi the old bent cap concrete is 2669 psi. It was tied to the bent cap using Abaqus tie constrains. Repair mortar model is as shown in Figure 5-8.

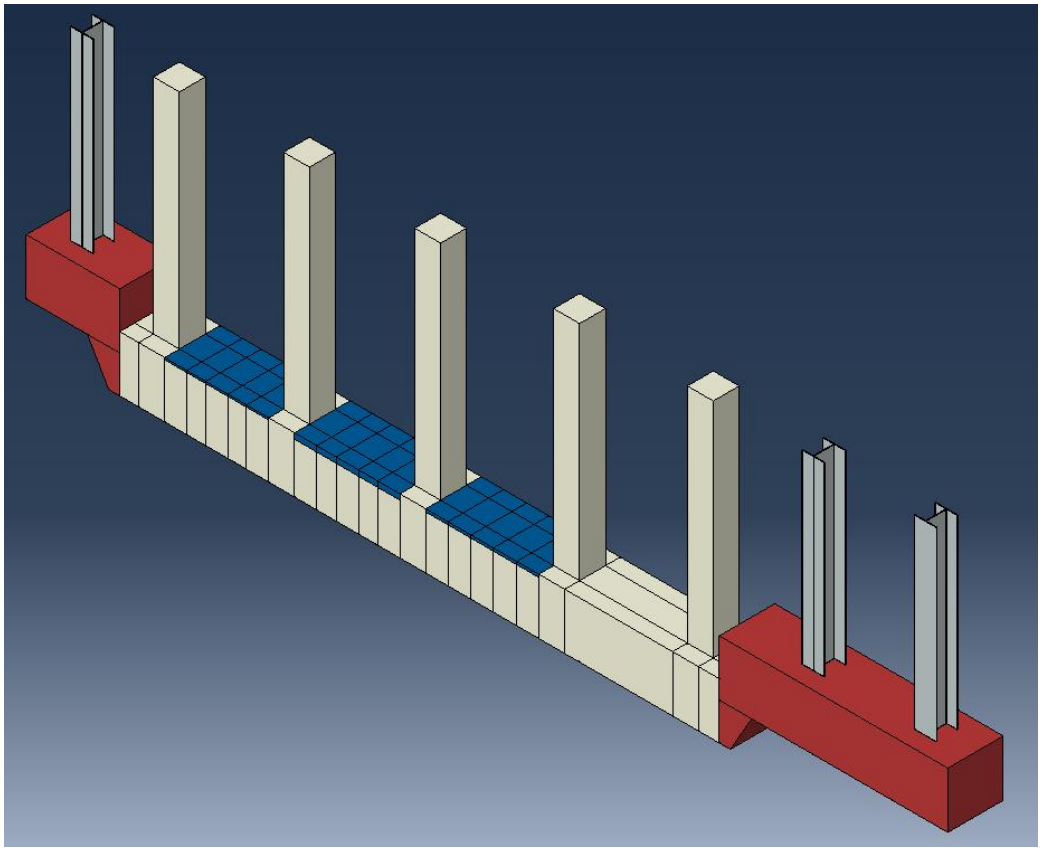

Figure 5-8 Repair mortar model

The second component is the FRP sheets. FRP Flexural and U-wrap sheets were added for the three repaired spans. FRP sheets were connected to the repair mortar using a cohesive bond. Epoxy and FRP properties were used to calculate the cohesive bond parameters to represent the actual behavior of the FRP. Figure 5-9 shows the modeling geometry of FRP sheets.

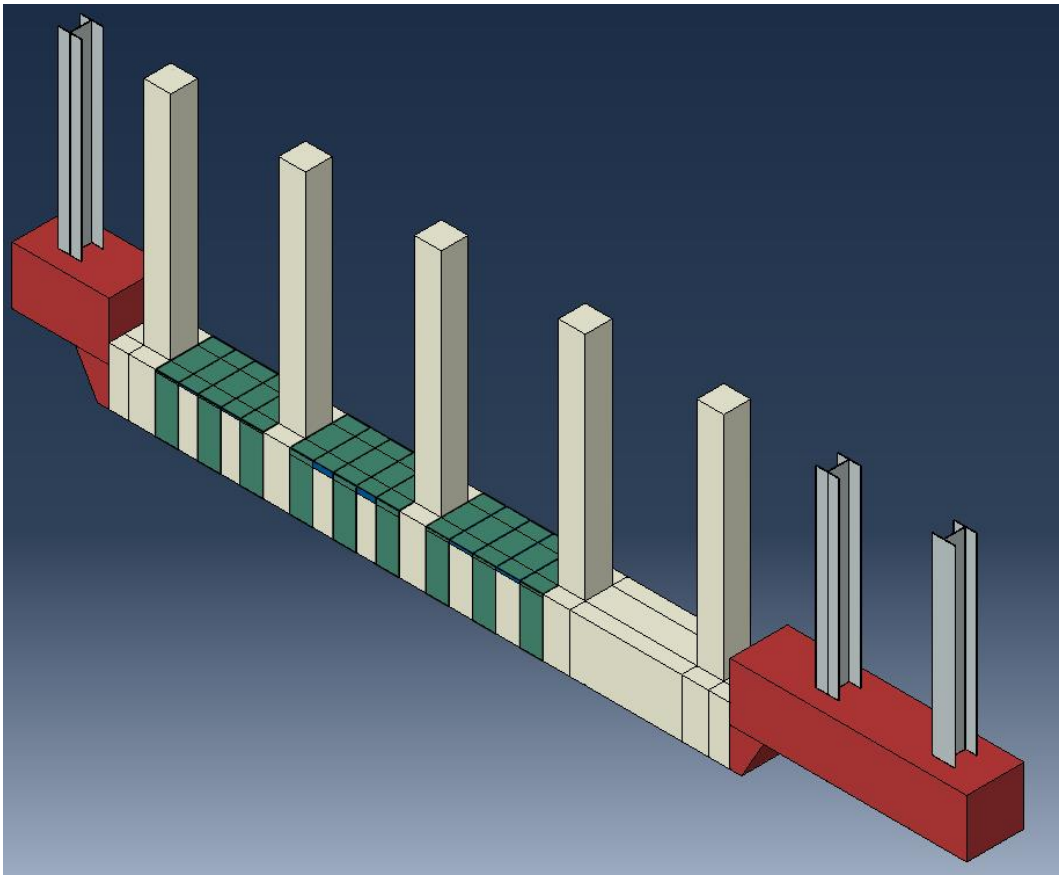

Figure 5-9 FRP sheets model

5.5 Meshing and Boundary Conditions

Meshing is required for finite element models. The model is divided into a number of small elements. After loading, stress, and strain are calculated at integration points of these small elements (Bathe 1996). Selection of the mesh density is an important step in finite element modeling. Convergence of results is obtained when an adequate number of

elements is used in a model (Kachlakev 2001). An even finer mesh gave almost the same result as the previous mesh, but more time was needed for computations (Obaidat 2011). In this study, a convergence study was carried out to determine an appropriate mesh density. Therefore, a three inch moderately fine mesh was chosen in this study. All structural members except the steel columns were given the same mesh size. Steel columns were given one inch and half mesh size since the web thickness is only one inch. Figure 5-10 illustrates the mesh used in this model.

Boundary conditions and loads were defined to complete the inputs of the ABAQUS model. The boundary conditions for the simulated bent cap was fixed support to simulate the condition of the experimental load tests. Figure 5-11 shows the boundary condition used in the Abaqus model at the base of the column.

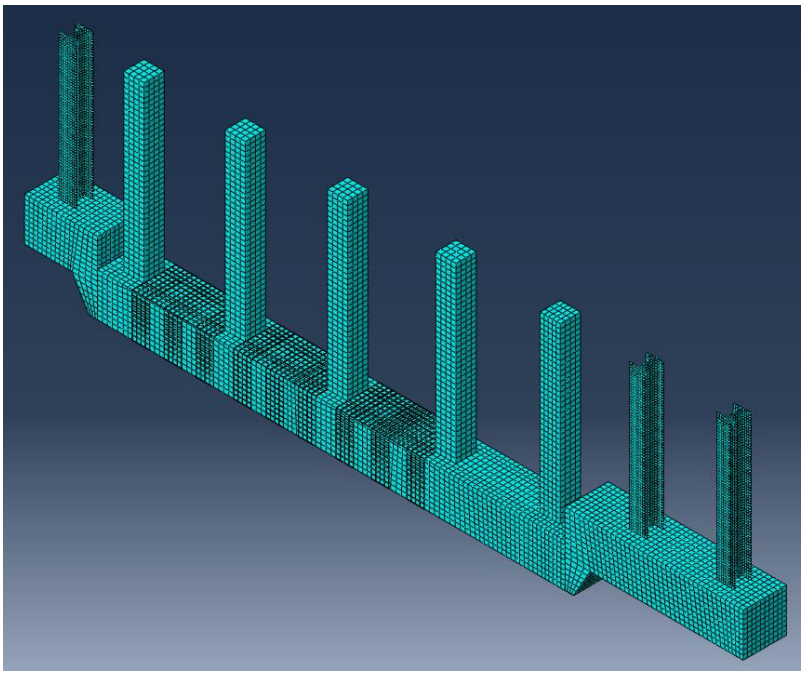

Figure 5-10 Mesh used in the model

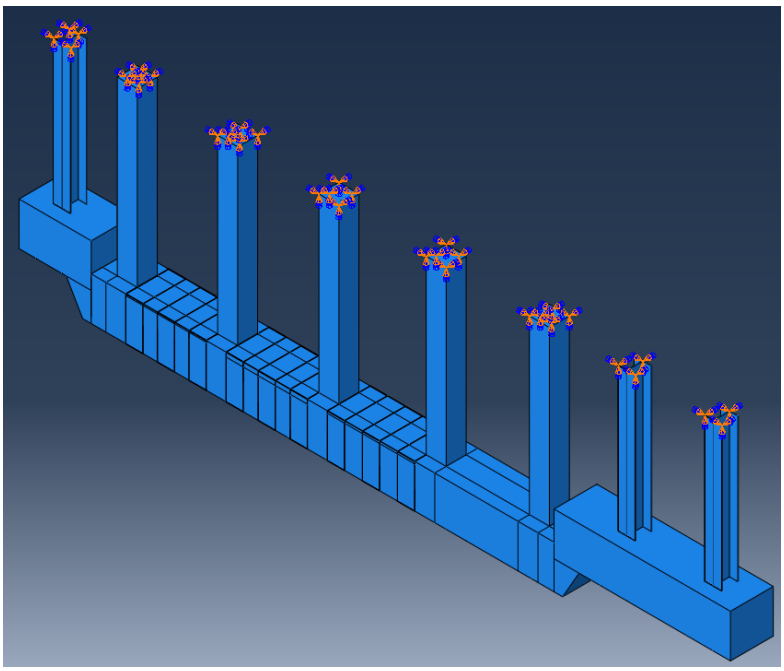

Figure 5-11 Model Boundary condition in Abaqus

5.6 Loads

The loads were applied at the girders locations which represent the actual case for the bridge bent caps. A finite element analysis model was created using CSIBridge software. It was used to determine the loads received by the bent cap from the girders. Figure 5-12 shows the bridge simulation using CSIBridge software. The area of the girders bottom surface attached to the bent caps top surface were calculated which sitting on the bent cap upper surface was calculated. Then, the loads were applied on the bridge bent cap using a surface load in Abaqus as shown in Figure 5-13.

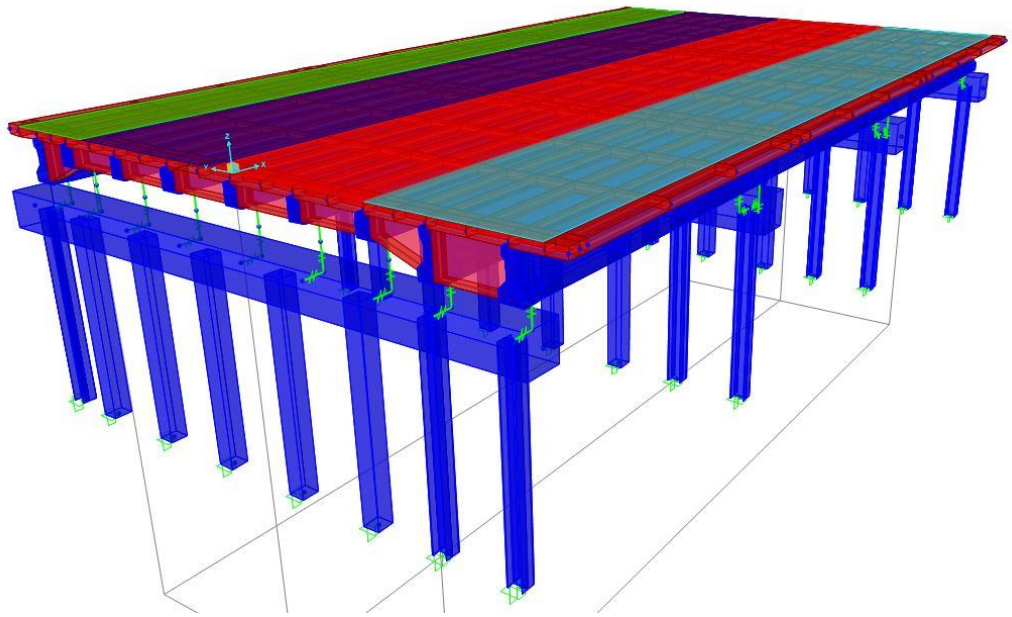

Figure 5-12 bridge model using CSIBridge

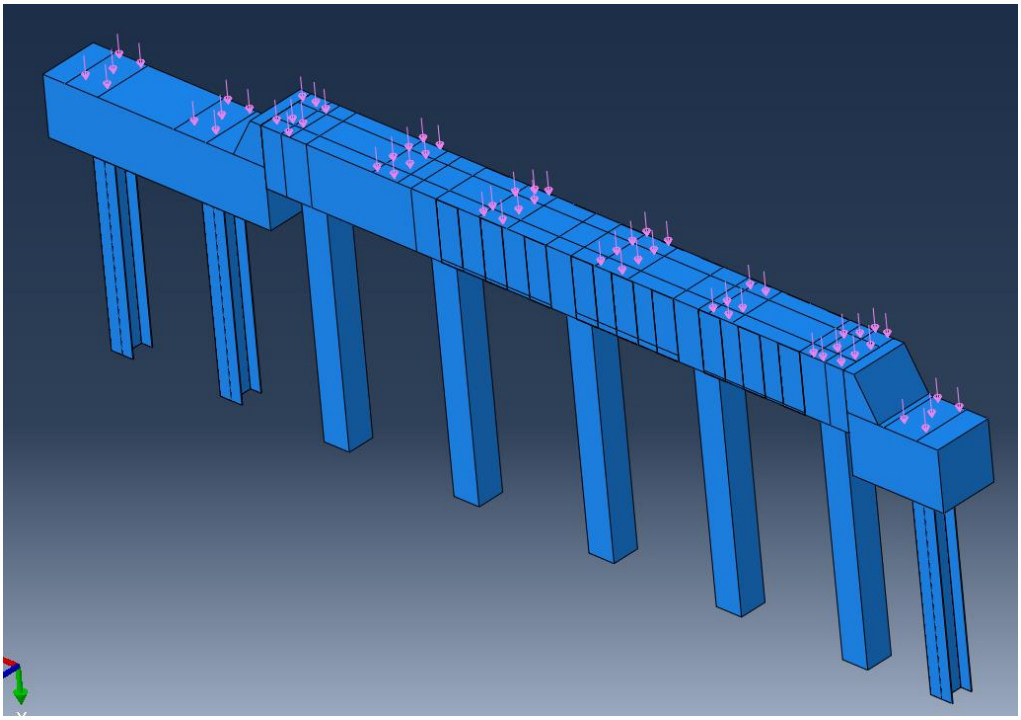

Figure 5-13 Surface loads model

Chapter 6
LOAD TESTS AND FINITE ELEMENT MODELING RESULTS

6.1 Load Tests Results

Load tests before and after repair of the west bound of US 80 over East Fork Trinity River Bridge in Dallas, Texas was carried out to investigate the performance of the mortar repair and the CFRP rehabilitation. A detailed plan was prepared for instrumentation, static and moving load tests. The load tests required a complete closure of traffic to avoid any participation of other vehicles in the data collection. The data acquisition systems were balanced and reset to zero before the beginning of the tests and after each run.

Four tests were conducted, one static and three crawl speed tests. The time was recorded when the second axle of the truck passed over each bent cap for all tests. The purpose of recording the time is to create intervals of time with known positions to convert the time domain to the position domain. This also can neglect any errors in the time domain since the truck cannot be perfectly driven at a constant speed through all the tests. The strain gages data was created using text files, which then were converted into excel sheets. After analyzing the strain data, it was determined that the peak strains from all the tests were just around 20 microstrains. These low peak strains can be attributed to the low weight of the test trucks, stiff bridge,

and short bent cap spans. Observations from the live load data indicated that the strain readings returned to zero once the truck was off the bridge. Hence, it can be concluded that the bridge behaved linear-elastically. However, the strain results for before and after repair load tests were used to evaluate the bent caps repair for various load configurations and to study the effect of the deterioration depth, and for modeling calibration.

6.1.1 Comparison between before and after Repair Load Tests

The strain results of bent caps 37 and 35 for steel, CFRP, and concrete gages used in the load tests before and after repair were analyzed to investigate the effectiveness of the bent caps repair. From the data recorded, it was observed that all but two of the strain gages behaved accordingly. Strain gages mounted on mid-span four of bent cap 37 and mid-span two of bent cap 35, were found to give erroneous results due to faulty strain gages. Crawl speed test with two lanes loaded was considered to perform the comparison since it is observed that the strains results are the highest for this loading sequence.

The results clearly show a small difference in strains between the load tests before and after repair for two spans in bent cap 37 and one span in bent cap 35. The results of the load test after repair for spans two and three of bent cap 37 show a strain reduction of 28% and 20%, respectively, as shown in Figures 6-1 and 6-2. Results of load test after repair for span

three of bent cap 35 show a reduction in strain of about 40% as shown in Figure 6-3. However, span one of bent caps 37 and 35 shows a negligible difference in strain as shown in Figures 6-4 and 6-5, respectively.

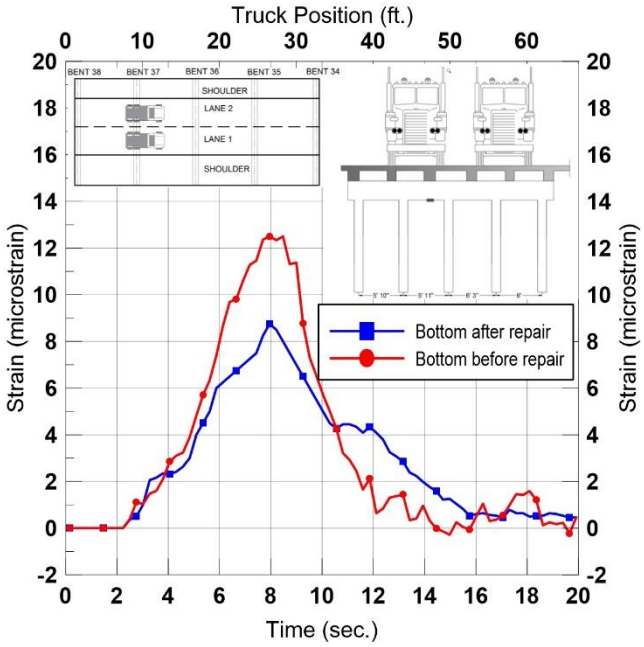

Figure 6-1 Strain comparison of span two of bent cap 37

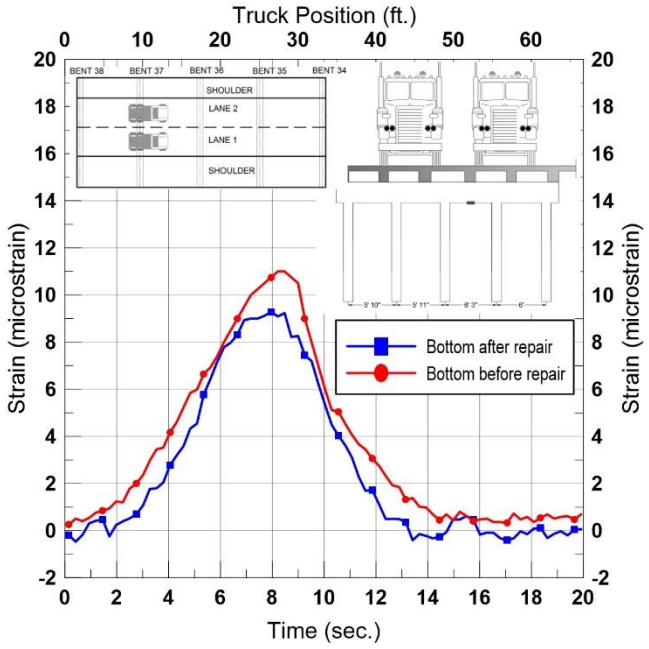

Figure 6-2 Strain comparison of span three of bent cap 37

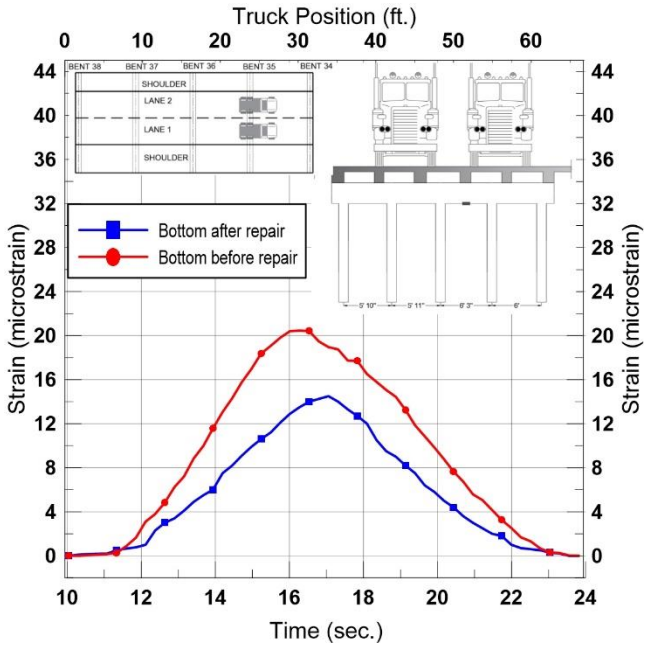

Figure 6-3 Strain comparison of span three of bent cap 35

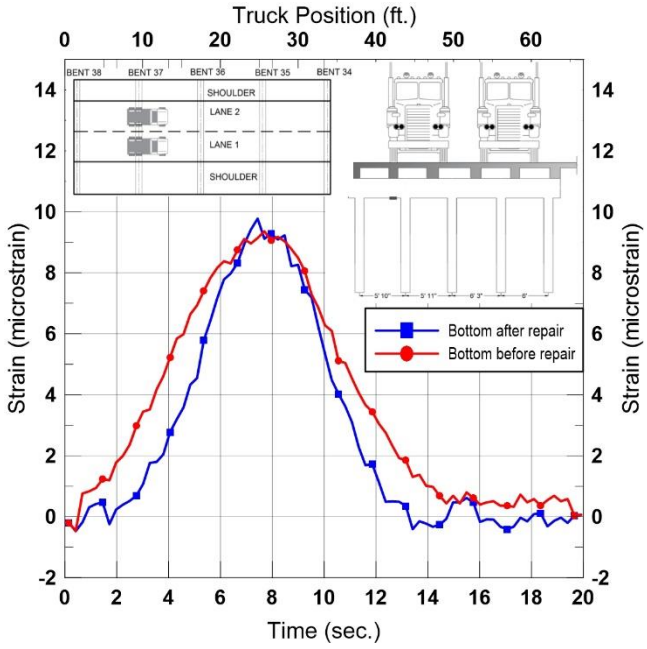

Figure 6-4 Strain comparison of span one of bent cap 37

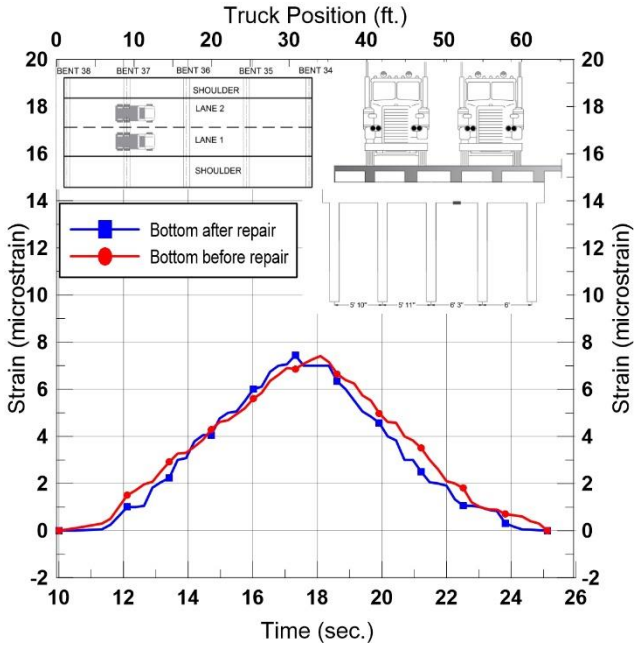

Figure 6-5 Strain comparison of span one of bent cap 35

The strain results of bent caps 37 and 35 clearly show that the CFRP composites participated in carrying the applied loads, as evident by the recorded nonzero strains on the sheets. The test results of the bent caps also indicated that the largest rebar and CFRP strains are induced in the two interior spans since the girders on top of these spans are located approximately in the middle of the bridge span, also these girders are close to the wheel loads. The test results indicated that the repair mortar and the CFRP sheets bonded to the bottom face of the bent caps had a noticeable effect on the overall strength of the bent caps.

The repair mortar has a compressive strength of 6500 psi while the original bent cap concrete has a 2690 psi compressive strength. Hence, this would affect the overall strength of the bent caps depending on the repair mortar depth. The repair mortar depth of spans one, two, and three of bent cap 37 were 1 in., 3in., and 2.5 in., respectively. Hence, it was expected to see a strain reduction in spans two and three since the repair mortar depth is high in these spans. Additionally, spans two and three of bent cap 37 exhibited some minor flexural cracks. CFRP was applied to resist opening of the flexural cracks and to increase the bent caps strength. Span one of bent caps 37 and 35 shows almost no change in strain after repair since the repair mortar depth is less than 1 in. and it did not exhibit any minor cracks. However, the experimental results could not quantify the exact contribution

of CFRP and the mortar in the bent cap strength gain since only one load test was carried out after CFRP rehabilitation.

6.1.2 Load Cases

For the bridge load tests before and after repair, different load cases were considered to collect the strain data. The load cases were designated to provide a wide variety of data that can be used to calibrate the FE model under different loading scenarios. Also, the load cases data was used to compare the bent cap behavior before and after repair. The load cases were left, right and two-lane loads. Figure 6-7 shows the strain in bent cap 37 before and after repair for different load cases. It can be noted that the left lane load produced the highest strain in span one while right lane load produced the highest strain in span three. This is due to the load distribution factor for the bridge girders. The load distribution factor depends on the truck position. If the distance between the girder and the truck wheels is close, it will take a higher distribution factor. Therefore, it was expected to see the high strain in span one for the left lane load. It can be observed from the figure that span one produced compression strain (-) for the right lane load since the truck is on the other side of the bent cap causing a tensile strain in spans three and four and compression strain in span one.

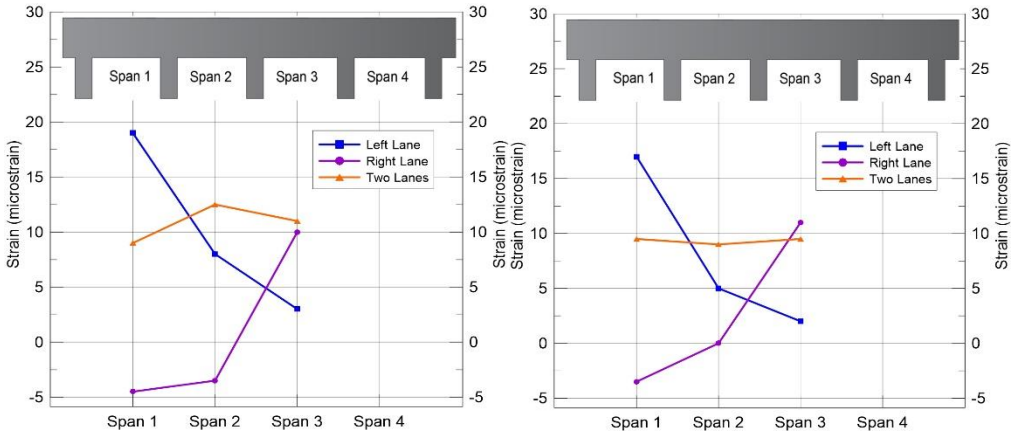

(a) (b)

Figure 6-6 strain measurement for the load cases (a) before repair, (b) after repair

6.2 Model Calibration

The preliminary model is based on theoretical values and equations from literature which does not take into consideration the actual materials and test conditions. Hence, it is required to calibrate the finite element model to accurately reflect the actual condition of the bridge bent cap. The first step in the model calibration is to determine the actual material properties of the bridge bent caps. Three concrete cores were taken from bent caps 35, 36, and 37. A Ground Penetration Radar (GPR) was used to locate the steel rebars before coring to avoid any rebar damage. The average diameter of the concrete cores was 3.81 in. and the average depth was 8 in. Strain gages were installed on one side of the concrete cores to

get the stress-strain curve of the concrete cores. The strain readings will be used for a better correlation between the calibrated values and experimental measurement. The concrete cores were tested according to the ASTM C39 specifications (ASTM C39 2014) as shown in Figure 6-9. The average compressive strength for bent caps 37, 36, and 35 were 2.69 ksi as shown in Table 6.1.

(a) (b)

(c) (d)

Figure 6-7 Concrete coring procedures: (a) Taking the cores, (b) GPR scanning, (c) Setting up the compression machine, (d) Tested sample

Table 6-1 Compressive strength of the bent caps

Bent Cap #	Concrete compressive strength (Ksi)
37	3.17
36	2.21
35	2.69
Average	2.69

The model calibration process included finding the values of strain in the mid-span region from the experimental load tests. For different load cases, only the maximum values of strain were considered for model calibration. The only truck live load was considered in the model while other loads such as dead load and lane load, were not considered since it is not measured by the test. A moving load case was created for every single load case in CSIBridge program. The loads values were taken from CSIBridge for different positions throughout the bridge spans. Afterward, the load values were applied in the ABAQUS model and the response was gathered. The strain measurements of the FEM was obtained from the model and compared with the experimental values. The comparison was made by using the correlation function as Equation 6.2. This function will account for the error and how optimal was the analyzed model. The correlation

coefficient value ranged from -1 and 1 which indicates to how close two variables are related to each other. A correlation coefficient of +1 indicates a perfect positive correlation, while -1 indicates a perfect negative correlation.

$$\frac{\sum(\varepsilon_m - \overline{\varepsilon_m})(\varepsilon_c - \overline{\varepsilon_c})}{\sum\sqrt{(\varepsilon_m - \overline{\varepsilon_m})^2(\varepsilon_c - \overline{\varepsilon_c})^2}} \qquad \text{Equation 6.2}$$

Where ε_m is the measured response, ε_c is the model response and $\overline{\varepsilon_m}$ $\overline{\varepsilon_c}$ are the means of the measured and model responses respectively. From this point, calibration is an iterative process that consists of changing the boundary conditions and material properties to optimize the model as quantified by the correlation function. The initial model of the bent cap before repair has an elastic modulus (E) value of 21,762 Mpa (3156 Ksi). The value of E was changed to 19,228 Mpa (2788 Ksi) for the calibrated model. Furthermore, the most recent value of E used in the bent cap before repair model was used in the after repair model. Only the value of E of the CFRP E was changed from 63,500 Mpa (9,209 Ksi) to 70,000 Mpa (10,152 ksi) for the calibrated model. Figure 6-10 shows the final calibrated values for the FEM and the experimental values used for calibration for each test. Once the FEM was calibrated, the model would constitute a calibrated

version of the bridge that could be used for further rating, study and as a validation for the modeling techniques used to describe bridge behavior.

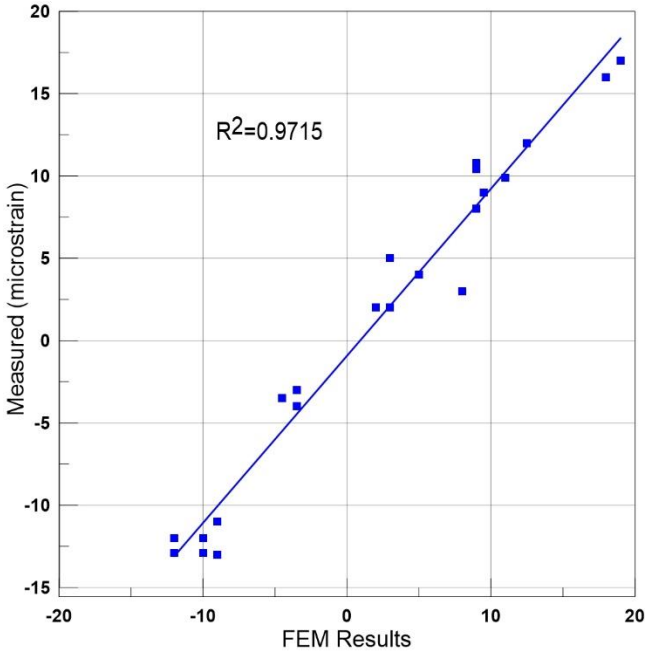

Figure 6-8 FEM results vs. experimental results

6.3 Model Results

6.3.1 Strain Results

The finite element should be checked by comparing the strains with the measured experimental results prior to predict the future behavior of the bent cap. Strains at the bent cap mid-span were considered the most critical since they reflect the bent cap behavior at locations that would experience the highest strains. A comparison of the measured and strain calculated from the finite element model for bent cap 37 before and after repair can be

seen in Figure 6-1 (a) and (b). It can be seen from these figures that an excellent correlation exists between the live load data and the finite element model. Although the data did not match up extremely close when the truck was on the opposite span, it should be mentioned that the finite element model was off by about only two microstrains from the live load data. Figure 6-9 shows the strains calculated from the model for the before and after repair bent cap. It can be noted the strain was reduced for the bent cap after repair for span two and three while it increased for span one. This is a close behavior to the live load test since span one repair depth is lesser than one inch.

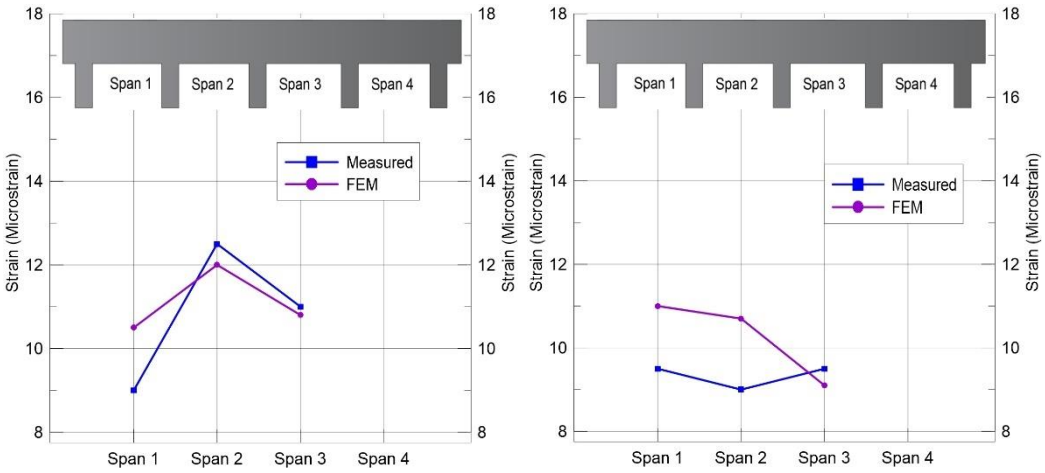

(a) (b)

Figure 6-9 Measured vs. FEM (a) before repair, (b) after repair

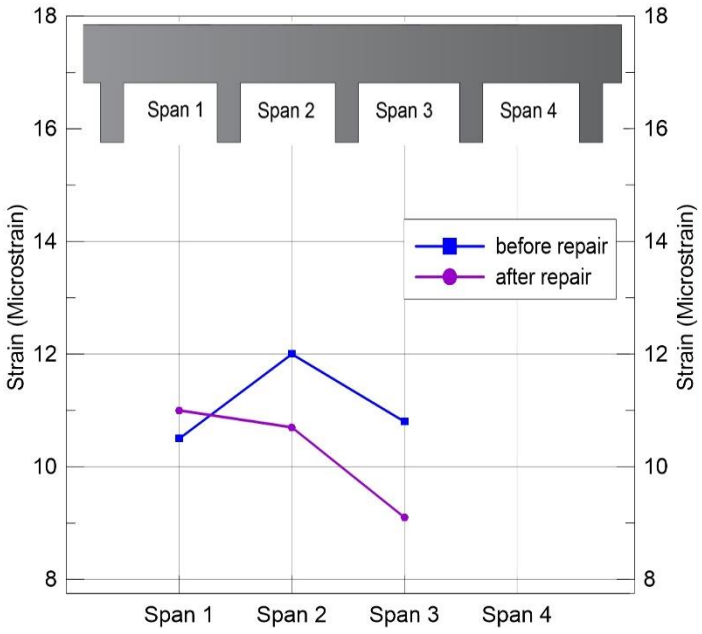

Figure 6-10 FEM results for the bent cap before and after repair

6.3.2 Neutral Axis Location

The principle theory for calculating the neutral axis location for simple beams is not applicable to deep beams even under the linear elastic assumption. The stress or strain distribution along the beam depth is no longer linear which varies depending on the aspect ratio of the beam. The neutral axis of bent cap 37 was calculated to investigate the effect of the CFRP on the neutral axis location. The location is found using the FE models as shown in Figure 6-11. Based on this investigation, it may be

concluded that the neutral axis moved slightly downwards after the FRP system was installed since the FRP reduced the strain at the bottom face.

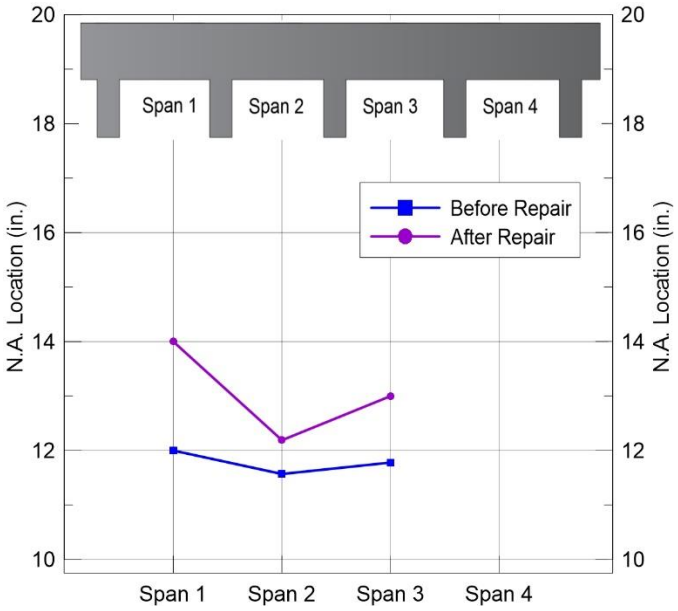

Figure 6-11Neutral Axis Location

6.3.3 Deterioration Effect

Corrosion of reinforcing steel is the leading cause of concrete deterioration. When the corroding steel expands, it creates tensile stresses which damage the surrounding concrete since the concrete has a low tensile strength. The possible damage includes cracking, spalling and delamination of concrete cover, loss of bond between concrete and reinforcements, and eventually degradation of member bearing capacity. However, the selected bent cap experienced section loss and steel

corrosion which reduced the flexural capacity. Four FE models were created based on the calibrated model to study the effect of concrete deterioration as shown in Table 6.2.

Table 6-2 Section loss variation

Model #	Properties
1	No section loss
2 (bent cap 37)	1.5 in.
3	2 in.
4	3 in.

The FE models were loaded till the first crack initiated. Figure 6-13 shows the tensile strains for all models. The first model with no section loss has the highest tensile capacity. Also, the tensile capacity decreased with the section loss increased. After the crack is initiated, the concrete would start the inelastic behavior along with the crack opening which explains the sudden increase in strain. Also, the flexural capacity depends on the concrete section loss if the steel is exposed. It depends on the exposure area of steel since the bond area between the concrete and steel will be reduced.

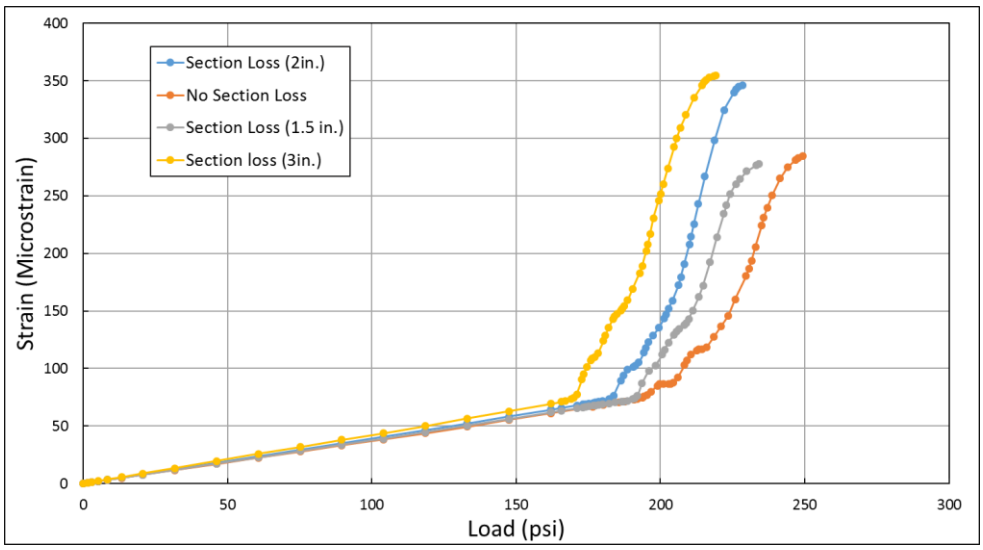

Figure 6-12 Tensile strain for all models

6.3.4 Comparison with HL-93 Truck

The bent cap before and after repair models were initially loaded with TxDOT vehicle with an average gross weight of 50 kips. However, the AASHTO code specified the HL-93 truck as the designed vehicle. The weight of the HL-93 truck is 72 kips which is higher than the truck used in this study. Hence, a comparison was performed to see the difference in the produced tensile strain. Figure 6-14 shows the bent cap before and after repair for both trucks. It can be noted that the HL-93 truck produced higher strain in span one and three since it has a higher weight. However, the tensile strain is lesser for HL-93 in span two. This is due to the difference in

the width between the two trucks. HL-93 truck has a width of six feet while the TxDOT truck has an eight feet width which resulting in different location of the wheels on the bridge.

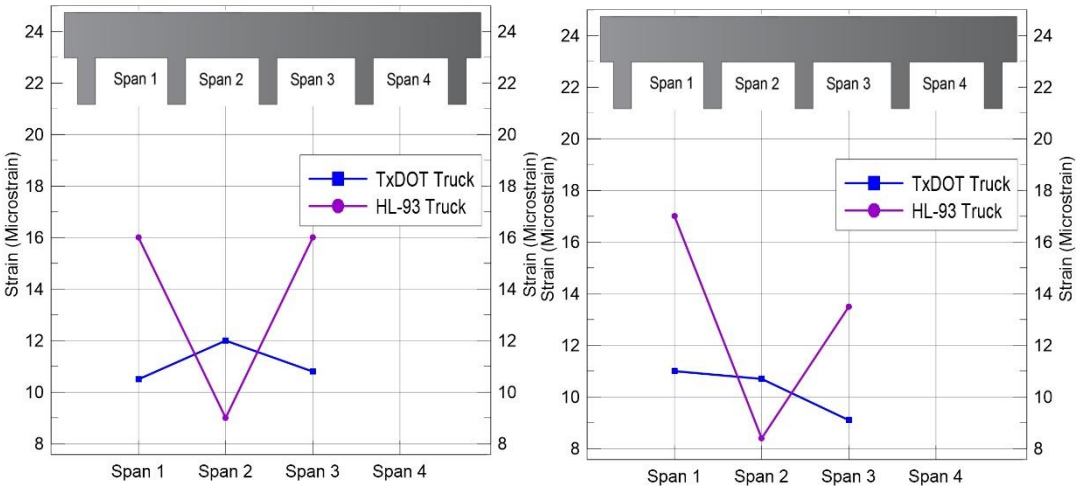

(a) (b)

Figure 6-13 HL-93 truck vs. TxDOT truck (a) bent cap before repair, (b) bent cap after repair

6.4 Bent Cap Capacity before and after Repair

The bent cap was designed according to the Working Stress Design (WSD) method since it was built in 1940. The moment capacity of the bent cap was found to be 187 k-ft. in the positive moment region and 128 k-ft in the negative moment region based on the WSD method. However, this method is no longer used since the 1970s since it is very conservative. Nowadays, LRFD is the method used for calculation the members capacity. The bent cap flexural capacity is 364 k-ft and 232 k-ft in the positive and negative moment region, respectively. Also, the bent cap shear capacity is 85 kips. However, the cracking moment was also calculated to find out at what load the crack starts in the bent cap. The cracking moments for the bent cap before and after the repair was found to be 161 k-ft and 196 k-ft, respectively. The applied moment from the truck was around 20 k-ft. which is much lesser than the cracking moment and the moment capacity.

The calibrated models for the bent cap before and after repair were loaded till failure to investigate the actual capacity of the bent cap. Figures 6-15 and 6-16 show the cracks pattern in span three for the bent cap before repair, repaired, and strengthened with CFRP models. The moments at which the crack begins was 147 k-ft and 238 k-ft, respectively. Hence, it is observed that the repair mortar along with the CFRP increased the cracking moment.

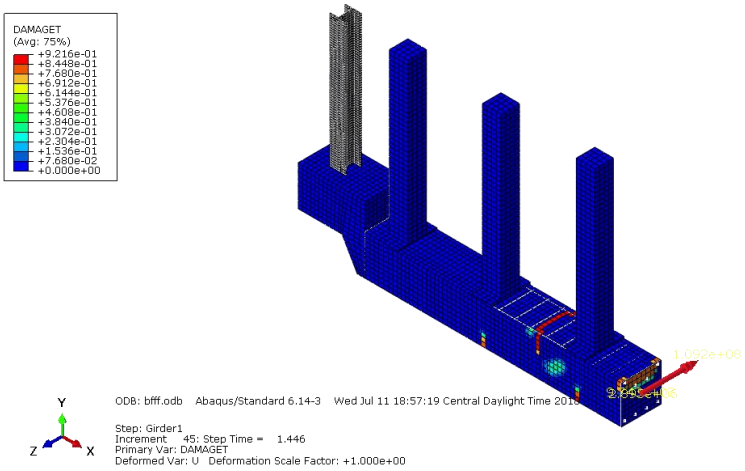

Figure 6-14 Cracked section of the bent cap before repair

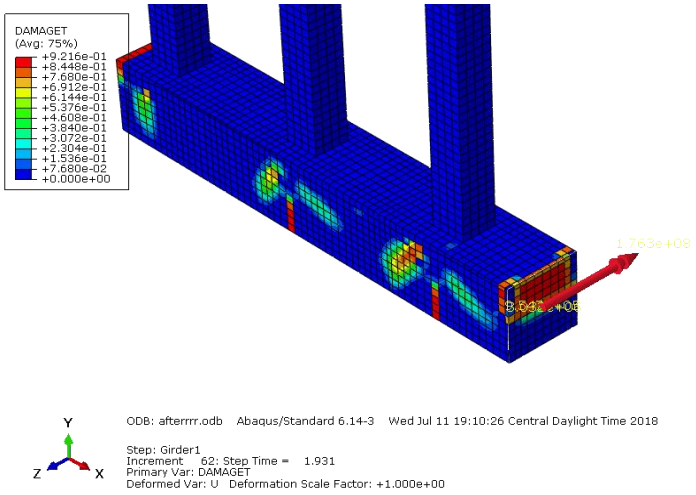

Figure 6-15 Cracked section of the repaired bent cap

The crack pattern shows some difference for the bent cap before and after repair as shown in Figures 6-17 and 6-18. The bent cap before repair

experienced flexural crack first in span two then shear compression cracks along with tensile cracks in the negative moment region. The bent cap after repair experienced tensile cracks in the negative moment region than shear compression cracks and finally a flexural cracks. Figure 6-19 shows the bent cap tensile behavior for the bent cap before and after repair, and the CFRP strengthened. It can be noted that the section of the bent cap before repair cracked at a load of 178 psi (510 kips) while the repaired bent cap at 204 psi (600 kips) and the CFRP strengthened at 260 psi (720 kips).

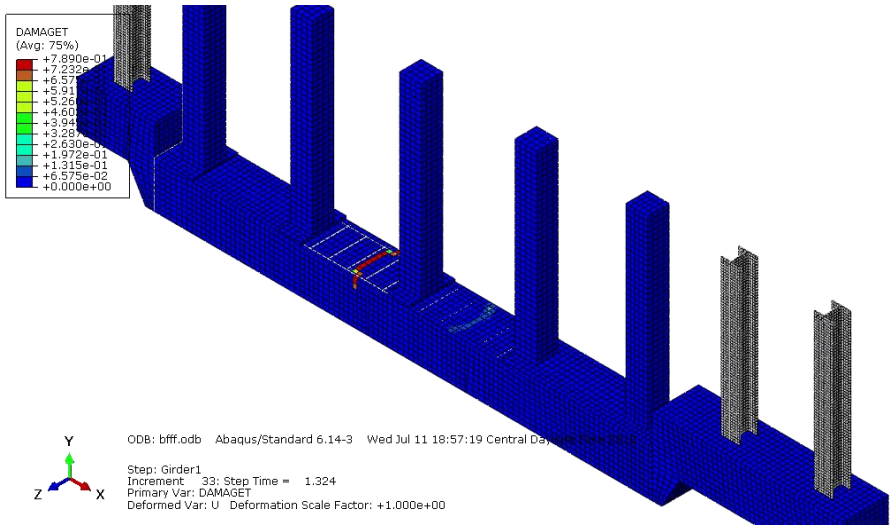

Figure 6-16 Crack pattern for the bent cap before repair

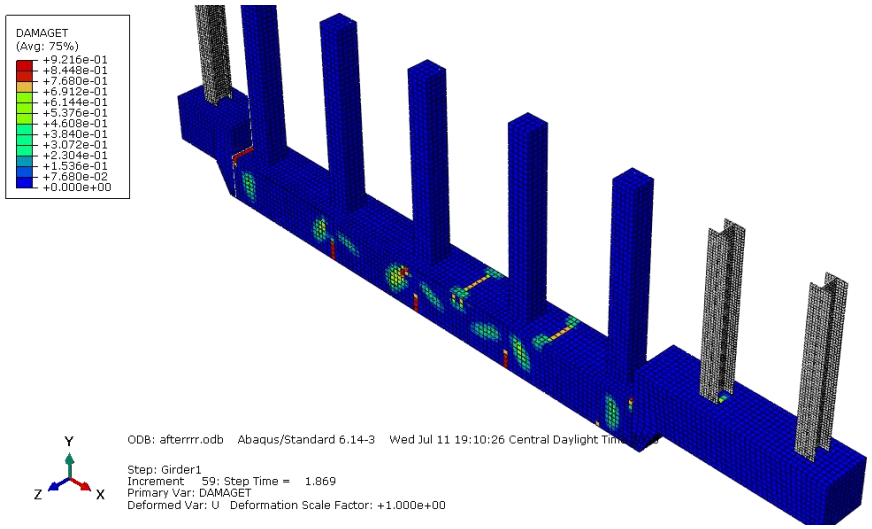

Figure 6-17 Cracks pattern for the bent cap after repair

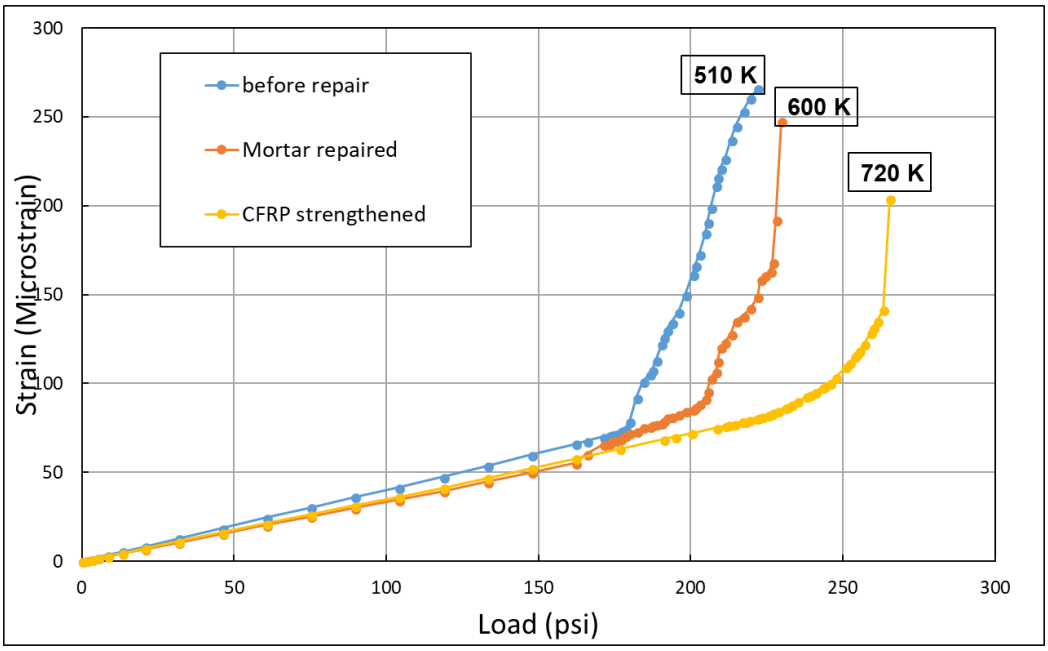

Figure 6-18 bent cap capacity

Chapter 7
CONCLUSIONS AND RECOMMENDATION

7.1 Summary

A 78-year-old reinforced concrete bridge located Dallas, Texas was repaired and evaluated through live load testing. The bridge bent caps had a significant deterioration exhibiting spalling concrete and exposed rebar. Eight such bent caps were selected for repair, FRP strengthening, and evaluation. The FRP performance was evaluated through full-scale load testing. The study involved three phases: load testing of deteriorated bent caps before repair, repair/strengthening of the bent caps using an epoxy mortar and longitudinal/transverse CFRP laminates, and follow-up load testing after CFRP repair/strengthening. The load tests involved placing pre-weighed trucks at specific positions on the bridge and collection of strain measurements. Load test data was used to calibrate the FEM model to simulate the structural behavior of the bridge bent cap. Then, the FE model was used to determine the capacity of the bent cap.

7.2 Summary of Findings and Conclusions

- The live load test data shows that the tensile strain was reduced in two spans in the range of 20% to 28% for the bent after repair resulting from the contribution of the repair mortar and the CFRP.

- Application of the CFRP to bridge bent cap was successfully performed using a simple and straightforward process.
- A compressive strain was produced in the positive moment region when the span position is not within the lane width.
- The neutral axis location shifted downwards after the CFRP strengthened the bridge bent cap.
- The bent cap repair word was done without affecting the traffic flow.
- The FE model was successfully calibrated using the live load tests data to investigate to investigate the effectiveness of the repair.
- The model strain results show a good agreement between the live load data and the finite element model.
- The bent cap section loss resulting from concrete deterioration had a reverse effect on the live load carrying capacity of the bent cap.
- The flexural load-carrying capacity of the damaged bridge was fully recovered and enhanced by applying CFRP sheets on the tensile side of the bent cap.
- Serviceability, especially crack control, was also improved after the CFRP strengthening.

- CFRP strengthening technique is recommended for bent cap repair.

- The study can be used as a bench mark for repair & diagnostic load test of damaged bent caps.

7.3 Future Research

- Long-term evaluation of FRP effectiveness. The long-term effectiveness of the FRP strengthening system applied by conducting several load tests over the next 10-20 years should be performed to determine any loss in the structural capacity of the strengthened bridge and the causes of that loss.
- A heavier truck can be used for the live load test since working with small strain data is difficult.
- The bridge girders can be instrumented along with bent cap to determine the distribution factor for each girder to quantify the applied load on the bent cap.
- Conduct the load test more than one time for each run since it is difficult to control the trucks drivers speed.

.

Appendix A

SUMMARY OF BRIDGE REPAIR MANUALS FOR ALL STATES HIGHWAY

#	State	Bent Cap Repair	FRP	Concrete Repair
1	Louisiana	✘	✘	The evaluation procedure is only provided.
2	Colorado	• Limit of removal of concrete (0.5-1)'' beyond the face of the reinforcing steel. • Apply patching material.	• <u>FRP for Substructure: Columns repair:</u> 1) Place concrete sealer on top of concrete columns. 2) Provide 4" gaps between FRP placement areas. No concrete sealer shall be placed in the area.	1) Patching
3	Nevada	• <u>External Pier Cap Post-Tensioning</u>: Tensioning strand or rods can be placed externally on the cap to add compression to the cap. Brackets, distribution plates and other components are needed to transfer the post-tensioning forces to the cap. If aesthetics is a concern, the cap can be widened with ducts placed internally for the post-tensioning.	• <u>FRP for Superstructures:</u> Inadequate internal shear reinforcement or damaged reinforcement can be strengthened with externally applied, fiber-reinforced polymer (FRP) laminate reinforcement bonded to the surfaces of the webs. Bending capacity can also be increased with the application of FRP reinforcement.	1) Patching. 2) Polymer Concrete Overlay 3) Resin Overlay 4) Waterproof Membrane/Asphalt Overlay 5) Epoxy-Resin Injection 6) Crack Sealant 7) Silane Seal 8) Joint Rehabilitation and Replacement 9) Upgrade/Retrofit Bridge Rails 10) Scour Mitigation

		Post-tensioning is usually symmetrical to the cap so that an eccentric force is not introduced. The designer must look at the stressing sequence to ensure that the cap is not overloaded eccentrically during post-tensioning operations.		11) External Pier Cap Post-tensioning 12) Micropile Underpinning 13) Ground Anchorage 14) Soil Stabilization
4	Indiana	✘	• <u>FRP for Substructure:</u> <u>Columns Jacketing:</u> Jacketing consists of adding confinement steel to round columns and covering it with concrete or the use of a fiber wrap.	1) Patching 2) Epoxy Resin Injection 3) Low-Viscosity Sealant for Crack Repair 4) Post-Tensioning Tendons
5	Ohio	• <u>Spalls in concrete.</u> Procedures: 1) Patch and seal spalls with epoxy/urethane. • <u>Cracks in Cantilever Cap.</u> Procedures: 1) Epoxy inject cracks 1/8" and less in width and inspect for larger cracks.	✘	1) Patching

		2) Install steel bands or post tensioning rods around pier cap.		
6	Mississippi	✘	✘	✘
7	Iowa	3)	• <u>FRP for Superstructures:</u> <u>Beams repair:</u> 1) Inspect the concrete substrate and remove and repair unsound concrete. Inject cracks and fill surface defects with an epoxy resin. Ensure that the resulting surface is clean and dry. 2) Using gloves, masks, and goggles, cut the FRP strip to size using heavy duty shears. 3) Prime the concrete surface with an epoxy resin using a spatula for a width approximately 0.5 inch wider than the FRP strip. 4) Coat the face of the FRP strip to be bonded to the concrete with	1) Epoxy Inject Deck Overlays 2) Patch Bridge Decks with Asphaltic Concrete 3) Patch Bridge members with concrete

			the same epoxy resin as used to prime the concrete substrate. 5) After preparation of concrete substrate and FRP strip, place the strip on the concrete and use a rubber roller and pressure to embed the FRP strip into the resin base. 6) Allow FRP repair to stand for 24 hours without disturbance. 7) After FRP has properly cured, the FRP must be coated with an approved paint to prevent degradation and deterioration of the FRP from exposure to ultraviolet light.	
8	California	✘	✘	1) Epoxy for Patching, Bonding, and Filling Voids in Concrete. 2) Portland cement for Patching. 3) Shotcrete
9	Florida	• Patching Material. Procedures:	✘	1) Epoxy Deck Patching 2) Patching of concrete

		1) Saw cut around concrete to be removed and avoid cutting reinforcement. 2) Remove deteriorated concrete to horizontal and vertical planes using pneumatic breakers. 3) Add new reinforcing steel where required. 4) Apply bonding material to prepared surface that will interface with new concrete.		
10	Georgia	• <u>Epoxy Resin Adhesive</u> Procedures: 1) Square and saw-cut the area 1'' deep around the spall parameter. 2) Clean any corroded reinforcing by sand blasting. 3) Use compressed air to remove loose concrete debris. 4) Apply Epoxy Resin Adhesive to concrete surface.	✘	1) Epoxy resin adhesive 2) Rapid Setting Patching Material
11	Texas	<u>Minor Spall:</u> Procedures:	<u>FRP for concrete repair:</u> 1) <u>Surface Preparation:</u>	

		1) Surface preparation. 2) Apply Epoxy. 3) Finishing. 4) Curing. <u>Intermediate Spall:</u> Procedure: 1) Surface preparation (includes saw-cut the patch perimeters) 2) Apply Epoxy. 3) Finishing <u>Major Spall:</u> Procedures: 1) Surface preparation. 2) Square the patch perimeters to eliminate feathered edges and to ensure that the repair material will be applied in depths no less than 1/2 inch. 3) Roughen the substrate to ensure that there will be a mechanical bond between the patch material and the parent concrete. 4) Epoxy Anchors.	Prepare concrete substrate surfaces to promote continuous intimate contact between the CFRP and the concrete by providing a clean, smooth, and flat or convex surface 2) <u>Installation:</u> Apply system using the wet lay-up method unless otherwise approved. Install the CFRP system in accordance with contract requirements, working drawings, and the manufacturer's recommendations. 3) <u>Testing:</u> Perform the following tests after the initial resin has cured at least 24 hours and in accordance with manufacturer's specifications: a visual inspection of the entire CFRP surface, an acoustic tap test of any areas	1) Pressure-Injected Epoxy, 2) Gravity-Fed Sealant, 3) Routing and Sealing, and 4) Surface Sealing. <u>Classifications:</u> <u>Minor Spall:</u> Procedures: 1) Surface preparation. 2) Apply Epoxy. 3) Finishing. 4) Curing. <u>Intermediate Spall:</u> Procedure: 1) Surface preparation (includes saw-cut the patch perimeters) 2) Apply Epoxy. 3) Finishing <u>Major Spall:</u> Procedures: 1) Surface preparation. 2) Square the patch perimeters to eliminate feathered edges and to ensure that the repair material will be applied in depths no less than 1/2 inch.

			suspected to contain air pockets, and at least 2 direct pull-off tests for each member strengthened in accordance with ASTM D4541 to verify the tensile bond between the concrete and the CFRP system	3) Roughen the substrate to ensure that there will be a mechanical bond between the patch material and the parent concrete. 4) Epoxy Anchors.
12	Arkansas	✘	✘	1) Patching
13	Alabama	✘	✘	✘
14	South Carolina	✘	✘	✘
15	Oklahoma	✘	✘	1) concrete grout 2) epoxy resin mixture
16	Utah	<u>Shotcrete</u>: Procedures: 1) Remove loose or spalling concrete down to or just below the existing reinforcing. 2) Replace corroded reinforcing when required to restore capacity. 3) Place welded wire fabric or replacement stirrups to	<u>FRP for Substructure:</u> <u>Columns Jacketing:</u> Use external reinforcing in the form of steel jackets, fiber wraps or prefabricated fiber reinforced polymer (FRP) shapes to increase capacity. Numerous methods are available to place or form the systems. The typical construction sequence for prefabricated FRP shapes	1) Concrete sealer. 2) Pothole patching 3) Epoxy injection

		replace deteriorated or missing stirrups. 4) Place shotcrete and shape the surface to match the original surface or as required to restore capacity. Shotcrete can be plain or fiber reinforced. 5) Develop a special provision, define the limits of removal and define required reinforcing replacement when specifying repairs using shotcrete.	removes deteriorated concrete, places the stay in place form and grouts the gap. Alternatively, wet layup systems remove loose and deteriorated concrete, reconstruct the surface, then place and cure the FRP system.	
17	Kansas	✘	✘	✘
18	Missouri	✘	✘	1) Rapid Set Concrete Patching Materials.
19	Tennessee	✘	✘	✘
20	North Carolina	✘	✘	✘
21	Kentucky	✘	✘	✘
22	Oregon	✘	✘	1) Concrete Sealing 2) methacrylate sealer 3) epoxy sealer

23	Idaho	✘	✘	✘
24	Wyoming	✘	✘	✘
25	Nebraska	✘	✘	✘
26	Illinois			1) Epoxy injection 2) Patching of concrete
27	West Virginia	✘	✘	1) epoxy resin mixture 2) Portland cement concrete
28	Virginia	✘	✘	✘
29	Washington	✘	✘	1) Concrete grout.
30	Montana	✘	✘	1) Shotcrete 2) Epoxy Injection 3) Post-Tensioning Tendons Strengthening
31	North Dakota	✘	✘	✘
32	South Dakota	✘	✘	1) Grout 2) Epoxy Injection Repairs
33	Minnesota	✘	✘	✘
34	Wisconsin	• <u>Pier cap repair.</u> Procedures: 1) Place a watertight expansion joint in the deck.	✘	1) Grout

		2) Consider whether bearing replacement is required. 3) Analyze the type of cap repair required. 4) Clean off spalled concrete and place new concrete. 5) Analyze capacity of bars still bonded to see if unbonded bars are needed. Use ultimate strength analysis. 6) Consider repair method for serious loss of bar steel capacity. Add 6” of cover to cap. Add additional bar steel. Grout in U shaped stirrups around bars using standard anchor techniques. Use steel plates and post-tensioning bars to place compression loads on both ends of cap. Cover exposed bars with concrete. Pour wing extension under pier caps beginning at base to take all loads in compression. This would alter pier shape.		

		7) Consider sloping top of pier to get better drainage. 8) Consider placing coating on pier top to resist water intrusion.		
35	Michigan	• <u>Patching.</u> Procedures: 1) Clean off spalled concrete 2) Patching mixtures include latex modified (LM) concrete as one of the choices. When substructure units are patched, the entire surface of the substructure unit shall be coated with "Penetrating Water Repellent Treatment" to prevent further deterioration.	1) <u>FRP for Substructure:</u> <u>Columns repair:</u> This work consists of repairing concrete pier columns by wrapping them with a fiber reinforced polymer (FRP) wrap.	1) Embedded Galvanic Anodes.
36	Maryland	✘		✘
37	Delaware	✘	• <u>FRP for Superstructures:</u> <u>Beams repair:</u> CFRP system shall be limited to prevent sudden failure of the beam under sustained service loads in the event the CFRP system is damaged. The designer	1) Shotcrete 2) Epoxy injection

			shall perform an analysis and design of the strengthened member to ensure that the member will fail in a flexure mode rather than a shear mode under overload conditions.	
38	New Jersey	✘	✘	✘
39	Connecticut	✘	✘	✘
40	Rhode Island	✘	✘	✘
41	Pennsylvania	✘	✘	1) Epoxy Coat 2) Post-tensioning ducts 3) Concrete Patching
42	New York	✘	✘	1) epoxy injection 2) Seal with Silicone
43	New Hampshire	✘	✘	✘
44	Vermont	✘	✘	✘
45	Massachusetts	✘	✘	1) HP Cement Concrete Overlays
46	Maine	✘	✘	1) Portland Cement 2) Bonding Agents
47	Alaska	✘	✘	✘

48	Hawaii	✘	✘	✘
49	Arizona	✘	✘	1) Epoxy Injection.
50	New Mexico	✘	`	1) Epoxy Injection 2) Crack Sealing Using Low-Viscosity Gravity-Fed Sealers.

References

- ABAQUS (2014). “ABAQUS standard user’s manual. Version 6.14, vol. I–III.” Pawtucket (America): Hibbitt, Karlsson & Sorensen, Inc.

- ACI. (2017). “Guide for the design and construction of externally bonded FRP systems for strengthening concrete structures.” ACI 440.2R-17, Farmington Hills, MI.

- Ainge, S. W. (2012). Repair and Strengthening of Bridge Substructures.

- Allen, R. T. L., Edwards, S. C., & Shaw, D. N. (Eds.). (1992). Repair of concrete structures. CRC Press.

- American Association of State Highway and Transportation Officials. (2016a). “Manual for Bridge Evaluation, 2nd Edition, with 2011, 2013, 2014, 2015, and 2016 Interim Revisions.” C3, Washington, DC.

- American Association of State Highway and Transportation Officials. (2016b). AASHTO LRFD Bridge Design Specifications, Customary U.S. Units, 7th Edition, with 2015 and 2016 Interim Revisions, Farmington Hills, MI.

- ASCE. (2017). ‘2017 report card for America’s infrastructure.’’ ASCE.

- ASTM C39/C39M (2014). “Standard Test Method for Compressive Strength of Cylindrical Concrete Specimens,” Annual Book of ASTM Standards, ASTM International, Vol. 04. 02, West Conshohocken, PA

- Bathe, K. J. (1996). Finite Element Procedures. Upper Saddle River, New Jersey, 07458.

- Bakht, B., & Jaeger, L. G. (1990). Bridge testing—A surprise every time. Journal of Structural Engineering, 116(5), 1370-1383.

- Beal, D. B. (1998). Manual for bridge rating through load testing. Research Results Digest, (234), 12-28.

- Bradberry, T. E., & Wallace, S. (2003). FRP reinforced concrete in Texas transportation past, present, future. Special Publication, 215, 3-36.

- Carolin, A. (2003). “Carbon Fiber Reinforced Polymers for Strengthening of Structural Elements”, Doctoral Thesis, Luleå University of Technology.

- Chajes, M. J., Mertz, D. R., & Commander, B. (1997). Experimental load rating of a posted bridge. Journal of Bridge Engineering, 2(1), 1-10.

- CSIBridge, C. B. 14 [Computer software]. Walnut Creek. CA, Computers and Structures.

- FHWA (Federal Highway Administration). (2012). Bridge inspector’s reference manual, Washington, DC.

- FOX 59 (2017). “ I-465 northbound at Rockville Road to be closed indefinitely after truck hits overpass” <<http://fox59.com/2017/01/10/i-465-northbound-closed-near-rockville-road-after-crash-leaves-debris-on-interstate/ >> accessed on Feb 11, 2018.

- Hag-Elsafi, O., Lund, R., & Alampalli, S. (2002). Strengthening of Church Street Bridge Pier Capbeam Using Bonded FRP Composite Plates: Strengthening and Load Testing (No. FHWA/NY/SR-02/138,). Transportation Research and Development Bureau, New York State Department of Transportation.

- Hansson, C. M., Poursaee, A., & Jaffer, S. J. (2007). Corrosion of reinforcing bars in concrete. R&D Serial, (3013).

- ICRI (2007). “Selecting and Specifying Concrete Surface Preparation for Sealers, Coatings, and Polymer Overlays”, Technical Guidelines Prepared by the International Concrete Repair Institute, Jan. 1997, International Concrete Repair Institute, Sterling, VA, USA

- Kachlakev, D. I., Miller, T. H., Potisuk, T., Yim, S. C., & Chansawat, K. (2001). Finite element modeling of reinforced concrete structures strengthened with FRP laminates (No. FHWA-OR-RD-01-XX). Oregon. Dept. of Transportation. Research Group.

- Kim, Y. J., Green, M. F., & Fallis, G. J. (2008). Repair of bridge girder damaged by impact loads with prestressed CFRP sheets. Journal of Bridge Engineering, 13(1), 15-23.

- Klaiber, F. W., Dunker, K. F., Wipf, T. J., & Sanders Jr, W. W. (1988). Methods of strengthening existing highway bridges (No. 1180).

- Lichtenstein, A. G. (1995). Bridge rating through nondestructive load testing. National Cooperative Highway Research Program Project, 12-28.

- Lu, C., Yang, J., Li, H., & Liu, R. (2017). Experimental Studies on Chloride Penetration and Steel Corrosion in Cracked Concrete Beams under Drying-Wetting Cycles. Journal of Materials in Civil Engineering, 29(9), 04017114.

- Mays, G. C. (Ed.). (2002). Durability of concrete structures: investigation, repair, protection. CRC Press.

- McCormac, J. C., & Brown, R. H. (2015). Design of reinforced concrete. John Wiley & Sons.

- Morgan, D. R. (1996). Compatibility of concrete repair materials and systems. Construction and building materials, 10(1), 57-67.

- Nemati, K. (2006). Point Shilshole Condominium Building Concrete Deterioration Causes and Repair Method. Point Shilshole Condominium inc.

- Nilson, A. (1997). Design of concrete structures (No. 12th Edition).

- Obaidat, Y. (2011). Structural retrofitting of concrete beams using FRP-debonding issues. Department of Construction Sciences, Lund University.

- Pantelides, C. P., Gergely, J., Reaveley, L. D., & Volnyy, V. A. (1999). Retrofit of RC bridge pier with CFRP advanced composites. Journal of Structural Engineering, 125(10), 1094-1099.

- Pham, H. B., Al-Mahaidi, R., & Saouma, V. (2006). Modelling of CFRP–concrete bond using smeared and discrete cracks. Composite structures, 75(1-4), 145-150.

- Piggott, M. Load bearing fibre composites, 2nd Edition. Kluwer Academic Publishers, Boston/ Dordrecht/ London. 2002.

- Pinjarkar, S. G., Guedelhoefer, O. C., Smith, B. J., and Kritzler, R. W. (1990). "Nondestructive load testing for evaluation and rating." Final Rep., NCHRP Proj. 12-28(13), Transp. Res. Board, Washington, D.C.

- Pino, V., Nanni, A., Arboleda, D., Roberts-Wollmann, C., & Cousins, T. (2016). Repair of Damaged Prestressed Concrete Girders with FRP and FRCM Composites. Journal of Composites for Construction, 21(3), 04016111.

- Poursaee, A. (2016). Corrosion of steel in concrete structures. In Corrosion of Steel in Concrete Structures (pp. 19-33).

- Radomski, W. (2002). Bridge rehabilitation (Vol. 13). London: Imperial College Press.

- Saraf, V., Sokolik, A., & Nowak, A. (1996). Proof load testing of highway bridges. Transportation Research Record: Journal of the Transportation Research Board, (1541), 51-57.

- Saenz, L. Discussion equation for the stress - strain curve of concrete, By Desayi P, Krishnan S, ACI J, 1964; 61, 1229–35.

- Sasher, W. C. (2008). Testing, assessment and FRP strengthening of concrete T-beam bridges in Pennsylvania. West Virginia University.

- Smith, J. L., & Virmani, Y. P. (1996). Performance of epoxy-coated rebars in bridge decks. Public Roads, 60(2).

- Smoak, G. (2002). Guide to concrete repair. The Minerva Group, Inc.

- Stallings, J. M., Tedesco, J. W., El-Mihilmy, M., & McCauley, M. (2000). Field performance of FRP bridge repairs. Journal of Bridge Engineering, 5(2), 107-113.

- Sudhakumar, J. (2001). Methods of repairing concrete structures. In Proc., 26th Conf. on Our World in Concrete and Structures (pp. 605-612).

- Tilly, G. P. (2011). Durability of concrete repairs. Concrete Repair: A practical guide, 231.

- Trejo, D., Halmen, C., & Reinschmidt, K. F. (2009). Corrosion performance tests for reinforcing steel in concrete: technical report (No. FHWA/TX-09/0-4825-1). Texas Transportation Institute, Texas A & M University System.

- TxDOT (2014). “Standard specifications for construction and maintenance of highways, streets, and bridges”. Texas Department of Transportation.

- TxDOT (2015). “Bridge Design Manual-LRFD.” Texas Department of Transportation.

- TxDOT (2015). “Concrete Repair Manual.” Texas Department of Transportation.

- TxDOT (2016). “Material Producer List” Texas Department of Transportation.

- Weyers, R. E., Prowell, B. D., Sprinkel, M. M., & Vorster, M. (1993). Concrete bridge protection, repair, and rehabilitation relative to reinforcement corrosion: A methods application manual. Contract, 100, 103.

- Wu, Z., & Hemdan, S. (2005). Debonding in FRP-strengthened flexural members with different shear-span ratios. In Proceeding of the 7th International Symposium on Fiber Reinforced Composite Reinforcement for Concrete Structures (pp. 411-426).

- Yang, D., Merrill, B. D., & Bradberry, T. E. (2011). Texas’ Use of CFRP to Repair Concrete Bridges. Special Publication, 277, 39-57.

- Zhao, Y., & Jin, W. (2016). Steel Corrosion-Induced Concrete Cracking. Butterworth-Heinemann.

Biographical Information

Yazan Almomani received his Bachelor of Science degree in civil engineering from University of Jordan, Jordan in 2013 and master's degree in Structural Engineering from University of Jordan, Jordan in 2015. He worked as a Structural Engineer in both site and design from 2013 to 2015. His Master's thesis was on Effect of Soil Structure Interaction Accompanied by Variation of Spectral Acceleration Values on the Dynamic Behavior of Multistory Reinforced Concrete Buildings. His research interest includes repair and rehabilitation of structures and structural health monitoring of bridges.